2013

DESIGN, SYNTHESES, AND BIOLOGICAL EVALUATION OF 14-N-SUBSTITUTED NALTREXONE DERIVATIVES AS OPIOID RECEPTOR LIGANDS

Orgil Elbegdorj
Virginia Commonwealth University

DESIGN, SYNTHESES, AND BIOLOGICAL EVALUATION OF 14-N-SUBSTITUTED NALTREXONE DERIVATIVES AS OPIOID RECEPTOR LIGANDS

A dissertation submitted in partial fulfillment of the requirements for the degree of Doctor of Philosophy at Virginia Commonwealth University.

by

Orgil Elbegdorj
Bachelor of Science in Biochemistry
Virginia Tech, 2008

Director: Yan Zhang, Associate Professor
Department of Medicinal Chemistry

Virginia Commonwealth University
Richmond, Virginia
January, 2013

Acknowledgement

Since I started this journey few years ago, there have been many people who have helped me on the way. First of all, I would like to thank my advisor Dr. Yan Zhang, who has been there from the beginning. He has motivated and encouraged me through many setbacks; his insights and guidance were always appreciated. I would like to thank Dr. Dana Selley, Dr. Phillip Gerk, Dr. Glen Kellogg, and Dr. Shijun Zhang for being in my committee and helping me with my dissertation. I would like to thank all the past and present members of the Yan Zhang lab group for their amiability as well as their input and assistance with my research. I would especially like to thank Dr. Guo Li and Dr. Yunyun Yuan for their assistance in organic chemistry. I would like to thank Dr. Dana Selley for giving me the opportunity to work in his lab and learn how to do radioligand binding assays. I want to thank Joanna Jacob and Jordan Cox for teaching me how to do the assays and cell culture work. Importantly, I want to thank my family and friends for all their love and care. There are many people who have not been mentioned here that helped me with this dissertation and I thank them for all their help and support as well.

Table of Contents

List of Tables

List of Figures

List of Schemes

List of Abbreviations

Å	angstroms
^{3}H	tritiated
β-FNA	beta-funaltrexamine
δ	delta
δ	chemical shift
^{0}C	degrees Celcius
ɣ	gamma
κ	kappa
µ	mu
µg	micrograms
µL	microliter
aq	aqueous
BBB	blood brain barrier
BBr_3	boron tribromide
B_{max}	receptor density
CHO	Chinese hamster ovarian
CNS	central nervous system
CO_2	carbon dioxide
CREB	cAMP response element-binding protein
d	doublet
DPN	diprenorphine
DMEM	Dulbecco's modified Eagle's medium
DMF	dimethylformamide
DMSO	dimethyl sulfoxide
DOR	delta opioid receptor
DPM	disintegrations per minute
EA	ethyl acetate
EC_{50}	half maximal effective concentration
EDTA	ethylenediaminetetraacetic acid
EGTA	ethylene glycol tetraacetic acid
EL	extracellular loop
E_{max}	maximum response
FBS	fetal bovine serum
FDA	Food and Drug Administration
g (centrifuges)	g-force
G148	geneticin
GDP	guanosine diphosphate
GNTI	5-guanidinonaltrindole
GPCR	g-protein coupled receptor
GTP	guanosine triphosphate
GTPɣS	guanosine 5'-O-[gamma-thio] triphosphate
h	hours

IC_{50}	half maximal inhibitory concentration
IR	infrared spectroscopy
K_2CO_3	potassium carbonate
K_i	binding affinity
KOR	kappa opioid receptor
m	multiplet
M	molar
MHz	megahertz
mM	millimolar
m.p.	melting point
MOR	mu opioid receptor
MS	mass spectroscopy
N	normality
N_2	nitrogen gas
Na^+	sodium ion
NaCl	sodium chloride
NaOH	sodium hydroxide
NH_4OH	ammonium hydroxide
NIDA	National Institute on Drug Abuse
NLX	naloxone
nM	nanomolar
NMR	nuclear magnetic resonance
NTI	naltrindole
norBNI	norbinaltorphimine
s	singlet
SAR	structure activity relationship
$SOCl_2$	thionyl chloride
TEA	triethylamine
THF	tetrahydrofuran
TM	transmembrane
Tris	trihydroxymethylaminomethane

Abstract

DESIGN, SYNTHESES, AND BIOLOGICAL EVALUATION OF 14-N-SUBSTITUTED NALTREXONE DERIVATIVES AS OPIOID RECEPTOR LIGANDS

By Orgil Elbegdorj, Ph.D.

A dissertation submitted in partial fulfillment of the requirements for the degree of Doctor of Philosophy at Virginia Commonwealth University.

Virginia Commonwealth University, 2013

Director: Yan Zhang, Associate Professor
Department of Medicinal Chemistry

Opium, the dried resin obtained from the unripe seedpods of the poppy flower, has been used for medicinal and euphoric purposes since ancient times. Morphine, the main active ingredient of opium, and other clinically useful opioid analgesics all mediate their effects through activating the mu opioid receptor. Studies involving the mu opioid receptor knockout mice showed that the interaction with the mu opioid receptor is also responsible for many notorious side effects associated with these drugs including dependence and addiction. Therefore, selective antagonists for the mu opioid receptor are needed to study its function in drug abuse and addiction. Previously, based on molecular modeling studies and the “message-address” concept, a series of 14-O-substituted naltrexone derivatives were designed and synthesized. These compounds carried an ester-linked heteroaromatic substitution at the 14-position of naltrexone

which was designed to interact with the putative “address” site, that was identified in the mu opioid receptor through molecular modeling studies. The lead compound of this series was determined to have a high affinity and selectivity for the mu opioid receptor. Because the 14-O-substituted naltrexone derivatives were not very stable, the ester linkage in these compounds was replaced by an amide one and a series of 14-N-substituted naltrexone derivatives were synthesized. The affinity and selectivity of these novel naltrexone derivatives were determined in a competitive radioligand binding assay. Interestingly, the 14-N-substituted naltrexone derivatives did not maintain the high selectivity of the 14-O-substituted series. It was hypothesized that the conformational constraint introduced by the amide linker was detrimental to the mu opioid receptor selectivity. Therefore, three 14-N-substituted naltrexone derivatives which carried more flexible linkages were synthesized and evaluated. The mu opioid receptor selectivity was not recovered by introducing rotational freedom into the linker. Some of these 14-N-substitued naltrexone derivatives were determined to be mu-kappa opioid receptor dual selective antagonists. Since the mu opioid receptor antagonists are effective at treating drug addiction, while growing evidence suggests that the kappa opioid receptor antagonists may be beneficial in lowering drug cravings, these novel mu-kappa opioid receptor dual selective antagonists may find unique clinical utility in the treatment of opioid dependence.

I. Introduction

Opium, the dried resin obtained from the unripe seedpod of the poppy flower (*Papaver Somniferum*), have been used for medicinal and euphoric purposes since antiquity. Opium contains more than 20 distinct alkaloids of which morphine is the main active constituent. In 1806, Friedrich Serturner reported the isolation of pure morphine from opium.[1] The strong pain-relieving characteristics of morphine are well established; even today with other treatment options available, opioids are generally considered the most effective analgesics.[2] However, morphine also produces many undesirable side-effects including respiratory depression, sedation, constipation, and dependence. Furthermore, the addictive potential of morphine has been known for centuries. Heroin, a synthetic derivative of morphine, was marketed by the Bayer pharmaceutical company in 1898 as a non-addictive morphine substitute. Unfortunately, heroin and all subsequent synthetic opioids that have been introduced into clinical use as analgesics share the addictive liabilities of classical opioids.[1]

The physiological targets of morphine and other opioids were largely unknown up until 1973, when three independent laboratories demonstrated the existence of opioid binding sites in the brain.[3-5] In the 1990s, the three main opioid receptors μ, δ, κ were cloned, further improving our understanding of the endogenous opioid system.[7] The discovery of the opioid binding sites in the brain stimulated the search for endogenous opioids which lead to the identification and later cloning of many biologically active peptides that interact with the opioid receptors. This family of endogenous opioid peptides includes Leu-enkephalin, Met-enkephalin, dynorphyn, β-endorphin and

endomorphins. These peptides with opioid activity are produced from larger precursors by selective action of different peptidases and other post-translational processing enzymes.[6] All of the opioid receptors are G-protein coupled receptors and the signal transduction mechanism is through $G_{i/o}$ proteins. Activation of opioid receptors leads to inhibition of adenylyl cyclase activity, resulting in decreased cAMP production, closure of voltage-gated Ca^{2+} channels, and stimulation of inwardly rectifying K^{+} channels. At the cellular level, all of these actions lead to strong inhibition of nerve firing and reduction in neurotransmitter release.[8]

Opioid receptors and their endogenous ligands are widely distributed through the CNS and peripheral tissues. This widespread anatomy is related to the important role that the opioid system plays in regulating major homeostatic and behavioral functions that include nociception, emotional well-being, learning and memory, regulation of reward circuits, food intake, respiration, and gastrointestinal motility.[9] All three opioid receptors are thought to be involved in analgesia. However, all clinically significant opioid analgesics are mu opioid receptor (MOR) agonists. Furthermore, studies involving mu opioid receptor knockout mice have revealed that the analgesic effect of morphine and its notorious side effects were abolished in MOR-deficient mice.[10,11] Since many of the side effects associated with the clinical administration of opioids are mediated by the MOR, compounds that are selective antagonists at the MOR will serve as valuable research tools and may be used as potential therapeutics.

Historically, opioid antagonists have been instrumental in identification and characterization of opioid receptors. Indeed, the action of an agonist is characterized as opioid-receptor-mediated only if its actions are competitively reversed by an opioid

antagonist.[12] Opioid receptor selective antagonists have not only been used as important pharmacological tools in opioid receptor research, but also have shown capacity to be effective at alleviating unwanted symptoms related to opioid agonist administration and used as treatment for various disease states. Nalorphine, the allyl derivative of morphine developed in 1944, is the first compound to be recognized as an opioid antagonist.[13] It is used as an opiate antidote but produces unpleasant side effects probably due to its agonist action at the kappa opioid receptor (KOR).[14] In the 1960's the first pure opioid antagonist naloxone was synthesized and pharmacologically evaluated.[15] It does not produce any effects similar to morphine and blocks the binding of receptor specific ligands at all three receptors with slightly higher K_i at the MOR and KOR compared to the delta opioid receptor (DOR). Due to its short elimination half-life and poor bioavailability, the use of naloxone is limited to emergency care settings where it is used to reverse the life-threating respiratory depression caused by opioid overdose.[16]

Soon after, naltrexone was developed by National Institute on Drug Abuse (NIDA) as a more potent, longer acting universal antagonist than naloxone.[17] Naltrexone is slightly more MOR selective as an antagonist when compared to naloxone and as a reversible opioid antagonist it blocks the euphoric effects of exogenously administered opioids and diminishes their reinforcing effects.[18] Naltrexone itself does not possess any addictive potential or lead to tolerance. When orally administered, naltrexone is well absorbed, reaching peak plasma levels being reached within one hour.[19] Due to these favorable properties, naltrexone has been approved by the FDA for the treatment of alcohol abuse and opioid dependence.[20] Naltrexone was shown to

counteract the stimulant and reinforcing effect of alcohol while enhancing the sedative effect. Furthermore, naltrexone has been found to reduce craving for alcohol in alcohol-dependent subjects in laboratory settings where they are exposed to alcohol.[77] Despite

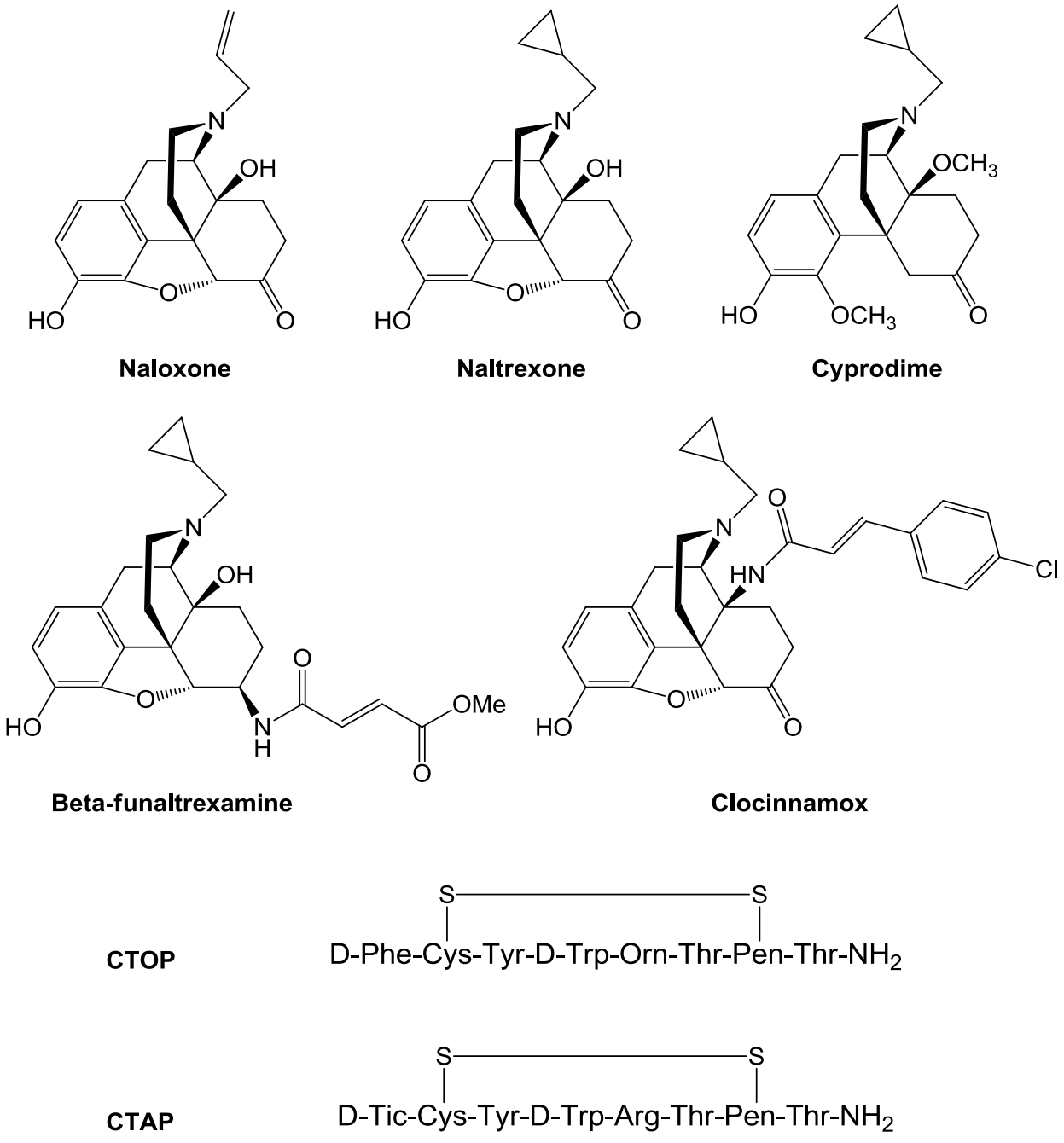

Figure 1. Mu opioid receptor antagonists.

its potential appeal as a treatment for alcohol and opioid dependence, naltrexone's clinical utility has been severely limited due to poor patient compliance and undesirable side effects.[21] Naltrexone has been shown to induce unpleasant dysphoric symptoms when administered in man.[23, 24] This may be due to naltrexone's poor selectivity and partial agonist activity at the KOR[28], since it is well known that KOR agonists and partial agonists produce psychotomimetic and dysphoric effects.[22] Nevertheless, naltrexone has been extensively utilized as a scaffold to develop important receptor selective antagonists as experimental tools.

In 1980, Portoghese reported the synthesis of β-funaltrexamine (β-FNA), the first selective MOR irreversible antagonist.[25] β-FNA structurally resembles naltrexone, with a fumarate group introduced at the 6-position. The fumarate group acts as a Michael acceptor for a nucleophilic attack, thus forming a covalent bond between β-FNA and the mu-opioid receptor. Initially, it was shown through site-directed mutagenesis studies that the Lys233 of the mu opioid receptor is covalently modified by β-FNA[26] and later confirmed when the crystal structure of the MOR bound to β-FNA was solved.[47] Clocinnamox, a derivative of naltrexone with a chlorocinnamoylamino group at the 14-position of naltrexone, is another selective irreversible antagonist of the MOR. It interacts with all three opioid receptors but only irreversibly inhibits the MOR.[27] Although, irreversible antagonists are essential tools in pharmacology for characterizing receptors and receptor function, the fact that they bind covalently and inactivate the receptor largely limits their utility. Irreversible antagonists are difficult to wash off the receptors in biological assays and prevent agonist action until new receptors are synthesized. Therefore, reversible antagonists are preferred in most cases because

they will temporarily block the receptor during the pharmacological study and then can be washed out from the binding site to revive the receptors.[29]

At this time, CTOP and CTAP are two of the most selective and reversible antagonists available at the mu opioid receptor.[30] CTOP and CTAP are cyclic, conformationally constrained peptide analogues of somatostatin, an important regulatory hormone that is widely distributed throughout the body with wide range of biological functions. Somatostatin was shown to bind the opioid receptors with low affinity but the chemically modified, rigid octapeptide analogs CTOP and CTAP have shown very high affinity and selectivity for the mu opioid receptor.[31] Although selective peptide antagonists were achieved through this novel approach, for a full pharmacological study both in vitro and in vivo activity is desired. Therefore, small molecule ligands are generally preferred due to their ability to penetrate the CNS, higher metabolic stability, and bioavailability.

Cyprodime was reported as a non-peptidic, reversible, neutral antagonist selective for the mu opioid receptor.[32] However, cyprodime has low affinity for the mu opioid receptor (K_i = 5.4 nM), its affinity is about 10-fold less than naloxone and 40-fold less than naltrexone. Moreover, cyprodime is only moderately selective for the mu opioid receptor in vitro (K_i value ratios, $\delta/\mu \approx 39$, $\kappa/\mu \approx 10$).[33] The low affinity and moderate selectivity of cyprodime limits its use as a tool to study the pharmacological characteristics of the mu opioid receptor. Further structure activity relationship studies on the cyprodime scaffold has not resulted in the development of a more potent and selective mu opioid antagonist without increasing the agonist activity.[33, 34] Therefore,

the synthesis of a nonpeptide, potent, selective, and reversible antagonist for the mu opioid receptor is still highly desirable.

The naltrexone structure may serve as a better scaffold for the development of mu selective antagonists. This scaffold has been previously utilized in the design of selective but irreversible antagonists β-FNA and clocinnamox for the mu opioid receptor. Furthermore, naltrexone was successfully adopted as the "message" moiety in the synthesis of naltrindole (NTI) and 5-guanidinonaltrindole (GNTI), reversible, highly selective, small molecule antagonists for the delta and kappa opioid receptors respectively, using the "message-address" concept.[35,36] The "message-address" concept was proposed Schwyzer who used it to analyze the structure-activity relationship of adrenocorticotropic hormone (ACTH) and related peptide hormones.[37] According to this concept, peptide hormones of the same class contain a "message" sequence and an "address" sequence of amino acids that are sequential or in close proximity to each other. The "message" sequence is responsible for signal transduction, while the address component of the peptide provides additional binding affinity and not necessary for the transduction process. Additionally, for a group of peptides that are associated with multiple receptors, the message component is structurally similar or invariant, while the address component is variable and becomes the primary determinant of selectivity for a specific receptor.[35]

Portoghese et al. reported the synthesis of NTI, the first non-peptide, potent, highly selective delta opioid receptor antagonist.[38] NTI encompasses a naltrexone-derived "message" component and an indole ring fused to the C-ring of the morphinan structure. The pyrrole moiety functions as a spacer that rigidly holds benzene, the

"address" component in proper orientation. The benzene group was envisioned to be an important delta opioid receptor "address" moiety from the analysis of endogenous opioid peptides, specifically leu-enkephalin. The conformational rigidity of the "address" component of NTI was essential, since it permitted binding with an "address" subsite that is unique to the delta receptor, while sterically hindering binding to "address" subsites associated with other opioid receptors.[39] Naltrindole retained the antagonist properties of its "message" component naltrexone while the addition of an "address" moiety specifically designed to interact with the delta opioid receptor, significantly increased its affinity therefore increasing its selectivity (K_i value ratios, μ/δ ≈ 152, κ/δ ≈ 276).[38] Naltrindole is widely used to study the delta opioid receptor pharmacology and the tritiated version has been a valuable tool in determining the affinity of novel ligands at the delta opioid receptor.

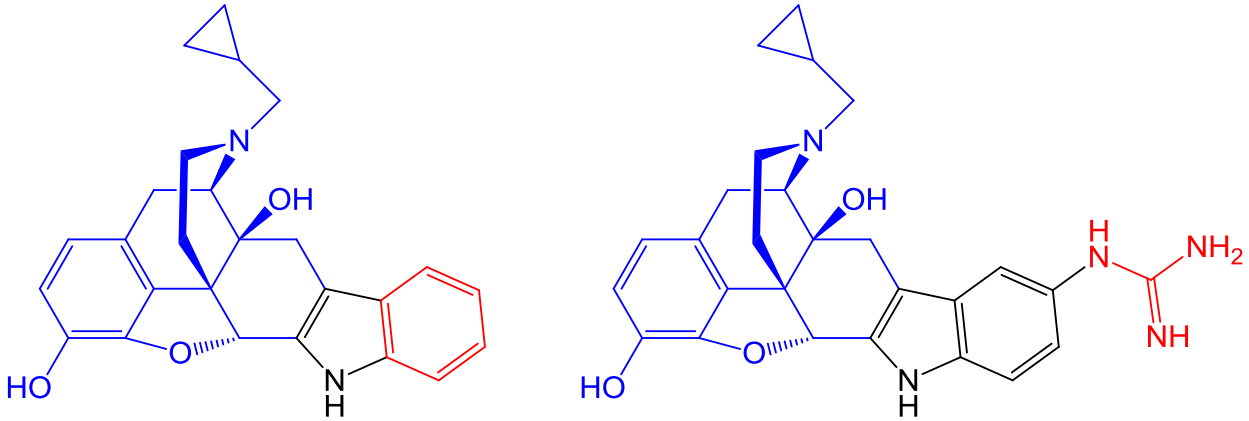

Figure 2. Delta opioid receptor selective antagonist NTI and kappa opioid receptor selective antagonist GNTI. The "message" component of these molecules are colored blue, while the "address" component is shown in red.

The “message-address” concept has been further expanded to kappa opioid receptor, where it has been successfully utilized to develop 5’-guanidinonaltrindole (GNTI), a potent and selective kappa opioid receptor antagonist (K_i value ratios, μ/κ ≈ 125, δ/κ ≈ 257).[40] The indole moiety in delta opioid receptor antagonist naltrindole was used to hold the guanidine group in proper orientation for an interaction with the kappa opioid receptor “address” subsite in the binding pocket.[36] Through a site-directed mutagenesis study, the kappa opioid receptor primary “address” recognition element was found to be the amino acid residue Glu297 at the top of the transmembrane helix 6 (TM6). Therefore, the strong ionic interaction specifically found in the kappa opioid receptor binding locus between the glutamate residue and the guanidine moiety of GNTI is responsible for its high selectivity.[41]

The application of the “message-address” concept towards the mu opioid receptor may also provide potent, highly selective, non-peptide, reversible antagonists for MOR. Introduction of specific chemical moieties onto the naltrexone scaffold, designed to interact with the mu opioid receptor “address” site may lead to the development of highly selective antagonists. Recently, based on molecular modeling studies and the “message-address concept,” a series of new 6α- and 6β-N-heterocyclic substituted naltrexamine derivatives were designed, synthesized, and characterized in our laboratory. Among these compounds, NAP and NAQ (**Figure 3**) were chosen as lead compounds for the development of MOR selective antagonists. NAP displayed high binding affinity for the MOR at K_i = 0.37 nM with over 700-fold selectivity for the MOR over the DOR and more than 150-fold selectivity over the KOR. NAQ also showed high affinity for the MOR at K_i = 0.55 nM with over 200-fold selectivity for the

MOR over the DOR and approximately 50-fold selectivity over the KOR.[29] Furthermore, NAP and NAQ both acted as potent antagonists in the in vivo tests without any significant agonist activity even at the very high dose of 100 mg/kg.[73] Further pharmacological and pharmacokinetic studies have revealed NAP to be a substrate of P-glycoprotein. Therefore, NAP seems to exhibit low permeability and limited ability to cross the BBB and it is now being developed as a peripheral selective MOR antagonist with potential clinical implication for the treatment of opioid-induced constipation.[74]

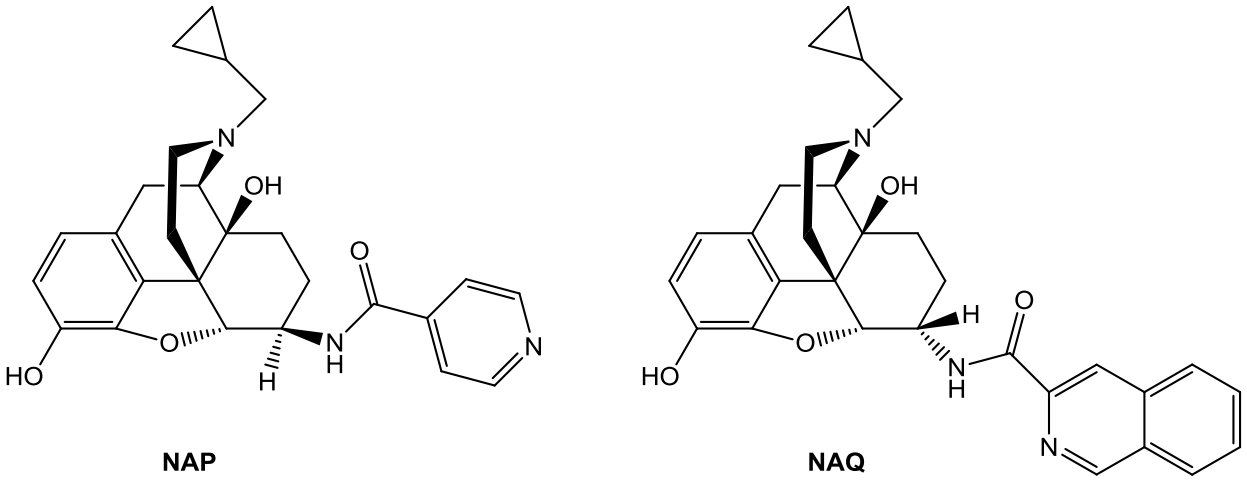

Figure 3. Mu opioid receptor selective antagonists currently being developed in our lab.

On the other hand, NAQ had have much better pharmacokinetic profile than NAP and may be assumed to have an absorption pattern similar to naltrexone.[75] Moreover, in a comparative opioid withdrawal study, NAQ did not elicit withdrawal symptoms at a dose 10 times higher than that of naloxone or naltrexone in morphine pelleted mice.[73] Therefore, NAQ may have a potential to be developed into a CNS active agent for the treatment opioid addiction and alcoholism. Indeed, the 6-N-substituted naltrexamine derivatives, NAP and NAQ, show a lot of promise as lead compounds for the development of MOR selective reversible antagonists but the research is still in its early

stage. Further manipulation of the naltrexone scaffold using the "message-address concept" may lead to the discovery of more favorable lead compounds with improved selectivity profile.

Prescription drug abuse has become a significant problem in the United States. The National Institute on Drug Abuse (NIDA) reports that in 2010, approximately 7.0 million people have used psychotherapeutic drugs nonmedically, of these 5.1 million used pain relievers. Furthermore, nearly 1 in 12 high school seniors reported nonmedical use of Vicodin and 1 in 20 reported abuse of OxyContin.[42] Admissions to substance abuse treatment programs increased by 400% between 1998 and 2008, with prescription painkillers being the second most prevalent type of abused drug after marijuana.[43] The National Survey on Drug Use and Health (NSDUH) estimates about 1.9 million people in the U.S. meet abuse or dependence criteria for prescription opioids. Unintentional overdose deaths involving prescription opioids have quadrupled since 1999 and now outnumber those from heroin and cocaine combined.[42] As discussed, addiction and abuse liabilities of opioids are primarily due to their interaction with the mu opioid receptor. Therefore, mu opioid receptor selective antagonists will be essential for the study of MOR function in drug abuse and addiction.

The use of naltrexone for the treatment of opioid dependence and maintenance therapy shows that mu opioid receptor antagonists can be effective at treating these conditions. Naltrexone's therapeutic use is hampered by its compliance issues possibly due to its low selectivity and partial agonist activity at the kappa opioid receptor. Novel non-peptide, highly selective, reversible antagonists targeting the mu opioid receptor will serve as valuable tools in understanding the role of this receptor in addiction and

dependence. Furthermore, selective mu antagonists with improved therapeutic profile may be used to treat conditions like opioid addiction and alcoholism more effectively.

This dissertation describes the synthesis of a series of 14-O-heterocyclic substituted naltrexone derivatives based on the “message-address” concept. The 14-position substituents in these compounds are designed to interact with a specific “address” site in the MOR binding site. It is hypothesized that the isosteric replacement of the O atom of the ester linkage of these compounds by NH of an amide linkage will not alter the pharmacological profile of these compounds.

II. Project Design

The main aim of this project was to design non-peptide, selective, reversible antagonists for the mu opioid receptor. The novel ligands were designed based on the lead compound that was identified in our lab. The proposed ligands were synthesized using organic chemistry techniques. In vitro pharmacological studies were carried out in order to determine the affinity of these novel compounds at all three opioid receptors. A [^{35}S]GTPγS binding functional assay was performed to see if these compounds act as agonists or antagonists at the mu opioid receptor. In addition, an in vivo assay was used to further characterize selected compounds based on the in vitro assay results. Finally, a molecular modeling study using the crystal structures of the opioid receptors was conducted in order to visualize and further analyze the binding modes of these ligands.

1. Molecular Design

It was reported that the third extracellular loop of the mu opioid receptor is critical for the binding of MOR-selective agonists.[44] Site-directed mutagenesis studies have also identified certain amino acid residues in this domain that may be essential for ligand selectivity for the MOR over the other two opioid receptors.[45] Comparative conformational analysis of mu opioid receptor selective agonists fentanyl, endomorphin 2, and the selective irreversible antagonist clocinnamox have revealed possible pharmacophoric elements that are important for MOR binding. The 17-cyclopropylmethyl group in clocinnamox was postulated to be the “message” part of the

molecule, while the p-chlorophenyl moiety at the 14-position was hypothesized to belong to the “address” component of the molecule that confers selectivity to MOR. Furthermore, when clocinnamox was docked into the MOR homology model, the 14-p-chlorophenyl moiety of clocinnamox, the putative “address” component of the molecule, was located in an aromatic binding pocket formed by EL2 and EL3. The amino acid residues within this aromatic pocket Tyr210, Phe313, and Trp318 are not conserved in the delta and kappa opioid receptors. These results led to the design and synthesis of a series of novel 14-O-heterocyclic substituted naltrexone derivatives. The heteroaromatic moieties at the 14-position of naltrexone are designed to interact with the aromatic binding locus formed by EL2 and EL3 of the mu opioid receptor. The nitrogen atom in these ring systems may also act as a possible hydrogen bond acceptor.

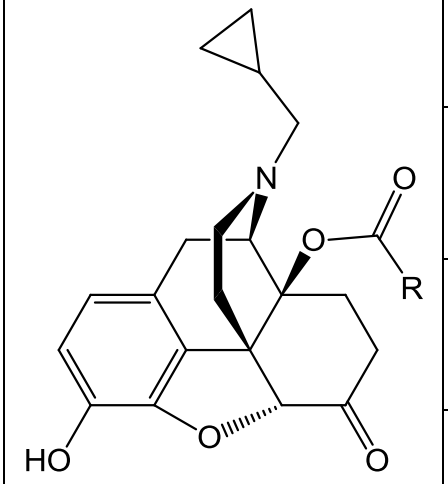

Compd	R-	Compd	R-
1	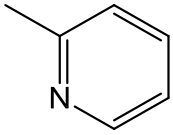	5	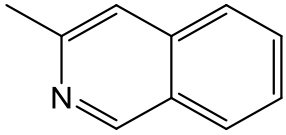
2	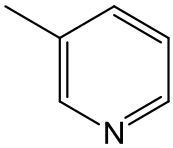	6	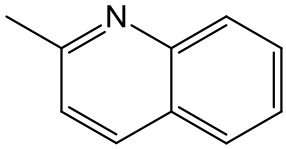
3	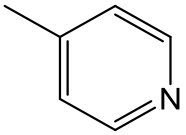	7	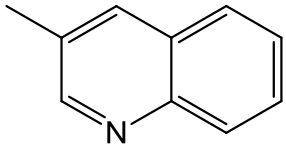
4	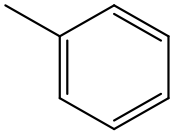	8	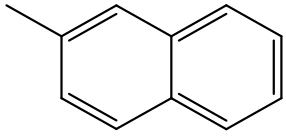

Figure 4. 14-O-heterocyclic substituted naltrexone derivatives previously synthesized in the lab.

In vitro biological assays revealed that these compounds bind the MOR with

nanomolar-to-subnanomolar affinities and generally had high selectivity for the MOR (**Table 1**). The lead compound in this series, compound **1** had approximately 800-fold selectivity for the MOR over the DOR and nearly 200-fold selectivity over the KOR.

Table 1. Competitive radioligand binding assay results for the 14-O-substituted naltrexone derivatives.

		K_i (nM) ± SEM			Selectivity Ratio	
Compd	Side Chain	MOR	KOR	DOR	κ/μ	δ/μ
1	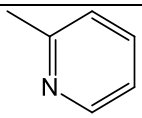	0.14 ± 0.03	25.50 ± 6.50	117.38 ± 17.97	182	838
2	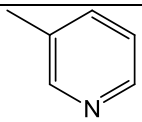	1.59 ± 0.61	47.81 ± 8.48	170.30 ± 12.64	30	107
3	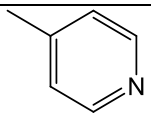	5.58 ± 1.34	49.21 ± 20.37	405.32 ± 234.68	9	73
4	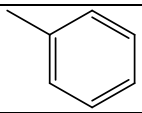	123.23 ± 38.23	586.42 ± 32.39	>10,000.00	5	>81
5	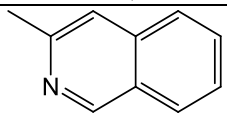	68.40 ± 6.04	>10,000.00	>10,000.00	>146	>146
6	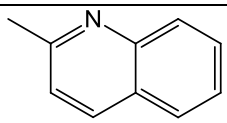	1.44 ± 0.32	67.15 ± 36.72	22.81 ± 19.52	47	16
7	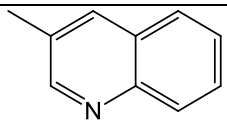	2.69 ± 0.72	148.23 ± 55.53	818.43 ± 507.23	55	304
8	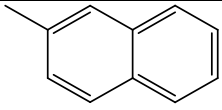	225.27 ± 46.6	46.57 ± 13.53	907.18 ± 192.99	<1	4

The K_i values for the mu, kappa, and delta opioid receptors represent the mean ± SEM of three independent experiments. [^{3}H] DAMGO, [^{3}H] norBNI, [^{3}H] NTI was used to label the mu, kappa, and delta opioid receptors, respectively.

Moreover, all compounds acted as neutral antagonists at the MOR except compound **8**. Overall, these results suggested that the 14-position substitutions introduced into naltrexone might interact with a unique aromatic binding locus found in the MOR. Furthermore the nitrogen atom in the heterocyclic ring might act as an H-bond acceptor, thus playing an important role in the selectivity of these compounds.[46] These compounds serve as a validation for the method of developing ligands that are selective antagonists at the mu opioid receptor.

However, a major drawback associated with these series of compounds was identified. The 14-O-substituted naltrexone derivatives were found to be not very stable, probably due to the reactive ester linkage introduced at the 14-position. To make these compounds more metabolically stable, the ester linkage was replaced by an amide linkage (**Figure 5**). Since the NH is an isostere of the O atom, it was hoped that these new 14-amino-substituted compounds would retain the pharmacologic profile of the 14-O-substituted naltrexone derivatives, i.e., the high selectivity for MOR and neutral antagonism. Although less reactive, the amide bond may provide less flexibility for the side chains compared to the ester bond. On the other hand, conformational constraint of a particular functional group in a favorable position may lead to increased affinity. Unlike naltrexone, the starting material for the 14-O-substituted series, the 14-amino-naltrexone is not commercially available. Therefore a viable synthetic route was found in order to introduce the amine functionality at the 14-position of naltrexone. After the amine group was synthesized, the heteroaromatic side chains were coupled to it, forming the amide bond.

2. Biological Evaluation

After synthesizing the novel naltrexone derivatives, biological assays were performed to determine their affinity and selectivity for the opioid receptors. Ideally these 14-amino-substituted compounds will retain the high selectivity that the 14-O-substituted ligands displayed for the MOR. The assays utilized CHO cells expressing mono-cloned opioid receptors. Competitive radioligand binding assays were used to determine the affinity of these compounds utilizing [^{3}H] NLX, [^{3}H] DPN, [^{3}H] NTI as radioligands for the mu, kappa, and delta opioid receptors, respectively. A functional [^{35}S]GTPγS assay was performed to determine if these compounds act as agonists, partial agonists, or antagonists at the mu opioid receptor.

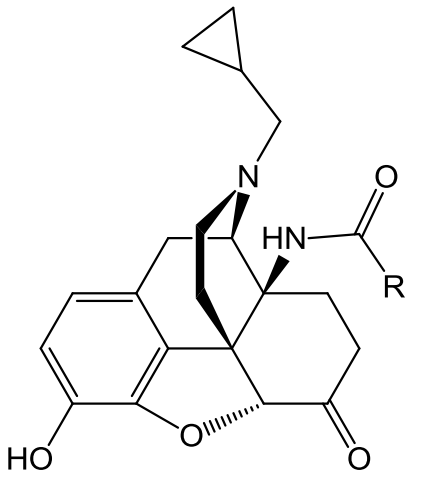

Compd	R-	Compd	R-
9	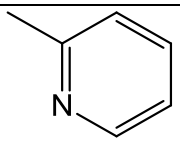	13	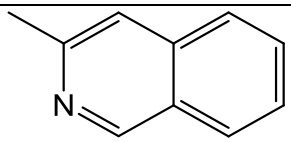
10	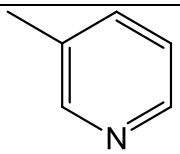	14	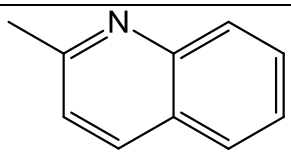
11	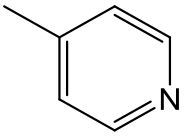	15	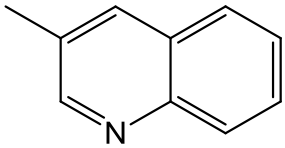
12	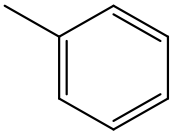	16	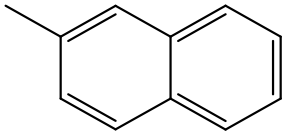

Figure 5. The newly designed 14-NH-heterocyclic substituted naltrexone derivatives.

3. Molecular Modeling Study

The crystal structures of all three opioid receptors have become available recently. The mu opioid receptor was crystallized with the irreversible antagonist β-FNA,[47] the kappa opioid receptor was crystallized in complex with JDTic,[48] and the delta opioid receptor was crystallized with the selective antagonist NTI bound in the binding site.[49] The 14-NH-heterocyclic substituted naltrexone derivatives were docked into the binding pocket of all three opioid receptor crystal structures using GOLD.[50] The docking studies were used to visualize the binding interactions and attempt to explain the pharmacological data.

III. Results and Discussion

1. Chemical Synthesis of 14-amino Derivatives of Naltrexone

The 14-amino naltrexone (**26**) is not commercially available; therefore it needed to be synthesized first before coupling it to various heteroaromatic ring systems. Using thebaine (**17**) as the starting material, the 14-amino naltrexone was synthesized in multiple steps (**Scheme 1**). Since the adopted synthetic route has been published in the literature,[51-56] the chemistry of this route is mature.

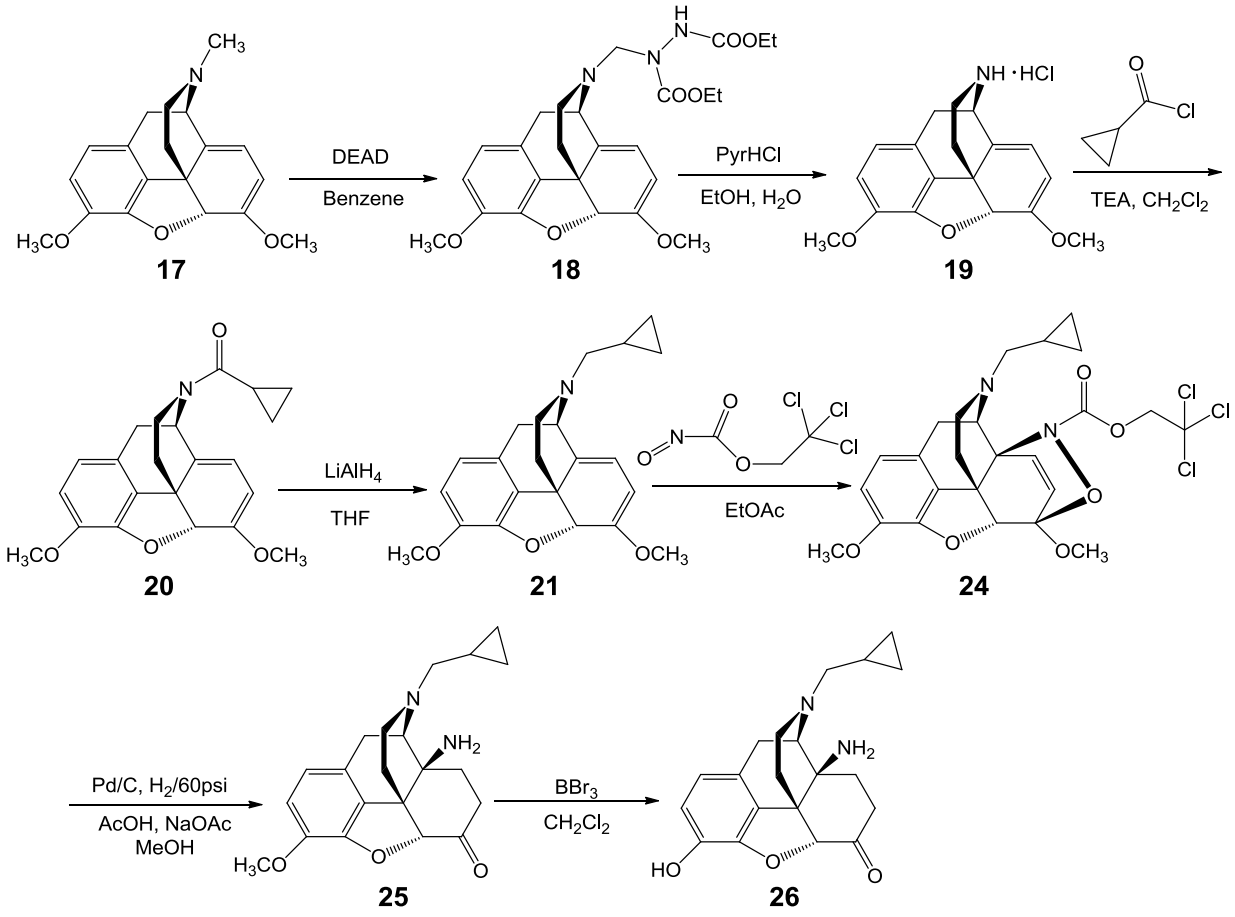

Scheme 1. The synthetic route towards 14-amino naltrexone from the starting material thebaine.

1.1 N-Dealkylation Reaction and Alternative Methods Attempted

The first reaction in **Scheme 1** involves the demethylation of the 17-position nitrogen in thebaine using the reagent DEAD. Initially toluene was used as a safer, less toxic substitute for benzene as the solvent. The first few attempts were unsuccessful and the intermediate was not isolated. The reaction was run at 85 ^{0}C for four hours and when monitored by TLC, significant quantities of starting material remained. After the reaction was run overnight, still most of the starting material was left unreacted. At that point another 0.5 more equivalent of DEAD was added and the reaction temperature was increased to 110 ^{0}C in order to push the reaction towards product. After 3 hours, the reaction was stopped and the major spot on the TLC plate was isolated, but it was not the desired product. The same reaction was repeated a few times in toluene at various temperatures but were not successful at furnishing the product. The literature was searched in order to find alternative methods for N-dealkylation. In total, three different N-demethylation reactions were tried, they are summarized in **Table 2**.

The first method is the classic Von Braun reaction that uses potassium carbonate and cyanogen bromide. After refluxing in CH_2Cl_2 for 17 hours, the K_2CO_3 was filtered out and the filtrate was added with 2:1 solution of H_2O:Concentrated NH_4OH and stirred for one hour. The reaction was very messy and produced more than five spots on the TLC and none of them were the product. The second reaction that was tried uses ethyl chloroformate as a N-demethylation reagent. After this reaction, product was not formed possibly, in this case, due to the harsh reaction conditions leading to the degradation of the starting material. In the third method, thebaine was added with 2,2,2-trichloroethyl chloroformate, K_2CO_3 and refluxed in dichloroethane. The crude

intermediate was not isolated and the crude reaction mix was dissolved in 90% acetic acid and added with Zn powder. After workup there were two major spots on TLC, one of them was 2,2,2-trichloroethyl chloroformate and the other spot was again not the product.

Table 2. Alternative N-demethylation reactions that were explored.

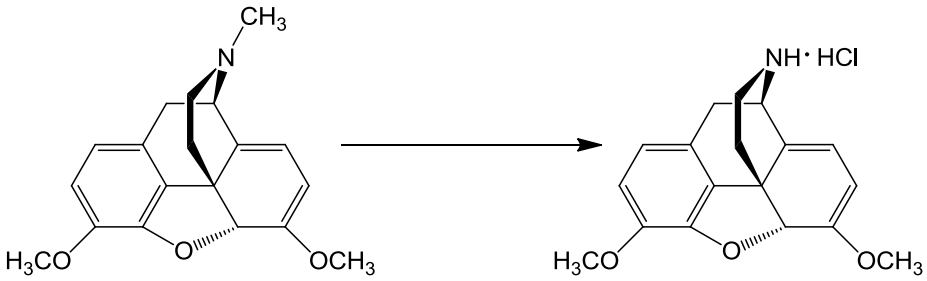

Method	Reagents and Condition	Reference
1	$\xrightarrow[CH_2Cl_2,\ reflux]{CNBr,\ K_2CO_3}$	57
2	A. 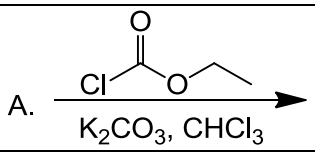 B. $\xrightarrow[reflux]{conc.\ HCl,\ HOAc}$	58
3	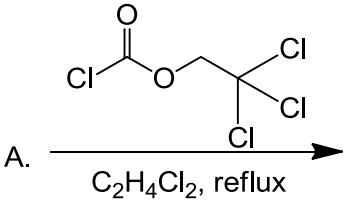 A. $\xrightarrow[C_2H_4Cl_2,\ reflux]{}$ B. $\xrightarrow[HOAc]{Zn\ powder}$	59

After attempting these reactions for weeks, the original method described in **Scheme 1** was attempted once again. However, this time no attempt was made to isolate the intermediate and the crude reaction mixture was dried and reacted with

pyridine hydrochloride in EtOH/H_2O mixture to give northebaine hydrochloride, the product. Initially, this reaction might have failed due to excess of DEAD leading to formation of side products. The reagent DEAD was also found to be unstable at temperatures over 100 ^{0}C. This N-dealkylation reaction had a very low yield of 30%. The yield needed to be further optimized, since this is the very first reaction in the synthetic route. Using benzene as a solvent and refluxing overnight at 85 ^{0}C seemed to improve yield. In the second part of the reaction, the crude intermediate is refluxed in 2:1 ratio of EtOH:H_2O for one hour, then stirred at room temperature for four hours. During this process northebaine hydrochloride precipitates out as a white solid. After washing with small amount of cold EtOH and drying, it can be used for the next reaction without further purification. By using this method northebaine HCl was synthesized from thebaine with yields of up to 83%. One caveat that was found with this reaction is that it cannot be scaled up without compromising the yield significantly. The maximum amount of thebaine used in this reaction with good yield was 3 grams. With starting material more than 3 grams the reaction yield suffered. In order to synthesize enough 14-amine naltrexone for the final 8 compounds, this reaction and the whole route had to be repeated numerous times.

In the next reaction the amine of **19** was N-acylated using cyclopropyl carbonyl chloride to provide 17-cyclopropylcarbonyl northebaine. The N-acylation reaction was simple and the product was obtained in near quantitative yield. The amide functionality at the 17-position was reduced to amine using lithium aluminum hydride, a strong reducing agent. The highest yield achieved for this reaction was 77% and this is close to the value reported in literature.

1.2 Heterocyclic Diels-Alder Reaction

The next step in the synthetic route involves the incorporation of an amino group to the 14β-position of **21** by utilizing a Diels-Alder reaction and catalytic hydrogenation. The synthesis of the hydroxycarbamate that is used in the reaction is shown in **Scheme 2**. It was prepared by N-acylation of hydroxylamine hydrochloride with trichloroethylchloroformate under basic conditions. In the cycloaddition reaction, the hydroxycarbamate **22** is oxidized by sodium periodate *in situ* to form nitrosoformate, the dienophile in the Diels-Alder reaction. The nitrosoformate immediately reacts with the diene of the alkaloid to form the Diels-Alder product.

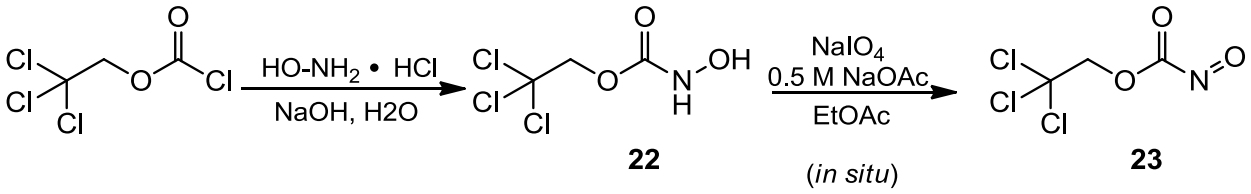

Scheme 2. Synthesis of nitrosoformate, the dienophile in the Diels-Alder reaction.

The reaction has been found to be stereospecific as only the β-regioisomer is observed.[54] The yield for the heterocyclic Diels-Alder reaction was usually around 60%.

In the next step, the Diels-Alder adduct **24** was reduced by catalytic hydrogenation. The reduction comprised of three steps: (a) hydrogenation of double bond at position 7-8, (b) cleavage of the trichloroethoxycarbonyl protecting group, and (c) reductive cleavage of N-O bond. The hemiketal formed at the 6-position was converted to ketone by acid catalyzed cleavage. The yield of this reaction was generally low, around 40%. The Diels-Alder adduct, the starting material for the

hydrogenation reaction, was found to be sparingly soluble in the mixture of 2N Acetic acid / 1.5N sodium acetate (1:1) and methanol mixture which was used as the solvent. As the hydrogenation reaction proceeded the precipitate disappeared with the formation of the soluble product. In order to increase reaction yield, it was found that the starting material should be both of fine particle size to increase solubility and pure so that the impurities will not poison the Pd/C catalyst. A new convenient method for the recrystallization/purification of the Diels-Alder product was found. The crude reaction mixture is added with small amount of methanol and sonicated. During this process the product precipitates out as white powder, which is filtered and washed with cold methanol to afford the product. The product obtained from this purification process is a pure white powder which can be readily used for the hydrogenation reaction.

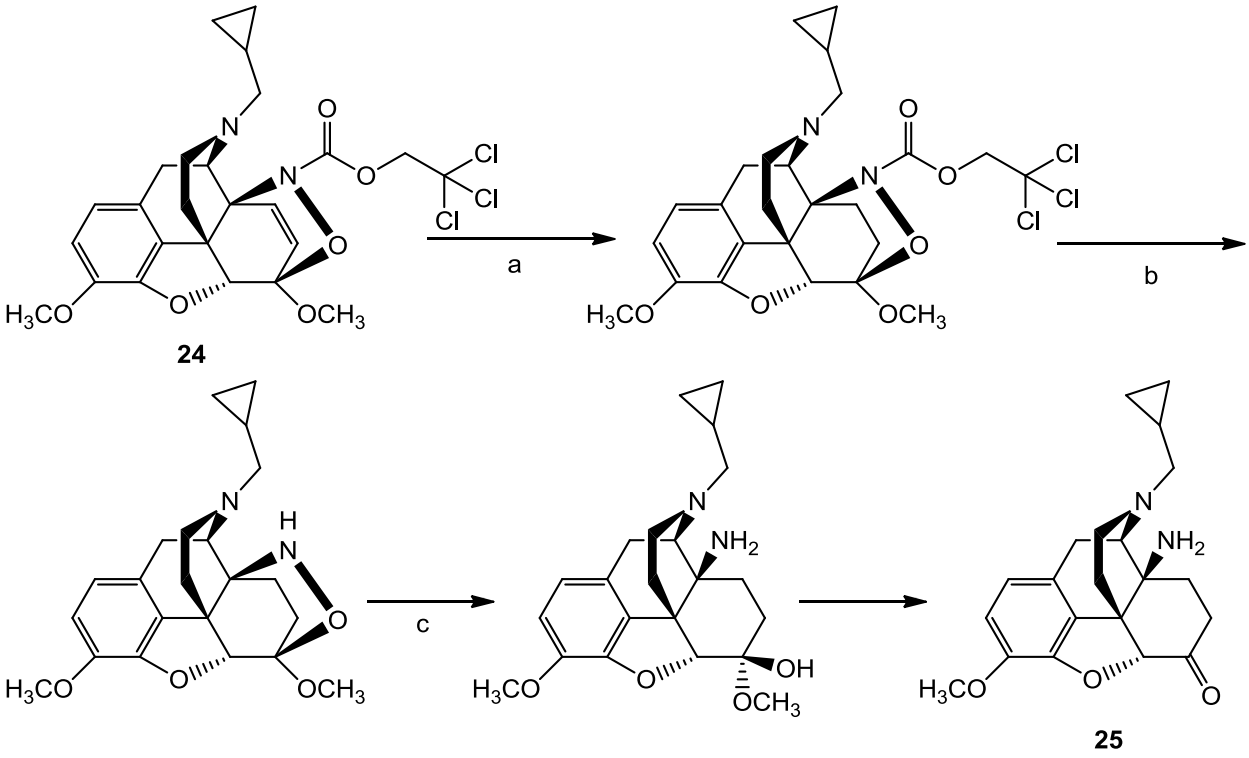

Scheme 3. Steps involved in the catalytic hydrogenation reaction.

1.3 O-Demethylation Reaction and Alternative Methods Attempted

The next step in the synthetic route involves 3-O-demethylation of **25** to obtain the 14-amino naltrexone. Boron tribromide, strong Lewis acid, is used as the demethylation reagent. The yield of this reaction was low (17%), probably due to harsh

Table 3. Alternative O-demethylation reactions that were attempted.

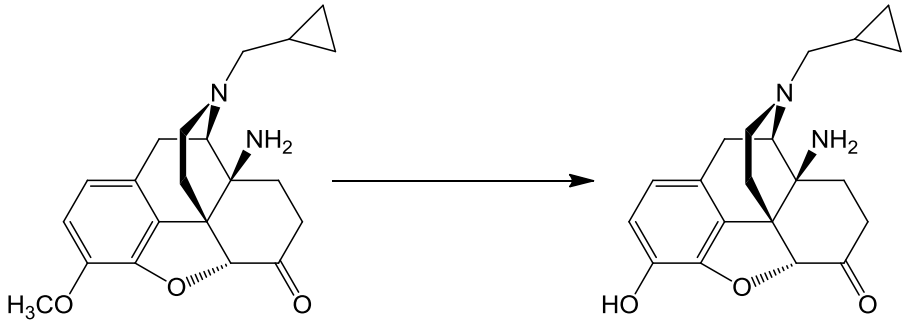

Method	Reagents and Condition	Reference
1	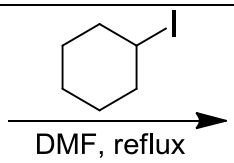	60
2	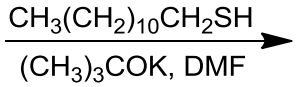	61
3	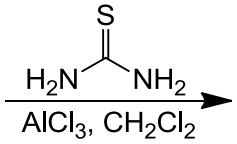	62

reaction conditions and the formation of unstable side products. Alternative O-demethylation reactions were sought out in hopes of finding a more efficient synthetic method with higher reaction yield. The reagent and reaction conditions for these

methods are shown in **Table 3**. In the first reaction, compound **25** was refluxed in DMF with cyclohexyl iodide. After two hours the reaction was monitored by TLC, and it was observed that all of the starting material had disappeared, but product was not formed. It appeared that the starting material had degraded. In the next reaction, the starting material was added to a stirred solution of potassium tert-butoxide and 1-dodecanethiol in anhydrous DMF at 0 ^{0}C. The reaction was continually monitored by TLC. After stirring overnight, no product was formed. In addition, it was found that the 1-dodecanethiol is very hard to deal with during phase separation as it has surfactant properties and readily dissolves in organic solvent compared to water. The last reaction that was attempted involved the refluxing of starting material, $AlCl_3$, and thiourea in dry DCM. The reaction was refluxed overnight and after workup, only starting material was isolated, no reaction took place.

The only O-demethylation reaction that worked, which used BBr_3, was revisited and further tweaked in order to maximize reaction yield. Instead of adding BBr_3 at 0^{0}C and stirring at room temperature, the demethylation reagent BBr_3 was added to the starting material at -78^{0}C, in order to minimize the formation of byproducts. The reaction was allowed to warm up to 0^{0}C slowly and stirred on an ice-water bath for one hour. Performing the reaction at low temperatures seemed to decrease the formation of side products and increased reaction yield. The highest yield achieved for this reaction was 44%.

1.4 Methods Attempted for the Direct Conversion of Naltrexone to 14-amino Naltrexone

In order to synthesize 14-amino naltrexone from thebaine, it took 8 steps and the whole route had a total yield of 8%, considering the maximum reaction yields that were achieved. If 14-amino naltrexone can be synthesized directly from naltrexone by transforming the alcohol group at the 14-position to amine in a simple one-pot reaction, it would be highly advantageous over the current strategy. Such a method would conserve resources and lead to the final compounds far more quickly, saving a lot of time and effort. However, there is no evidence that naltrexone goes through such transformation, it is not known if this synthetic conversion is even feasible. Nevertheless, the most common reactions utilized to convert alcohols to amines were adopted for naltrexone to see if the 14-amine naltrexone can be synthesized in a more convenient manner. All the reaction conditions and the results are summarized in **Table 4**. One of the most common approaches employed for the preparation of amines from alcohols involves three steps. First, the alcohol is converted to their corresponding halides or sulfonates, then nucleophilic substitution by an azide anion occurs. Finally, the azide is reduced to the amine using various reagents. There are methods that have been reported which do not require the conversion of the alcohol to a halide initially.

In the first method naltrexone was reacted with sodium azide and triphenylphosphine in CCl_4-DMF solvent system. It was envisioned that the azide group will replace the hydroxyl group at the 14-position through a S_N1 type of reaction. S_N2 substitution reaction cannot take place since the 14-position carbon is a tertiary carbon but it may form a relatively stable carbocation with the hydroxyl group leaving. Since the azide is mildly nucleophilic it will attack the carbocation at this position and form the single bond. The Staudinger reaction is employed to reduce the azide to an amine.[68]

Table 4. Reactions attempted to directly convert naltrexone into 14-amino naltrexone.

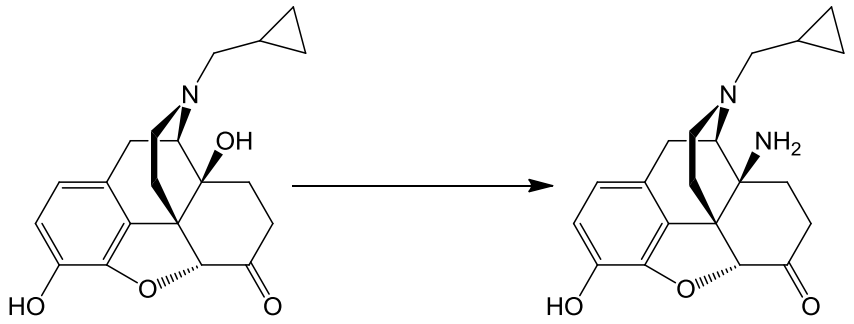

Method	Reagents and Condition	Reference
1	A. NaN_3, PPh_3 / CCl_4-DMF (1:4) → B. H_2O →	63
2	A. NaN_3, $BF_3O(C_2H_5)_2$ / THF, reflux → B. PPh_3 / THF → C. H_2O →	64
3	A. $(CH_3)_3SiN_3$, $BF_3O(C_2H_5)_2$ / CH_2Cl_2 → B. PPh_3 / THF → C. H_2O →	65
4	$SOCl_2$, NH_4^+ / CH_2Cl_2 →	66
5	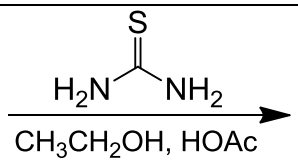	67

The azide reacts with triphenylphosphine to form phosphazide which loses nitrogen to give the iminophosphorane intermediate. The intermediate is hydrolyzed to give the amine and the triphenylphosphine oxide as the side product. This reaction is a particularly mild method of reducing an azide to an amine. After attempting the reaction

on naltrexone, two new spots have formed on the TLC. One of the spots was the side product triphenylphosphine oxide and the other spot was not the product. The reaction might have failed since the hydroxyl is not a good leaving group.

In the methods 2 and 3, boron trifluoride etherate, a Lewis acid, is added in order to make the hydroxyl a better leaving group and trimethylsilyl azide was used as a safer and more soluble alternate to sodium azide. The method 3 was reported to be regioselective for tertiary alcohols. After running both reactions for over 24 hours, only starting material was observed, no reaction took place. The fourth method uses thionyl chloride and ammonia gas to convert tertiary alcohols to corresponding amines. The compound that was isolated after the reaction was not the 14-amine product. The last method attempted was reported in a patent and successfully utilized to convert a tertiary alcohol, albeit with a simple structure, into an amine. Unfortunately, this reaction also failed to provide the desired product possibly due to the harsh reaction conditions.

There are not many reactions reported that can readily transform tertiary alcohol to an amine. All the methods that were attempted turned out to be unsuccessful at converting the 14-OH group of naltrexone into an amine. The main reason for this may be that the 14-position is unreactive due to high steric hindrance. Also the 6-position phenolic hydroxyl group and the 3-position carbonyl group might react with the various reagents and lead to undesirable side products. Therefore, the already established synthetic route shown in **Scheme 1** was used to synthesize more 14-amino naltrexone.

1.5 Chemical Synthesis of Final Compounds

In order to synthesize the final compounds, the side chains were introduced into

the morphinan skeleton using two different coupling methods (**Scheme 4**). The first procedure involves the direct coupling reaction of an acyl chloride with 14-amino naltrexone under basic conditions. In this reaction, the acid chloride is added to a solution of **26** dissolved in anhydrous DCM at 0 ºC under nitrogen atmosphere. The reaction is usually complete after stirring overnight. In the second procedure, the carboxylic acid of the aromatic side chain is coupled to the 14-amino naltrexone in the

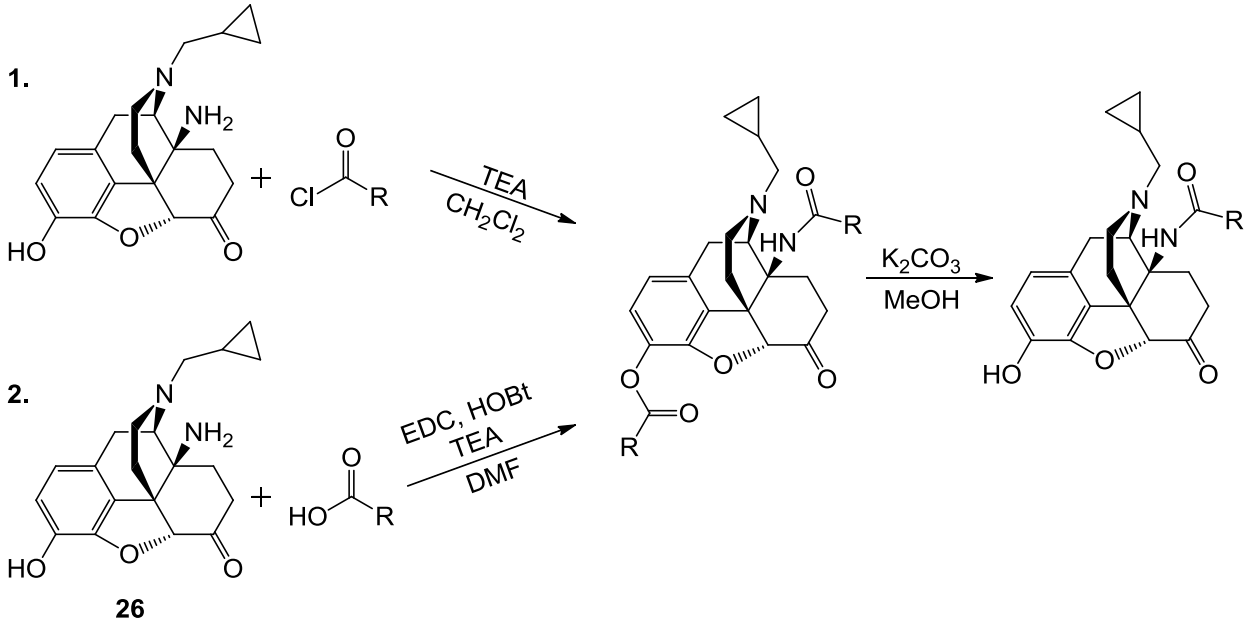

Scheme 4. Coupling of side chains to 14-amino naltrexone.

presence of 1-Ethyl-3-(3-dimethylaminopropyl)carbodiimide hydrochloride (EDC-HCl) and 1-hydroxybenzotriazole (HOBt) in the general peptide coupling reaction.[69] To a stirred solution of acid, EDC, HOBt, and TEA dissolved in DMF, was added 14-amine naltrexone and the reaction mixture was stirred for 18 hours at room temperature under nitrogen atmosphere. Also molecular sieves were added to neutralize the excess water the reaction produced. Generally, the second procedure seemed to be milder compared to the first method, which uses the acid chloride, as it produced less by

Table 5. The final coupling reaction percent yield of 14-NH-heterocyclic substituted naltrexone derivatives.

Compound	14-NH-heterocyclic Substituent	Procedure	Yield (%)
9	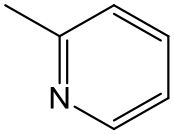	2	45
10	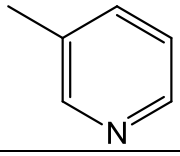	1	62
11	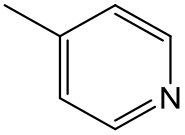	1	77
12	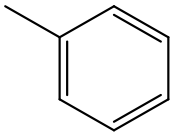	2	60
13	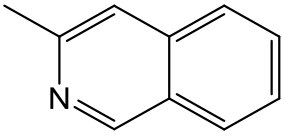	2	44
14	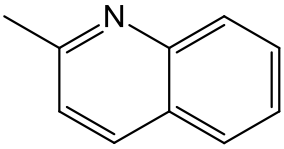	2	40
15	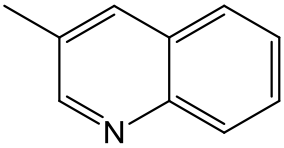	2	48
16	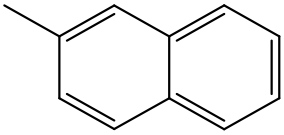	2	45

products. Both methods lead to the addition of the heterocyclic side chain moiety to 3- and 14-positions of the alkaloid. In the next step, the 3-position moiety is selectively removed by stirring the di-substituted intermediate with potassium carbonate in methanol. The phenyl ester moiety at the 3-position is highly unstable under basic

conditions and it is readily hydrolyzed in the saponification reaction while the amide bond is relatively stable and remains intact. All the final compounds were purified using column chromatography and then fully characterized. The final yields of these compounds are shown in **Table 5.**

2. Pharmacological Evaluation of 14-NH-Heterocyclic Substituted Naltrexone Derivatives

The 14-NH-heterocyclic derivatives of naltrexone were subjected to two different radioligand binding assays. The competition binding assay was performed to determine the affinity and the selectivity of these compounds at the opioid receptors. The functional [^{35}S] GTPγS assay was used to determine the potential agonist activity of the naltrexone derivatives.

2.1 Cell Culture of CHO Cells Overexpressing Opioid Receptors

For all the pharmacological assays that were performed, CHO cells expressing different mono-cloned opioid receptors were used. Before the assay could be performed, these cells had to be thawed and grown in optimal media. The MOR- and the KOR-CHO cells were grown in DMEM/F12 media containing 5% fetal bovine serum (FBS), 1% penicillin-streptomycin, and 0.25 mg/mL geneticin (G418). The DOR-CHO cells were cultured in the same media, except 10% FBS was added. All the cells were grown for about 7 days while being split continually, until they were grown to near confluence in 16 large culture dishes (150 mm × 25 mm). At this point, these cells were

harvested and membrane preparations were made. The membrane preparations are stored at -80 ^{0}C until they were thawed and used for the binding assay.

2.2 Competition Binding Assay

The competition binding assays were performed to study the selectivity and affinity of the newly synthesized ligands using mono-cloned opioid receptors expressed in CHO cells. [^{3}H] NLX, [^{3}H] DPN, and [^{3}H] NTI were used to label the mu, kappa, and delta opioid receptors respectively. The radioligands employed for the biological assays are highly selective for their corresponding receptors. The K_d values for the tritiated compounds and the B_{max} value for the CHO cell lines expressing the different opioid receptors have been previously determined in the laboratory. In this assay, varying concentrations of the naltrexone derivatives compete with a constant concentration of the radioligand, usually set between 1 to 2 times their K_d values. The potency of the new compounds in displacing the specific binding of the radioligand was determined from using linear regression analysis of Hill plots. The IC_{50} values are then calculated and corrected to K_i values using the Cheng-Prusoff equation, $K_i = IC_{50} / (1 + [L] / K_d)$.[70]

A. Mu Opioid Receptor

The affinity of the 14-NH-heterocyclic substituted naltrexone derivatives for the MOR was determined by competing varying concentrations of these drugs with 2 nM of [^{3}H] NLX. The non-specific binding was determined by using 5 µM of cold naltrexone. Membranes prepared from MOR-CHO cells (Dr. Selley's laboratory at VCU) were used for the assay and 30 µg of protein was added to each tube. The Bradford protein

assay[71] was utilized to determine and adjust the concentration of protein required for the assay. The total volume in each test tube was 500 µL and the tubes were incubated at 30 ºC for 90 minutes. The bound radioactive ligand was separated from the free radioligand by rapid vacuum filtration through a GF/B glass fiber filter paper using the Brandel harvester. The radioactivity was quantified by utilizing a scintillation counter. All assays were determined in triplicate and repeated at least three times.

B. Kappa Opioid Receptor

The affinity of the newly synthesized 14-NH-heterocyclic substituted naltrexone derivatives for the kappa opioid receptor was determined by competing varying concentrations of these drugs with 0.5 nM of [^{3}H] DPN. The non-specific binding was determined by using 5 µM of cold U-50488, a selective kappa opioid receptor agonist. Membranes prepared from KOR-CHO cells (Dr. Selley's lab at VCU) were used for the assay and 30 µg of protein was added to each tube. The Bradford protein assay was utilized to determine and adjust the concentration of protein required for the assay. The total volume in each test tube was 500 µL and the tubes were incubated at 30 ºC for 90 minutes. The bound radioactive ligand was separated from the free radioligand by rapid vacuum filtration as described above. The radioactivity was quantified by utilizing a scintillation counter. K_i values are result of 3 independent experiments.

C. Delta Opioid Receptor

The affinity of the 14-NH-heterocyclic substituted naltrexone derivatives for the delta opioid receptor was determined by competing varying concentrations of these

drugs with 0.5 nM of [^{3}H] NTI. The non-specific binding was determined by using 5 µM of cold SNC-80, a selective agonist at the delta opioid receptor. Membranes prepared from DOR-CHO cells (Dr. Selley's laboratory at VCU) were used for the assay and 30 µg of protein was added to each tube. The Bradford protein assay was utilized to determine and adjust the concentration of protein required for the assay. The total volume in each test tube was 500 µL and the tubes were incubated at 30 ºC for 90 minutes. The bound radioactive ligand was separated from the free radioligand by filtration as described above. The radioactivity was quantified by utilizing a liquid scintillation counter. All assays were determined in triplicate and repeated at least three times.

Initially, there were a few problems encountered with this assay. When the DOR-CHO cells in Dr. Selley's laboratory were used for the assay, the non-specific binding was found to be extremely high. In some instances the non-specific was higher than the total binding, making the data unusable. After a few attempts, the data was not reproducible and had very high SEM values. Saturation binding assays were performed to determine the B_{max} for the DOR-CHO cells. These cells had very low B_{max} values, indicating that the receptor expression was too low for K_i determinations. New DOR-CHO cells were received from Dr. Lee-Yuan Liu-Chen at Temple University that had been transfected recently. These cells were grown and new membranes were prepared. The saturation binding assay showed that these cells had a relatively high B_{max} value compared to the previous batch. The results from the competitive radioligand binding assay were a lot better, although the non-specific was still high compared to the other assays. In order to decrease the non-specific binding further, the

filter papers were soaked in 1% polyethylenimine solution before harvesting, and it was rinsed through with cold tris buffer four times. These measures lead to lower non-specific and a more reproducible data.

2.3 [^{35}S]GTPγS Functional Assay

A. Mu Opioid Receptor

[^{35}S]GTPγS functional assay was performed to determine the agonist activity of the 14-substituted naltrexone derivatives at the mu opioid receptor. In this assay, 10 µg of MOR-CHO membrane was incubated with 10 µM GDP, 0.1 nM [^{35}S] GTPγS and varying concentrations of the compounds under investigation for 90 minutes in a 30 ºC water bath. The Bradford protein assay was utilized to determine and adjust the concentration of protein required for the assay. The non-specific binding was determined with 20 µM unlabeled GTPγS. TME buffer with 100 mM NaCl was used to increase agonist stimulated binding and the final volume in each assay tube was 500 µL. Furthermore, 3 µM of DAMGO was included in the assay as a maximally effective concentration of a full agonist for the mu opioid receptor. The net stimulation produced by each test compound was normalized to the stimulation produced by 3 µM of DAMGO, which was considered to be 100%. After the incubation, the bound radioactive ligand was separated from the free radioligand by filtration through a GF/B glass fiber filter paper using the Brandel harvester. The results were determined by utilizing a scintillation counter. All assays were determined in triplicate and repeated at least three times.

B. Kappa Opioid Receptor

[^{35}S]GTPɣS functional assay was performed to determine the agonist activity of the 14-substituted naltrexone derivatives at the kappa opioid receptor. In this assay, 10 µg of KOR-CHO membrane was incubated with 10 µM GDP, 0.1 nM [^{35}S] GTPɣS and varying concentrations of the compounds under investigation for 90 minutes in a 30 ºC water bath. The Bradford protein assay was utilized to determine and adjust the concentration of protein required for the assay. The non-specific binding was determined with 20 µM unlabeled GTPɣS. TME buffer with 100 mM NaCl was used to increase agonist stimulated binding and the final volume in each assay tube was 500 µL. Furthermore, 5 µM of U50,488 was included in the assay as a maximally effective concentration of a full agonist for the kappa opioid receptor. The net stimulation produced by each test compound was normalized to the stimulation produced by 5 µM of U-50488, which was considered to be 100%. After the incubation, the bound radioactive ligand was separated from the free radioligand by filtration as described above. The results were determined by utilizing a scintillation counter. All assays were done in triplicate and repeated at least three times.

2.4 In Vivo Pharmacological Assays

Naltrexone derivatives with good selectivity profiles and antagonist actions in the in vitro assays for the mu opioid receptor were selected and tested in the in vivo assays. The selected compounds were tested for their acute antinociceptive agonistic and antagonistic effects in the mouse tail immersion assay. In addition, comparative opioid withdrawal assay were performed in morphine pelleted mice.

3. Pharmacological Assay Results for the 14-NH-Heterocyclic Substituted Naltrexone Derivatives

3.1 Competitive Radioligand Binding Assay Results

The competitive binding assay results show that the naltrexone derivatives with the amide linkage to various heterocyclic aromatic rings have a subnanomolar to nanomolar affinity to the mu opioid receptor. Interestingly, the 14-NH-substituted series of compounds did not maintain the high selectivity of the 14-O-heterocyclic substituted naltrexone derivatives for the MOR (**Table 6**). All the compounds that were tested have K_i values in the subnanomolar range for the KOR. The 14-NH-substituted derivatives also have higher affinity for the DOR compared to the 14-O-substituted compounds. In general, the 14-NH-substituted naltrexone derivatives seem to be dually selective for the mu and kappa opioid receptors over the delta opioid receptor.

A. Mu Opioid Receptor

The biological assay results for the mu opioid receptor show that the compounds with pyridinyl substitution bind with slightly higher affinity compared to the compounds with quinolynyl substitution. The nitrogen atom in the aromatic ring seems to make a small difference in the binding of the pyridinyl series, since the control compound binds with lower affinity compared to the aromatic rings containing a nitrogen atom. It is harder to see the same trend in the compounds with quinolinyl substitution. It is not clear if the nitrogen atom in the aromatic ring plays a significant role in binding of these 14-NH-substituted naltrexone derivatives to the mu opioid receptor.

Table 6. The binding affinity and selectivity of 14-NH-substituted naltrexone derivatives.

		K_i (nM) ± SEM			Selectivity Ratio		
Compd	Side Chain	MOR	KOR	DOR	κ/μ	δ/μ	δ/κ
NTX		0.34 ± 0.03	0.90 ± 0.11	95.46 ± 6.09	2.6	281	106
9	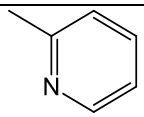	1.51 ± 0.34	0.36 ± 0.01	94.54 ± 6.48	0.24	63	263
10	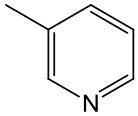	0.75 ± 0.28	0.16 ± 0.01	39.88 ± 0.50	0.21	53	249
11	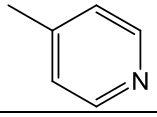	0.82 ± 0.33	0.33 ± 0.01	10.86 ± 1.31	0.40	13	33
12	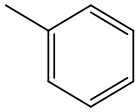	4.34 ± 0.70	0.12 ± 0.001	57.32 ± 4.33	0.03	13	477
13	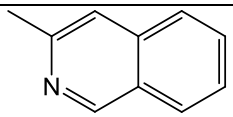	3.50 ± 1.87	0.27 ± 0.02	25.07 ± 1.84	0.07	7.2	93
14	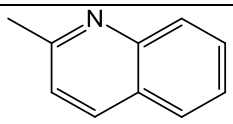	9.09 ± 4.94	0.26 ± 0.004	15.13 ± 0.63	0.03	1.7	58
15	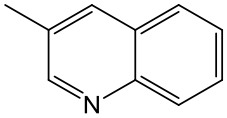	1.13 ± 0.25	0.13 ± 0.02	1.48 ± 0.05	0.12	1.3	11
16	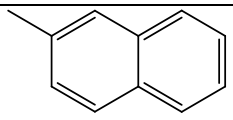	6.22 ± 4.01	0.33 ± 0.02	10.54 ± 1.35	0.05	1.7	32

The Ki values for all three receptors represent the mean ± SEM of 3 independent experiments. [^{3}H] NLX, [^{3}H] DPN, [^{3}H] NTI was used to label the mu, kappa, and delta opioid receptors respectively.

B. Kappa Opioid Receptor

The competitive radioligand binding assay results for the kappa opioid receptor show that the 14-NH-substituted compounds bind the kappa opioid receptor with K_i values in the subnanomolar range. These compounds have higher affinity for the kappa opioid receptor compared to the mu opioid receptor. Unlike the mu opioid receptor, both pyridinyl and quinolinyl substituted naltrexone derivatives bind with similar affinity. Furthermore, the nitrogen in the aromatic ring of these compounds does not seem to affect binding to the kappa opioid receptor. This might be explained by the absence of hydrogen bonding interaction for the heteroaromatic rings of the side chain in the binding pocket of the kappa opioid receptor.

C. Delta Opioid Receptor

The competitive binding assay data for the delta opioid receptor show that these compounds bind the delta opioid receptor with lower affinity compared to both mu and kappa opioid receptors. In general, the pyridinyl substituted naltrexone derivatives had lower affinity compared to the quinolinyl substituted derivatives. Compound **9** of the pyridinyl series and the compound **13** of the quinolinyl series had the lowest affinity for the delta opioid receptor. The nitrogen atom in both of these compounds might be oriented in a specific position that clashes with certain amino acid residue in the delta opioid receptor binding pocket, thus resulting in lowered affinity compared to the other derivatives. Moreover, the compounds in the quinolinyl series might have higher affinity due to their larger side chain reaching deeper in the binding pocket, increasing the potential for a positive interaction in the delta-opioid receptor binding pocket.

3.2 [^{35}S]GTPγS Binding Functional Assay Results

The [^{35}S] GTPγS binding assay was performed to determine the agonist potential of the 14-NH-substituted naltrexone derivatives at the mu opioid receptor. The results of this assay are summarized in **Table 7**. Compounds **9**, **10**, and **13** did not produce any significant stimulation in the functional assay and seem to act as antagonists at the mu opioid receptor. The nitrogen position of the derivative with 2-pyridyl substitution as in compound **9** and 3-isoquinolyl substitution in compound **13** might be in a specific orientation that promotes antagonist activity. A minor stimulation was produced by compounds **11** and **12**. Compound **14** acts as a partial agonist at the mu opioid receptor.

Table 7. The efficacy and potency of 14-NH-substituted naltrexone derivatives in [^{35}S]GTPγS binding functional assay in MOR-CHO cells.

		MOR	
Compd	Side Chain	EC_{50} (nM)	E_{max} (% max of DAMGO)
NTX		0.38 ± 0.10	7.18 ± 0.57
9	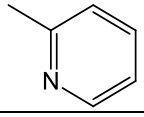	ND[a]	0.90 ± 0.42[b]
10	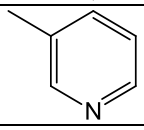	ND[a]	5.09 ± 0.57[b]
11	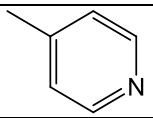	1.67 ± 0.99	7.74 ± 0.69
12	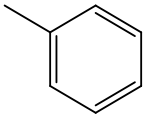	7.20 ± 1.74	5.79 ± 1.35
13	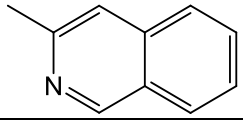	ND[a]	2.84 ± 1.62[b]
14	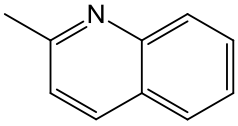	38.85 ± 17.98	34.40 ± 5.43
15	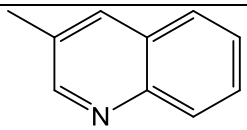	2.81 ± 0.29	15.76 ± 5.61
16	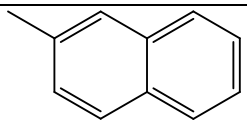	11.13 ± 5.11	16.52 ± 1.97

EC_{50} and E_{max} values represent the mean ± SEM of 3 independent determinations. E_{max} values are normalized to the signal in the presence of 3 µM DAMGO (100% stimulation).

[a] Not determined, dose dependent stimulation was not produced and the data did not fit non-linear regression

[b] percent stimulation produced at the maximum concentration of 10 µM tested, normalized to stimulation produced by 3 µM DAMGO.

4. Molecular Design of Second Generation 14-NH-Substituted Naltrexone Derivatives

The 14-NH-substituted naltrexone derivatives did not retain the mu opioid receptor selectivity of the 14-O-substituted series. The amide linkage in the 14-NH-substituted compounds might be limiting the rotational flexibility of the side chains compared to the ester linkage found in the 14-O-substituted series. The amide bond has a partial double bond character, thus it is more rigid and may be locking the side chains in an unfavorable position. As predicted, the newly synthesized naltrexone derivatives with an amide linkage were more stable than the previous ester-linked compounds and did not suffer from degradation problems.

From the first series of 14-amino naltrexone derivatives, compound **9** was chosen to be the lead compound. Compound **9** had high affinity for both mu and kappa opioid receptors and compared to all other compounds its affinity at the delta opioid receptor was the lowest. Also in the functional assay, it was shown that compound **9** did not possess any agonist activity at the mu opioid receptor. Looking at all the pharmacological assay results, compound **9** was the best choice to further optimize and try to recover the selectivity that the 14-O-substituted series had. It was envisioned that the 14-NH-linked naltrexone derivatives would gain mu opioid receptor selectivity if the side chain was able to rotate freely. As discussed, the only difference between these two series of compounds is the nature of the linkage, one being ester and the other amide, that connects the side chain to the morphinan skeleton.

Three new compounds were synthesized that carry the 2-pyridyl substituent from compound **9** (**Figure 6**). A methylene group was added to the linker to make the side

chain rotationally flexible. The other two compounds have flexible linkers with increasing length in order to see the effect of chain length on affinity and selectivity of these compounds.

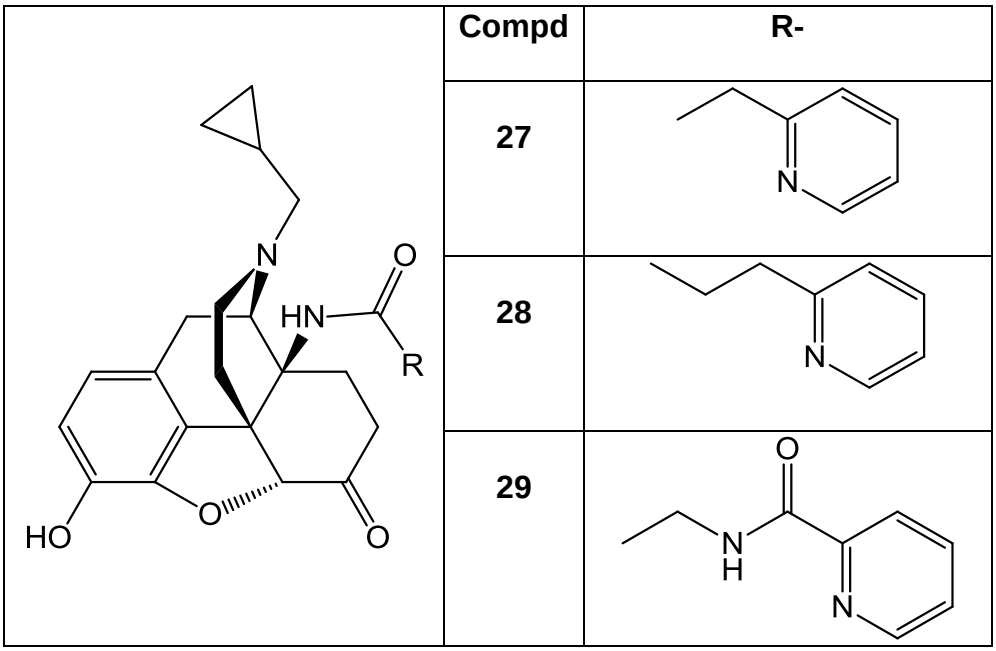

Figure 6. Designed second generation 14-NH-sustituted naltrexone derivatives.

4.1 Chemical Synthesis of Second Generation 14-NH-Substitued Derivatives of Naltrexone

The 14-amino naltrexone intermediate was prepared as discussed previously in **Scheme 1**. The 2-pyridyl acetic acid hydrochloride, side chain for compound **27**, was commercially available from Sigma Aldrich. The second side chain, 3-(pyridine-2-yl)propanoic acid was synthesized from 2-pyridine propanol by reacting it with potassium permanganate in a mixture of sulfuric acid and water (**Scheme 5**). The potassium permanganate, a strong oxidizing agent, was added into the reaction mixture slowly, over a 30 min period. The reaction was stirred for one hour at 80 ºC. After

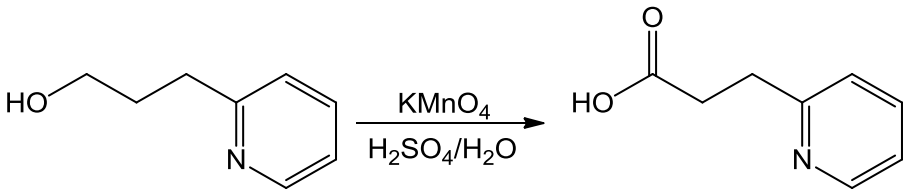

Scheme 5. Synthesis of 3-(pyridin-2-yl)propanoic acid, side chain of compound **28**.

workup, the product was crystallized from hot ethanol as a white solid. The product structure was confirmed by ^{1}H NMR and the reaction yield was 43%.

The side chain for compound **29** was prepared by coupling 2-picolinic acid with glycine ethyl ester hydrochloride using EDC and HOBt as previously described (**Scheme 6**).

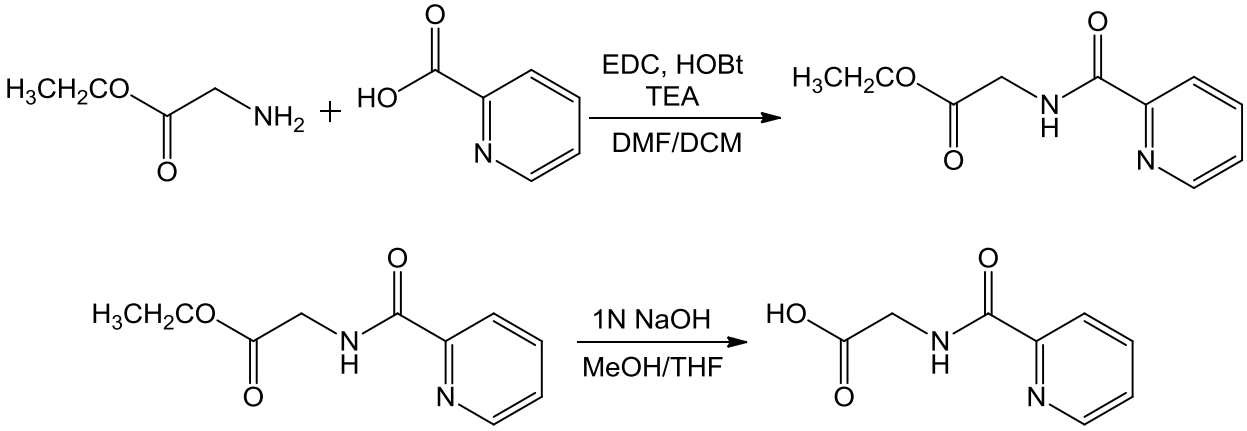

Scheme 6. Synthesis of 2-(picolinamido)acetic acid, side chain of compound **29**.

The alkyl protecting group of the intermediate was hydrolyzed under basic conditions. The product structure was confirmed by ^{1}H NMR and the overall reaction yield was 40%. All side chains were coupled to 14-amine naltrexone using procedure 1 shown in **Scheme 4**. The yields of the coupling reaction are shown in **Table 8**.

Table 8. Coupling reaction percent yield for the second generation of 14-NH-substituted naltrexone derivatives.

Compound	14-NH-heterocyclic Substituent	Procedure	Yield (%)
27	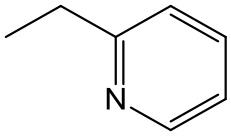	1	43
28	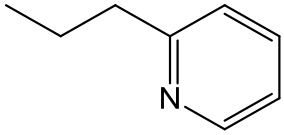	1	38
29	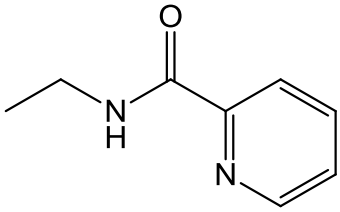	1	37

4.2 Pharmacological Assay Results for the Second Generation 14-NH-Substituted Naltrexone Derivatives

A. Competitive Radioligand Binding Assay Results

The pharmacological assay for the second series of 14-NH-substituted naltrexone derivatives were carried out as previously described. The three new compounds had subnanomolar affinity for both the mu and the kappa opioid receptor (**Table 9**). The introduction of rotational freedom and flexibility for the side chain did not lead to increased selectivity for the mu opioid receptor. Therefore, the rigidity of the linker must not be responsible for the altered selectivity profile of the 14-NH-substituted series of compounds. As the chain length increased to 5 atoms in compound **29**, its affinity for the delta opioid receptor also increased and the selectivity over delta opioid receptor was not maintained. There may be multiple explanations for this: as the

Table 9. The binding affinity and selectivity of the second generation 14-NH-substituted naltrexone derivatives.

		K_i (nM) ± SEM			Selectivity Ratio		
Compd	Side Chain	MOR	KOR	DOR	κ/μ	δ/μ	δ/κ
NTX		0.34 ± 0.03	0.90 ± 0.11	95.46 ± 6.09	2.6	281	106
27	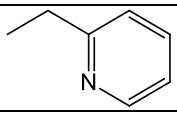	0.29 ± 0.04	0.19 ± 0.03	3.92 ± 0.12	0.66	14	21
28	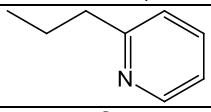	0.32 ± 0.04	0.17 ± 0.02	9.13 ± 0.52	0.53	29	54
29	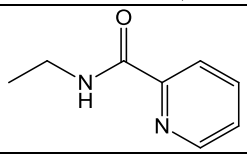	0.30 ± 0.01	0.14 ± 0.01	0.37 ± 0.04	0.47	1.2	3

The Ki values for all three receptors represent the mean ± SEM of 3 independent experiments. [^{3}H] NLX, [^{3}H] DPN, [^{3}H] NTI was used to label the mu, kappa, and delta opioid receptors respectively.

chain length increased, it is possible that the heteroaromatic side chain was placed in a favorable position possibly for a pi-pi stacking or a hydrophobic interaction that was previously unreachable with a shorter linker. Also, it is possible that the glycine linker may be participating in a hydrogen bonding interaction since it has two extra hydrogen bond donor and an acceptor groups compared to the other two side chains. In this series, compound **28** is the only naltrexone derivative that retained some of its dual selective ligand properties. Compound **28** is almost 30-fold more selective for mu opioid receptor over delta and 54-fold more selective for kappa over the delta opioid receptor. However, compared to compound **28**, the lead compound **9** is still a better dual-selective ligand, as it has higher selectivity for mu and kappa over the delta opioid receptor. In general, increasing linker length increased the affinity of the compounds for all three receptors but the selectivity was diminished.

B. [^{35}S]GTPγS Binding Functional Assay Results

The functional assay results are summarized in **Table 10**. The results showed that increasing the linker length of the lead compound by one atom (i.e., three-atom linker) lead to compound **27** having a significant agonist activity at both mu and kappa opioid receptors. Compound **28**, with a chain length of four atoms, acted as an antagonist at both mu and kappa opioid receptors. Further increasing the linker length by one atom lead to compound **29**, which retained antagonist properties at the mu opioid receptor but acted as a partial agonist at the kappa opioid receptor. In addition to the three new second generation compounds, the lead compound **9** was also tested in the [^{35}S]GTPγS functional assay at the kappa opioid receptor. Compound **9** produced substantial stimulation in the functional assay compared to maximal stimulation of U-50488.

Table 10. The efficacy and potency of the second generation 14-NH-substituted naltrexone derivatives in [^{35}S]GTPγS binding functional assay in MOR-CHO and KOR-CHO cells.

		MOR		KOR	
Compd	Side Chain	EC_{50} (nM)	E_{max} (% max of DAMGO)	EC_{50} (nM)	E_{max} (% max of U-50488)
NTX		0.38 ± 0.10	7.18 ± 0.57	2.24 ± 0.73	25.70 ± 5.29
9	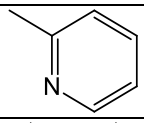	ND[a]	0.90 ± 042[b]	1.74 ± 0.50	24.91 ± 2.02
27	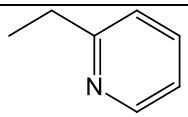	0.15 ± 0.03	77.96 ± 2.66	0.82 ± 0.18	64.88 ± 0.59
28	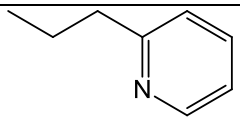	0.32 ± 0.05	12.71 ± 0.20	0.35 ± 0.09	11.55 ± 1.76
29	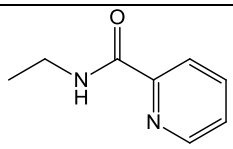	0.41 ± 0.16	11.83 ± 0.39	0.23 ± 0.02	47.90 ± 3.86

EC_{50} and E_{max} values represent the mean ± SEM of 3 independent determinations. E_{max} values at the mu opioid receptor are normalized to the signal in the presence of 3 µM DAMGO (100% stimulation). E_{max} values at the kappa-opioid receptor are normalized to the signal in the presence of 5 µM U-50488 (100% stimulation).

[a] Not determined, dose dependent stimulation was not produced and the data did not fit non-linear regression

[b] percent stimulation produced at the maximum concentration of 10 µM tested, normalized to stimulation produced by 3 µM DAMGO.

5. Preliminary In Vivo Pharmacological Evaluation Results

Based on the in vitro biological assay results, several 14-NH-substituted naltrexone derivatives were sent for in vivo pharmacological evaluation. Specifically, compounds **9**, **10**, and **13** were chosen due to their high affinity for the MOR, selectivity over the DOR, and absence of agonist activity in the [^{35}S]GTPγS functional assay. Initially, these compounds were tested for acute agonistic and antagonistic effects in mice. The 14-NH-substituted naltrexone derivatives were assessed for their ability to produce antinociception and to antagonize the antinociceptive effects of morphine in the mouse tail immersion assay. As shown in **Table 11**, all three compounds were found to be potent antagonists of morphine and did not produce any agonist effect themselves in this test. The in vivo assay results support the in vitro functional assay data for these compounds.

Table 11. AD_{50} Values for Antagonizing Morphine (10 mg/kg) Antinociception in Warm-Water Tail Immersion Assay.

Compd	AD_{50} values (mg/kg) for blockade of morphine antinociception
9	0.25
10	0.55
13	0.87

Additionally, these compounds were characterized in the comparative opioid withdrawal precipitation study. In chronically morphine exposed mice, the well-known opioid antagonists naltrexone and naloxone precipitate acute withdrawal symptoms upon administration. The withdrawal symptoms are manifested as jumps and wet dog

shakes in mice. It is hypothesized that inverse agonists with higher negative intrinsic activity at the mu opioid receptor will precipitate more vigorous withdrawal signs.[76] In this study, withdrawal symptoms produced in morphine pelleted mice by three different doses of the naltrexone derivatives were compared with that of naltrexone and naloxone (**Figures 7** and **8**). Compound **9** at a dose of 3 mg/kg precipitated jumps more than compared to both naloxone and naltrexone. Interestingly, lower and lower numbers of jumps were counted as the dose increased to 10 and 30 mg/kg. On the other hand, at a dose of 3 mg/kg, compound **9** only slightly precipitated wet dog shakes compared to the traditional antagonists. At the lowest dose of 3 mg/kg tested, compound **10** failed to precipitate any opiate withdrawal signs. As the dose increased, compound **10**

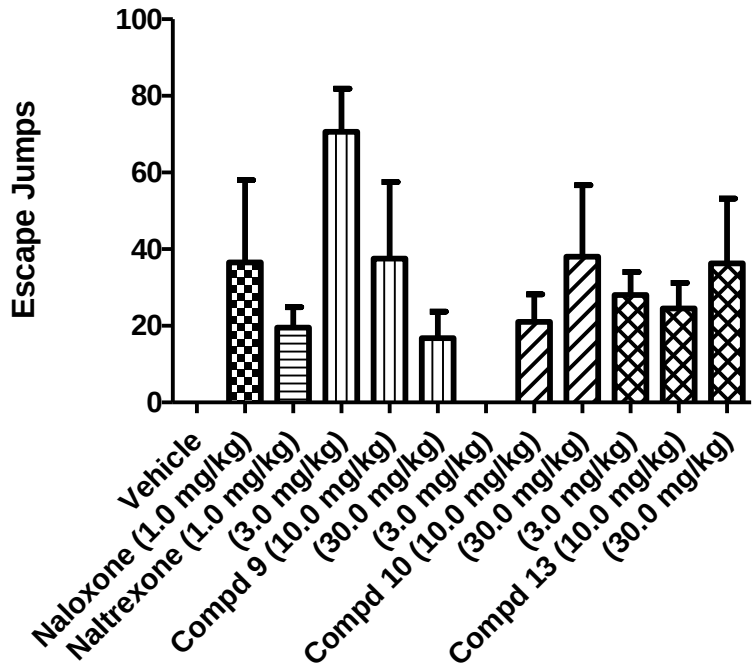

Figure 7. Naltrexone derivatives in comparative withdrawal assay in chronic morphine exposed mice: Escape jumps.

apparently precipitated both withdrawal symptoms. Compound **13**, dose dependently increased the number of wet dog shakes observed. At all doses tested, compound **13** precipitated escape jumps comparable to naloxone (1.0 mg/kg).

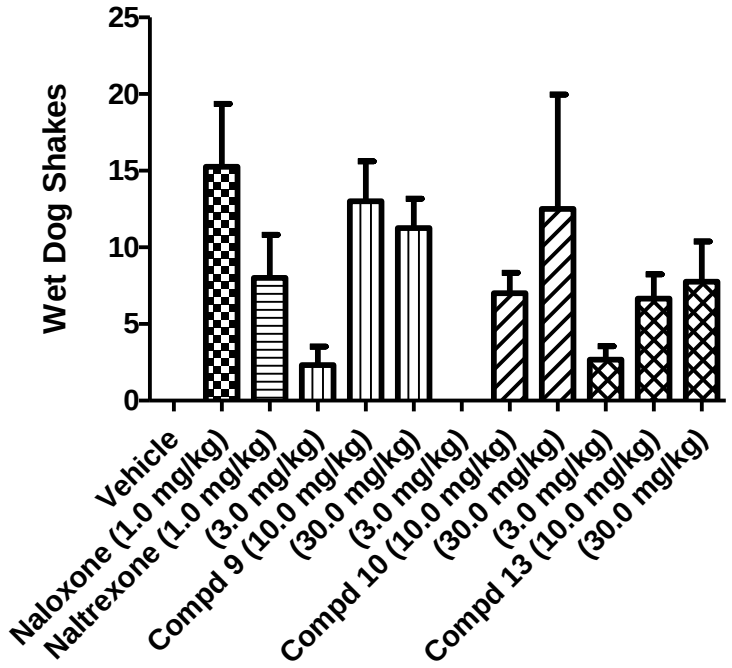

Figure 8. Naltrexone derivatives in comparative withdrawal assay in chronic morphine exposed mice: Wet dog shakes.

6. Molecular Modeling Study of the 14-Substituted Naltrexone Derivatives

A computational docking study was conducted on both series of 14-O-substituted and 14-NH-substituted naltrexone derivatives in order to analyze their interaction with the opioid receptors. Despite the small difference between these two series of compounds, namely in the nature of the linker that is holding the heteroaromatic side chains, their experimental radioligand binding assay results differ quite substantially. The 14-O-substituted series of compounds seemed to be mu opioid receptor selective, but when the ester linkage was replaced with an amide linkage in the 14-NH-substituted naltrexone derivatives, the selectivity profile of the novel compounds was altered.

6.1 Dynamics Simulation of Lead Compounds

Before the docking study, lead compounds from both series (compound **1** and compound **9**) were subjected to short dynamics simulations to determine if their lowest energy conformations might differ from each other. Using the molecular modeling package Sybyl 8.1, both compounds were placed in a water box and the dynamics simulation was run. As expected, the results show that the lowest energy conformations of both molecules are virtually identical, with the only difference being one extra hydrogen in compound **9** (**Figure 9**).

6.2 Computational Docking Studies of 14-Amino Naltrexone Derivatives

For the docking study, 8 compounds of the 14-O-substituted series and all 11 compounds from the 14-NH-substituted series were docked into the crystal structures of all three opioid receptors. By comparing the docking modes of these two series of

compounds, it may be possible to determine a reason for the differing selectivity profiles. All ligands used in the docking study were built with standard bond lengths and

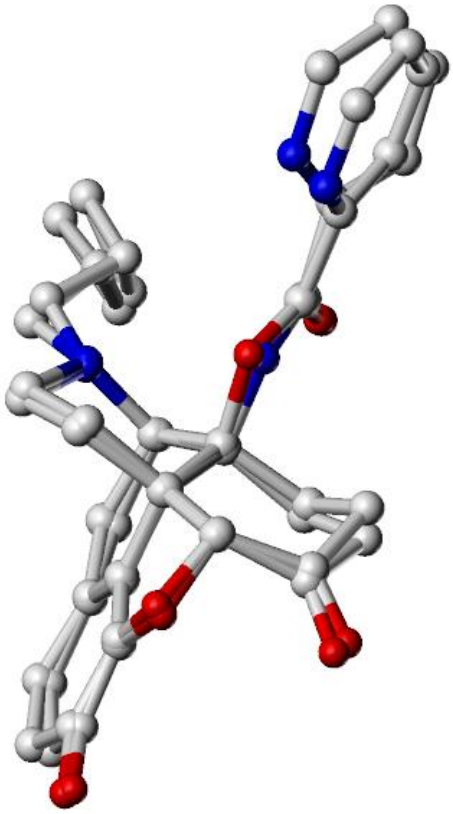

Figure 9. The lowest energy conformations of compound **1** and compound **9** obtained after a dynamics simulation. Carbon atoms are shown in white, oxygen atoms are shown in red, and nitrogen atoms are shown in blue.

angles using the molecular modeling software SYBYL 8.1. The small molecules were assigned Gasteiger-Huckel charges and energy minimized with the Tripos Force Field (TFF). The 19 ligands that were used in this study were docked into all three opioid receptor crystal structures using GOLD 5.1. For the docking study, the binding site of the receptor was defined to be all atoms within 15 Å radius of an oxygen atom on an Asp residue that is conserved in all opioid receptors. The compounds were docked 40

times each with standard GOLD parameters. The docked poses were scored using both CHEMPLP and the standard GOLD fitness score.

A. 14-Substituted Naltrexone Derivatives Docked into the Mu Opioid Receptor Crystal Structure

The crystal structure of the mu opioid receptor was solved in an inactive state bound to the irreversible antagonist β-FNA.[47] The binding site for the docking was defined to be all atoms in a volume of 15 Å radius of oxygen atom OD2 on Asp147$^{3.32}$. Furthermore, a 4 Å distance constraint was set between this Asp 147$^{3.32}$ oxygen atom and the positively charged nitrogen atom at the 17-position of the naltrexone derivatives. The Asp residue is conserved in all three opioid receptors and it functions as a critical anchor for a strong charge-to-charge interaction with the basic moiety in opiate compounds. The best scored binding modes of two representative compounds of each series, compound **1** and compound **9** are shown in **Figure 10**. The naltrexone derivatives appear to bind in a very similar manner to β-FNA in the mu opioid receptor binding pocket probably due to their identical “message” components. All the major interactions that were observed in the binding of β-FNA were also present in the model binding of the naltrexone derivatives to the mu opioid receptor. The positively charged 17-position nitrogen of the naltrexone derivatives forms a salt bridge with the Asp147$^{3.32}$ and Tyr 148$^{3.33}$ makes a hydrogen bond to the D-ring oxygen. The cyclopropyl group seems to be participating in a nonpolar interaction with the aromatic residues Tyr326$^{7.43}$ and Trp293$^{6.48}$. Trp$^{6.48}$ is conserved in most GPCRs and it is thought to be a key residue responsible for the activation of the receptor.[68]

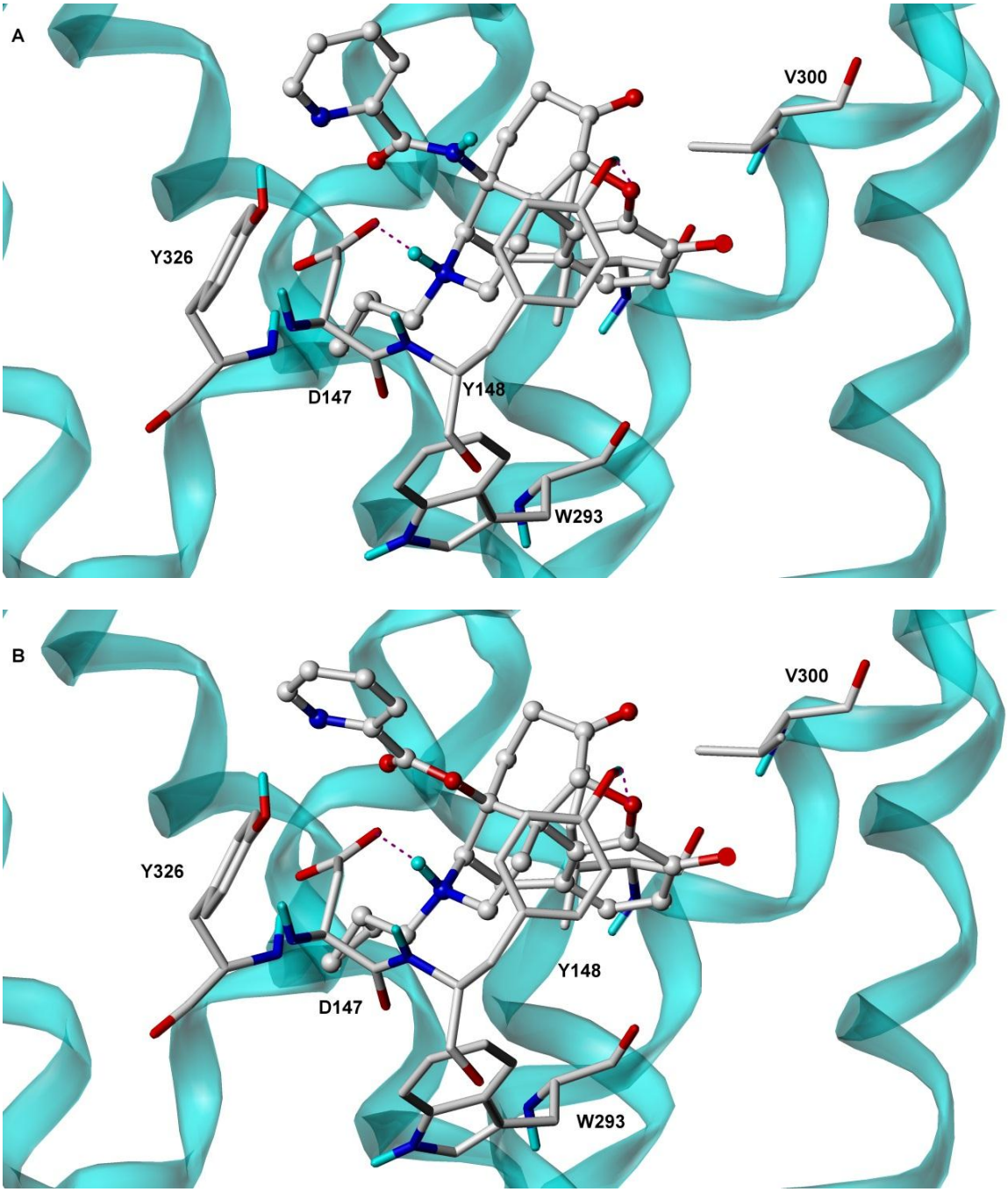

Figure 10. Comparison of binding modes of compound **9** (A) and compound **1** (B) docked into the MOR binding site. MOR transmembrane helices are shown in cyan, important amino acid residues are rendered as capped-stick, and the docked ligand is shown in ball-stick representation.

In all three opioid receptors, $Trp^{6.48}$ interacts with the cyclopropyl methyl group at the 17-position of naltrexone derivatives. The bulky nonpolar substituents at this position,

i.e., cyclopropyl and allyl groups of the opioid antagonists, may interact with the Trp$^{6.48}$ residue and lock it in an inactive conformation. The smaller 17-methyl group of the agonists may be too far to interact with Trp$^{6.48}$ to lock it in position, thus leading to the activation of the receptor. From the docking study, both compounds **1** and **9** seem to bind in a very similar manner. Although compound **9** has one extra hydrogen bond donor that can interact with Asp147$^{3.32}$ compared to compound **1**, the amide hydrogen was not shown to be participating in an H-bonding interaction in the docking results for the mu opioid receptor. Also the side chains of both series of compounds were not interacting with the putative "address" residue of the mu opioid receptor Trp318$^{7.35}$. In fact, the side chains were pointing in the opposite direction away from Trp318$^{7.35}$ and were positioned in a large cavity with no apparent interactions present. The discrepancy between the original computational modeling study and the current docking study is likely explained by the fact that the original study used a homology model of MOR based on the bovine rhodopsin structure, which was the only GPCR crystal structure available at the time.

B. 14-Substituted Naltrexone Derivatives Docked into the Kappa Opioid Receptor Crystal Structure

The crystal structure of the kappa opioid receptor was solved in an inactive state in complex with the selective antagonist JDTic.[48] The binding site for the docking was defined to be all atoms in a volume of 15 Å radius around oxygen atom OD1 on Asp138$^{3.32}$. Furthermore, a 4 Å distance constraint was set between the Asp138$^{3.32}$ oxygen atom and the positively charged nitrogen atom at the 17-posititon of the

naltrexone derivatives. The best scored docking results for two representative compounds of each series are presented in **Figure 11**. The important anchor residue of

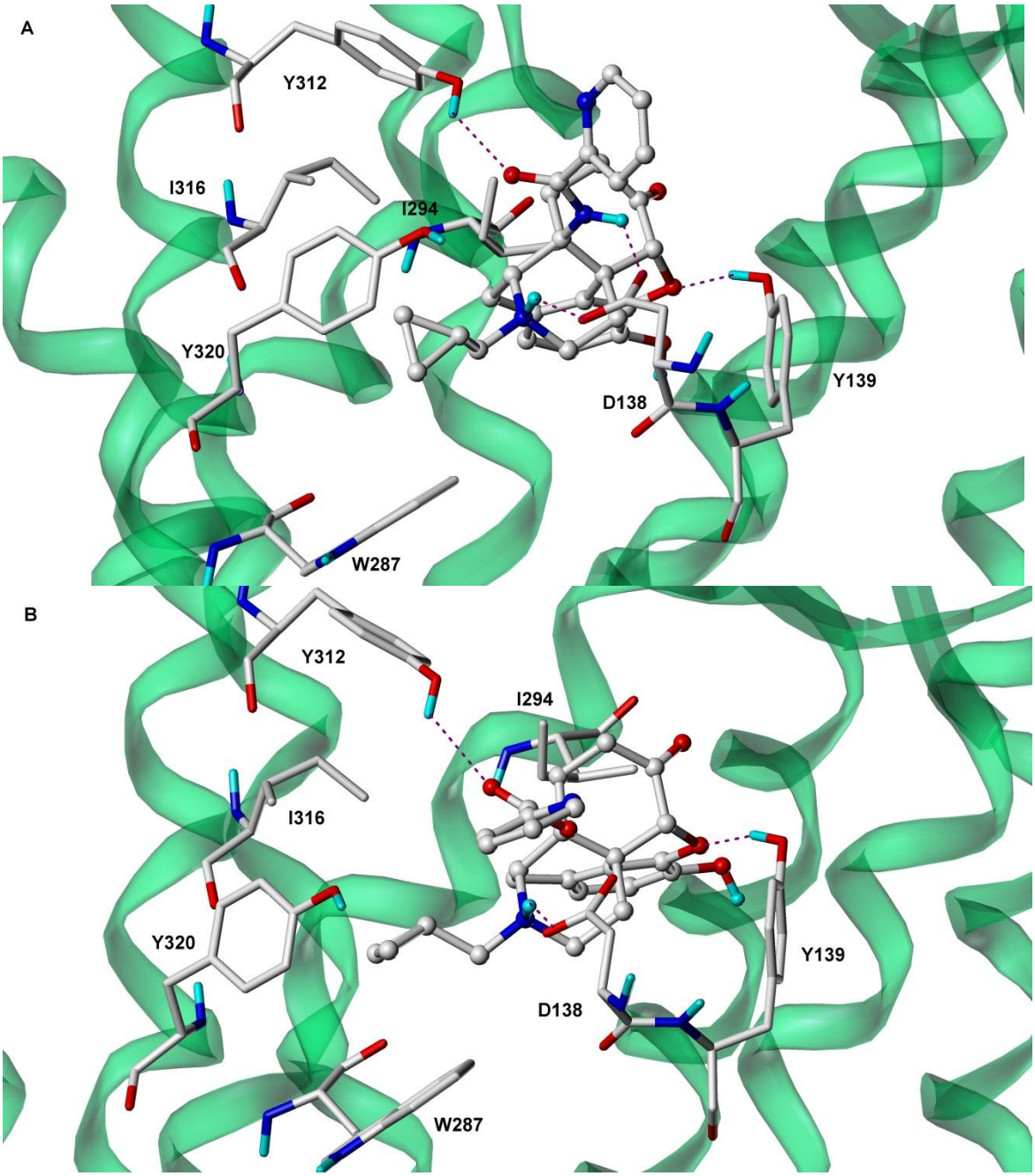

Figure 11. Comparison of binding modes of compound **9** (A) and compound **1** (B) docked into the KOR binding site. KOR transmembrane helices are shown in green-blue, important amino acid residues are rendered as capped-stick, and the docked ligand is shown in ball-stick representation.

the kappa opioid receptor Asp138$^{3.32}$ interacts with both the 17-position nitrogen and the amine at the 14-position of compound **9**. While the lead compound of the 14-O-heterocyclic substituted naltrexone derivatives, compound **1** only has one interaction with Asp138$^{3.32}$. Moreover, in the kappa opioid receptor binding site, Tyr312$^{7.35}$ hydrogen bonds to the amide carbonyl of both series of naltrexone derivatives. It is important to note that Tyr312$^{7.35}$ is one of the four non-conserved amino acid residues in the binding pocket of the kappa opioid receptor that interacts with JDTic and thought to contribute to its subtype selectivity. Tyr312$^{7.35}$ was shown to hydrogen bond to amide carbonyl found in JDTic, while the corresponding Trp$^{7.35}$ and Leu$^{7.35}$ found in mu and delta opioid receptors respectively does not participate in this critical polar interaction.[48] Therefore, compared to mu opioid receptor docking results, there are two additional polar interactions in the binding site of the kappa opioid receptor for the 14-NH-substituted series of naltrexone derivatives. Asp138$^{3.32}$ makes one extra hydrogen bond to amine at the 14-position and the unique Tyr312$^{7.35}$ residue not found in other related opioid receptors, interacts with the carbonyl group of the linker. These computational docking results may explain why the 14-NH-substituted series of compounds have high affinity for the kappa opioid receptor and have lost their selectivity for mu opioid receptor. Additional interactions in the KOR binding site include a hydrophobic interaction between Ile294$^{6.55}$ and ring C of naltrexone. The side chain of Tyr139$^{3.33}$ hydrogen bonds to furan oxygen. Amino acid residues Tyr320$^{7.43}$ and Trp287$^{6.48}$ seem to participate in a nonpolar interaction with the cyclopropylmethyl group of the naltrexone derivatives. It is postulated that the opioid antagonists block the activation related conformational changes in the Trp$^{6.48}$, thus locking the receptor in an

inactive state.

C. 14-Substituted Naltrexone Derivatives Docked into the Delta Opioid Receptor Crystal Structure

The crystal structure of the delta opioid receptor was solved in an inactive state in complex with the selective antagonist naltrindole.[49] The binding site for the docking was defined to be all atoms in a volume of 15 Å radius around oxygen atom OD2 on Asp128$^{3.32}$. For the docking study, a 4 Å distance constraint was set between the Asp128$^{3.32}$ oxygen atom and the positively charged nitrogen atom at the 17-posititon of the naltrexone derivatives. The best scored docking results for two representative compounds of each series are presented in **Figure 12**. As expected the Asp128$^{3.32}$ makes an ionic interaction to the 17-position nitrogen of naltrexone scaffold in both series of compounds, while the 14-NH-substituted derivatives also have an additional hydrogen bond between Asp128$^{3.32}$ and the amide at the 14-position. This extra interaction between naltrexone derivatives with an amide linker and the Asp128$^{3.32}$ of the delta opioid receptor may explain their increased affinity for the DOR compared to the compounds with an ester linkage. Otherwise, both series of compounds were docked virtually in the same manner in the delta opioid receptor binding pocket and shared the same interactions. The amino acid residue Tyr129$^{3.33}$ hydrogen bonds to the furan oxygen of naltrexone. Ile277$^{6.51}$ has a nonpolar interaction with the naltrexone derivatives. The cyclopropylmethyl group at the 17-position of both series of compounds seems to interact with Tyr308$^{7.43}$ and Trp274$^{6.48}$. The side chains at the 14-position of these compounds occupy a large cavity not in contact with any residues. The amino acid residue Leu125 seems to be closest to the side chain. As the linker

length increased in compounds **27**-**29**, the pyridine side chain might have gotten close to the Leu125 for a positive nonpolar interaction.

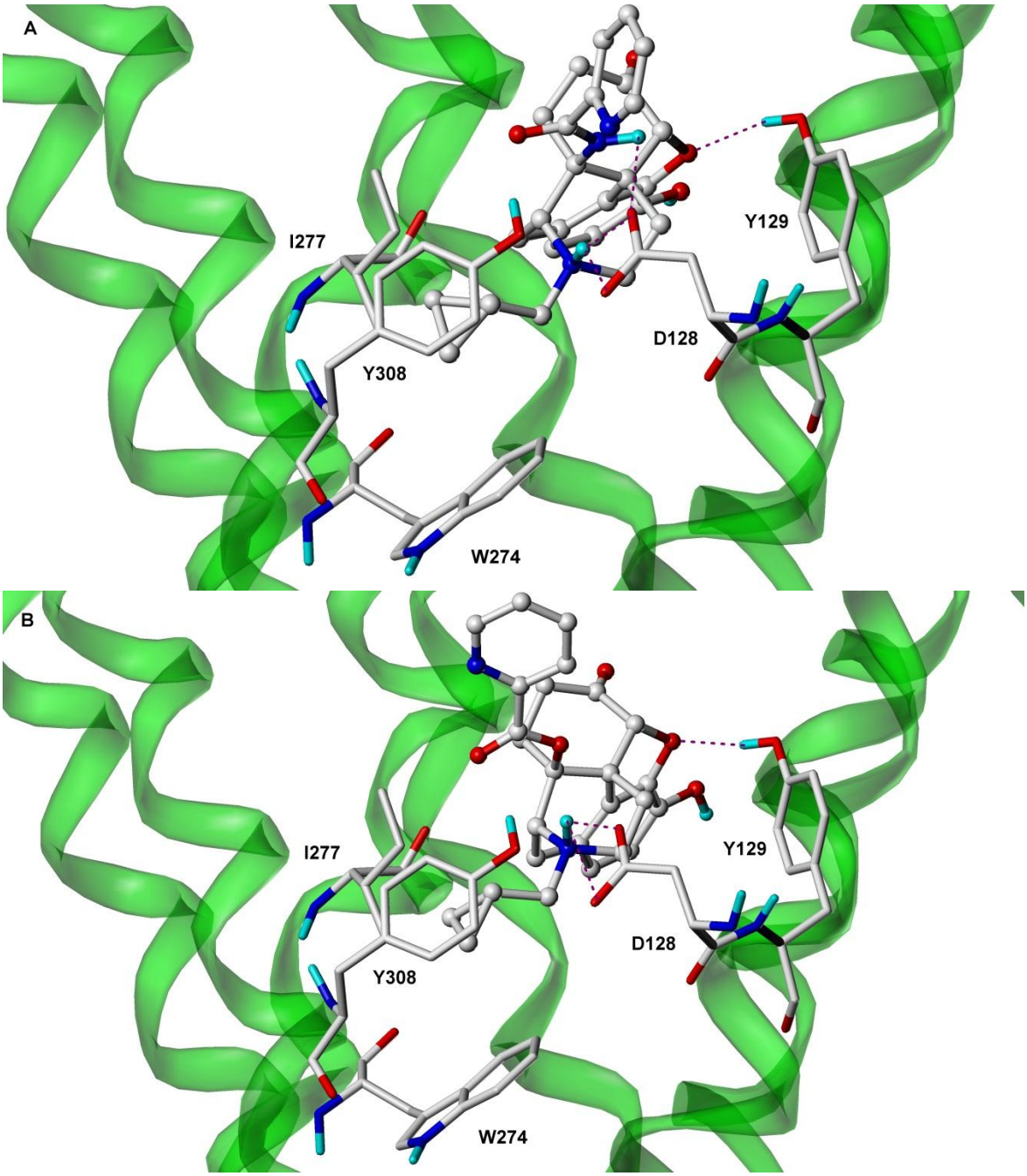

Figure 12. Comparison of binding modes of compound **9** (A) and compound **1** (B) docked into the DOR binding site. DOR transmembrane helices are shown in green, important amino acid residues are rendered as capped-stick, and the docked ligand is shown in ball-stick representation.

7. MOR and KOR Dual-selective Antagonists and Possible Implications in Drug Dependence and Addiction

Synthesis and biological evaluation of a series of 14-NH-substituted naltrexone derivatives led to the identification of two lead compounds as MOR and KOR dual-selective antagonists (**Figure 13**). Compound **9**, as a dual-selective antagonist, is about 60-fold more selective for the MOR and KOR over the DOR. Furthermore, compound **9** was shown to be a mu opioid receptor antagonist in both in vivo and in vitro assays. In the KOR [^{35}S]GTPγS functional assay, the E_{max} of compound **9** was slightly higher than that of compound **28**. Conversely, compound **28** has very high affinity for both MOR and KOR, but its selectivity over the DOR is low compared to compound **9**. Notably, compound **28** was shown to be an antagonist at both MOR and KOR in the in vitro functional assay. In vivo pharmacological evaluations have yet to be performed on compound **28**.

The unique MOR and KOR dual-antagonist nature of these compounds may be more advantageous than current naltrexone therapy for opioid dependence, although compounds with this particular pharmacological profile have not been described in the literature as possible therapeutics for drug addiction. Individually, MOR antagonists are well established as effective treatment option for various addictions.[77-79] Recently there is growing evidence that implicates the dynorphin/kappa opioid receptor system as an important modulator in the neurobiology of drug addiction and dependence. Additionally, kappa opioid receptor antagonists might be effective therapeutics in curbing drug craving and preventing relapse in abstinence therapy.

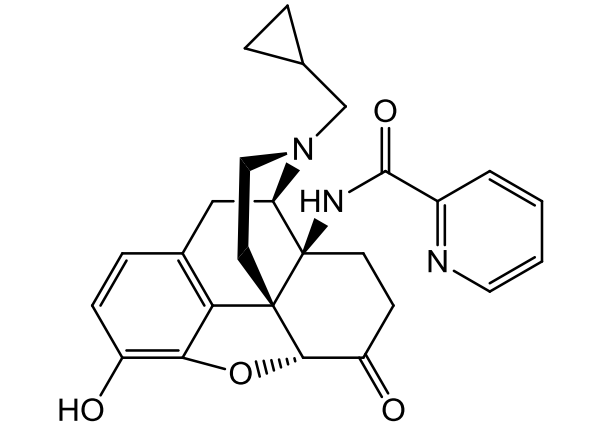

9

K_i (nM) ± SEM		
MOR	KOR	DOR
1.51 ± 0.34	0.36 ± 0.11	94.54 ± 6.09

MOR Agonist Activity	
EC_{50} (nM)	E_{max}
ND	0.90 ± 0.42

KOR Agonist Activity	
EC_{50} (nM)	E_{max}
1.74 ±0.50	24.91 ± 2.02

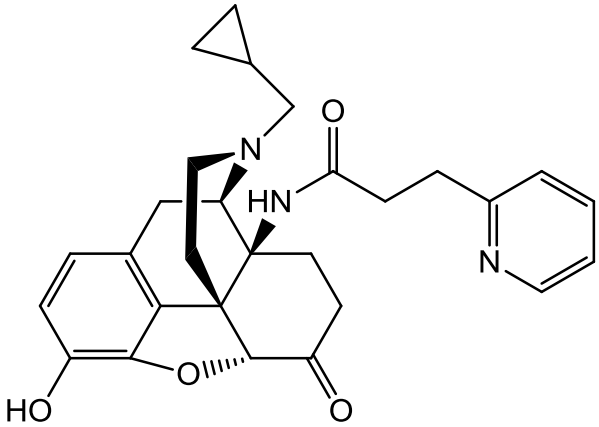

28

K_i (nM) ± SEM		
MOR	KOR	DOR
0.32 ± 0.04	0.17 ± 0.02	9.13 ± 0.52

MOR Agonist Activity	
EC_{50} (nM)	E_{max}
0.32 ± 0.05	12.71 ± 0.20

KOR Agonist Activity	
EC_{50} (nM)	E_{max}
0.35 ± 0.09	11.55 ± 1.76

Figure 13. Possible mu-kappa opioid receptor dual selective antagonist lead compounds and their in vitro pharmacological assay results summary.

Chronic stress is well known to induce despair and increase the risk of mood disorders and drug abuse. There are two major families of stress neuropeptides that have been identified, the corticotropin-releasing factor (CRF) and the dynorphins.[80] Dynorphins are endogenous opioid peptides that arise from the cleaving of prodynorphin precursor protein. Dynorphins are mostly selective for the kappa opioid receptor and have widespread distribution in the CNS including areas of the

dopaminergic nigrostriatal and mesolimbic-mesocortical systems.[81] KOR and dynorphin peptides play an important role in the modulation of reward to natural reinforcers and to various drugs of abuse, presumably through modulation of basal and reward/drug-induced changes in dopaminergic tone. The release of dynorphins and the activation of KOR mediate dysphoria and anhedonia associated with drug withdrawal, stress-induced aversion states, and stress-induced relaple-like behavior.[82]

The dynorphin/KOR system was found to play a major role in the stress response affecting the reinforcing properties of cocaine. It was found that repeated swim stress before cocaine conditioning significantly enhanced subsequent place preference to cocaine-paired compartment in wild-type mice, while stress did not affect conditioned place preference in mice pretreated with the KOR antagonist norBNI or mice with prodynorphin gene disruption.[83] In addition, the KOR selective agonist U50,488 mimicked stress exposure and significantly potentiated cocaine conditioned place preference.[83] The results from this study indicate that repeated stress exposure induced the release of endogenous dynorphins which activated the kappa opioid receptors and subsequently enhanced the rewarding properties of cocaine.[84] Later, the same research group investigated the role of KOR/dynorphin in animal models of relapse that identified triggers for reinstatement of drug self-administration. It was shown that stress exposure and the KOR agonist U50,488 all effectively reinstated cocaine-seeking behavior in mice previously conditioned to cocaine. Stress-induced reinstatement was completely blocked by norBNI and was not evident in KOR or dynorphin knockout mice.[84]

The KOR/dynorphin system was also shown to be implicated in dependence and addiction of other drugs of abuse including heroin, alcohol, and nicotine.[80-82,85] Although it is clear that this stress-related system modulates the rewarding effects of addictive drugs, the underlying neurobiological mechanism is still not well understood. However, most addicting drugs seem to ubiquitously affect the dopamine mesolimbic reward system directly or indirectly, acutely increasing dopamine levels. The increased neurotransmitter release in this brain region is thought to be responsible for the initial euphoric and rewarding effects of many drugs of abuse. All three opioid receptors are expressed in this region and play distinctly different roles. The chronic administration of drugs (e.g., cocaine, heroin, alcohol) is known to upregulate the cAMP pathway in the NAc, one part of the brain reward circuit, and the activation of CREB, a transcription factor, which leads

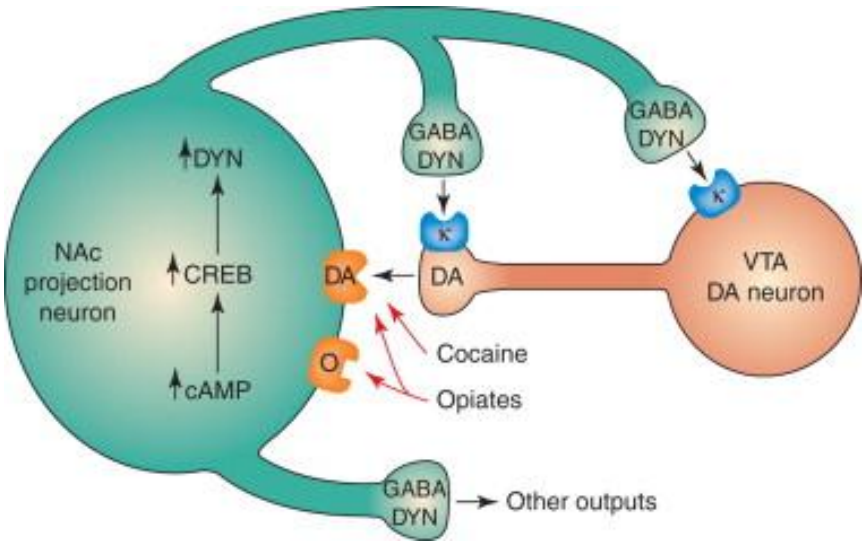

Figure 14. Regulation of CREB by drugs of abuse. DYN acts as a negative feedback mechanism in this circuit. Chronic exposure to various drugs of abuse upregulates this pathway.[86]

to the expression of genes encoding various proteins and neurotransmitters including dynorphins.[86] It has been shown that stress and chronic drug exposure enhances dynorphin expression and KOR signaling.[82] As mentioned above, activation of KOR leads to a diminishing of neurotransmitter release. Decreases in reward neurotransmitters have been hypothesized to lead to the negative motivational state associated with acute drug abstinence and long-term biochemical changes that contribute to the vulnerability to relapse.[87]

The acute dopaminergic stimulation in the mesolimbic reward region caused by addictive substances and the activation of the counter-modulatory KOR/dynorphin response seems to be responsible for the euphoric and dysphoric cycles of drug addiction/dependence. The dysphoric state coupled with potential neuropsychiatric comorbidity of anxiety and depression caused by this system may lead to compulsive, uncontrollable drug seeking behavior in an addicted individual compromising his progress towards abstinence. Therefore, the beginning period of an abstinence program may be a possible point of therapeutic intervention for MOR and KOR dual-antagonists. As reported, in animal models of relapse, KOR antagonist norBNI completely blocked stress- and KOR agonist-induced reinstatement in mice previously conditioned to cocaine.[84] Furthermore, depressant-like or anhedonic effects observed after stress exposure or during drug withdrawal can be blocked by KOR antagonists.[88,89]

Ideally, the MOR-KOR dual-antagonists will find utility in opioid dependence including heroin and prescription opioid analgesics, which is becoming a growing problem in this country, but may also be used for treating other addictions. The KOR antagonist component will block the dysphoric and anxiolytic effects of chronic

withdrawal thus decreasing the chance of relapse. While the MOR antagonist component will work to inhibit the euphoric effects of exogenously administered opiates if a relapse does occur. In the absence of the euphoric and rewarding effects of the illicit drug, the individual may possibly cease the drug seeking behavior. It is granted that this dual-antagonist approach to drug dependence/addiction has not yet been validated or even formally proposed. Nevertheless, the clinical utility of the individual MOR and KOR antagonists in this field has been thoroughly established.

Currently, naltrexone is the only opioid antagonist that is being used for alcohol and opioid dependence. Its use in this regard has been hampered by poor patient compliance, mainly due to its dysphoric and unpleasant side effects possibly caused by its partial agonist activity at the KOR.[23,79] The MOR-KOR dual-antagonist approach that is being proposed here has two presumed advantageous over naltrexone. First of all, the dual-antagonist will have no partial agonist activity at KOR, which might improve compliance. Secondly, the KOR antagonist component missing in naltrexone will function as an anti-depressant and anxiolytic thus decreasing the chance of relapse.

The two compounds that are presented here are lead compounds toward MOR and KOR dual-antagonists. As such, their pharmacological profile may need to be improved. Although compound **9** has modest selectivity over DOR, its E_{max} at the KOR is comparable to that of naltrexone. On the other hand, compound **28** is an antagonist at both MOR and KOR but it lacks high selectivity over DOR. Structure activity relationship studies need to be conducted in order to improve these parameters. Looking at the three second generation naltrexone derivatives, the side chain of compound **28** seems to ideal, since either increasing or decreasing the chain length

decreases selectivity over DOR and increases KOR agonist activity. Introducing rotational flexibility to the side chain of compound **9** by selectively reducing the amide carbonyl group or by using a different coupling method to link the side chain may decrease its KOR agonism. The 14-position amino group seems to be partly responsible for the increased affinity of these compounds for the KOR, thus should not be altered in future studies.

IV. Conclusion

Crude opium extracted from the unripe seedpods of the poppy flower have been used for medicinal purposes for centuries. The main active ingredient in opium, morphine, was isolated in 1806. The physiological targets of morphine and other opioids in the CNS were identified with the advent of radioligand binding techniques and highly selective ligands for each receptor. Soon after, endogenous opioid peptides were discovered and identified. The understanding of the endogenous opioid system was further elevated with the cloning of mu, delta, and kappa opioid receptor in the early 1990s.

The strong pain-relieving characteristics of opioids are well established. Therefore, opioid analgesics are the most popular treatment options for various kinds of pain. Unfortunately, these compounds produce many undesirable side effects including respiratory depression, sedation, constipation, tolerance, and dependence. All clinically significant opioid analgesics are mu opioid receptor agonists. It is known that the mu opioid receptor is responsible for the analgesic and addictive effects of morphine. Since many of the side effects associated with the clinical administration of opioids are mediated by the mu opioid receptor, compounds that are selective antagonists at the MOR may serve as valuable research tools or as potential therapeutics.

Historically, opioid antagonists have been instrumental in identification and characterization of opioid receptors. Naltrexone is a well-known opioid universal antagonist that was developed by NIDA. It is a reversible antagonist that blocks the euphoric effects of exogenously administered opioids and diminishes their reinforcing

effects. Naltrexone itself does not possess any addictive potential or lead to tolerance after repeated administration. As such, it was approved by the FDA for the treatment of alcohol and opioid dependence. Due to its undesirable side effects and poor patient compliance, the use of naltrexone for this purpose is severely limited. These dysphoric side effects may be caused by its partial agonist activity at the kappa opioid receptor. Nevertheless, the naltrexone structural scaffold has been widely utilized for the development of many important opioid antagonists.

β-FNA and clocinnamox are selective irreversible antagonists for the mu opioid receptor that structurally resemble naltrexone. They have limited utility in opioid research since they bind covalently to the receptor. CTOP and CTAP are highly selective reversible peptidyl antagonists at the mu opioid receptor. Due to their peptide nature, they may undergo metabolic inactivation rapidly. Therefore, the development of a non-peptide, highly selective, and reversible antagonist for the mu opioid receptor is still highly desirable.

The “message-address” concept may be applied to the MOR in order to develop highly selective, small molecule antagonists. Portoghese et al. successfully utilized the “message-address” concept previously and developed highly selective ligands for the KOR and the DOR (e.g. GNTI and NTI). Introduction of specific chemical moieties onto the naltrexone scaffold, designed to interact with the mu opioid receptor “address” site, may lead to the synthesis of selective antagonists. Recently, the “message-address” concept was adopted in our lab and lead to the identification of two 6α- and 6β-N-heterocyclic substituted naltrexamine (NAP and NAQ respectively) derivatives as lead

compounds for the development of MOR selective antagonists. Both compounds were assessed to be potent and highly selective for the MOR in pharmacological assays.

Further manipulation of the naltrexone structure, ideally at a different position, based on the “message-address” concept may lead to the discovery of more favorable lead compounds with a unique pharmacological profile. As opioid abuse becomes a growing problem, these compounds will be essential for the study of MOR function in drug abuse and addiction.

The current project involved the design, synthesis, and biological evaluation of non-peptide, selective, reversible antagonists for the mu opioid receptor. The novel ligands were designed based on the lead compound that was identified in the lab. Previously, a series of 14-O-heterocyclic substituted naltrexone derivatives were synthesized in our lab. The heteroaromatic moieties at the 14-position of these compounds were designed to interact with the aromatic binding locus formed by the EL2 and EL3, the putative “address” site of the mu opioid receptor. The in vitro biological assays revealed that the lead compound **1** had high affinity for the MOR and approximately 800-fold selectivity over the DOR and 200-fold selectivity over the KOR. These results validated the rationale of using “message-address” concept for the development of selective antagonists for the MOR. Regrettably, the 14-O-substituted naltrexone derivatives were found to be metabolically unstable. In order to make these compounds more stable, the ester linkage was replaced by an amide linkage. Therefore, 8 new compounds were synthesized that contained an amide bond at the 14-position of naltrexone that linked it to the heteroaromatic side chains.

Since the 14-amino naltrexone is not commercially available, it was synthesized from thebaine in multiple steps. Although the synthetic methods were previously reported, some difficulties were encountered, especially in the dealkylation reaction using the reagent DEAD and the O-demethylation reaction. Some alternative reactions were researched to accomplish these transformations but ultimately the original methods provided the product. In order to synthesize the final compounds, the side chains were introduced into the morphinan skeleton using either of two different coupling methods: the acid chloride of the side chain was directly coupled to the 14-position amine or the carboxylic acid of the side chain was coupled using the peptide coupling reaction.

The final compounds were then tested in a competitive radioligand binding assay at the MOR, KOR, and DOR using [^{3}H] NLX, [^{3}H] DPN, and [^{3}H] NTI to label the receptors respectively. The [^{35}S]GTPɣS assay was employed to determine the relative efficacy of these compounds at the MOR. The competitive binding assay results show that the naltrexone derivatives with the amide linkage to various heterocyclic aromatic rings have a subnanomolar to nanomolar affinity for the mu opioid receptor. Surprisingly, compared to the 14-O-substituted series of compounds, the 14-NH-substituted derivatives were no longer selective for the MOR over the KOR. In the functional assay, every compound in the series was found to be an antagonist at the MOR, except compound **14** which seems to be a partial agonist. These compounds seemed to be MOR-KOR dual selective ligands.

From this series of compounds, compound **9** was chosen to be the lead compound, since it had the highest selectivity over the DOR and it was shown to be a

mu opioid receptor antagonist. It was hypothesized that the limited rotational flexibility brought on by the amide linkage in the 14-NH-substituted compounds might be detrimental to MOR selectivity compared to the ester linkage found in the 14-O-substituted series. In order to test this hypothesis, three new compounds were synthesized. These compounds had an amide linkage that increased in length and were freely rotatable which carried the heteroaromatic ring found in compound **9**. In vitro pharmacological assay results revealed that the newly synthesized naltrexone derivatives had high affinity for both the MOR and KOR. The introduction of rotational freedom and flexibility for the side chain did not increase selectivity for the MOR. Additionally, these compounds were tested in the [^{35}S]GTPγS functional assay for the MOR and KOR. It was shown that compound **28** was a neutral antagonist at both MOR and KOR.

A computational docking study was conducted on both 14-O- and 14-NH-substituted naltrexone derivatives in an attempt to explain the discrepancies found in the biological assay results of these two series of compounds. The lead compound of the ester-linked series had high selectivity for the MOR, while the lead compound of the amide-linked series had no selectivity for the MOR; in fact it binds to the KOR with higher affinity. For the docking study, all 19 compounds were docked into the crystal structures of all three opioid receptors. The naltrexone derivatives bind to all receptors in a similar manner and participate in the major interactions that are well established for opioids. Namely, the positively charged 17-position nitrogen atom of all compounds participate in an ionic interaction with a conserved Asp residue and a conserved Tyr residue hydrogen bonds to the furan oxygen of these derivatives. The methyl

cyclopropyl group of all compounds participates in an important nonpolar interaction. However, a major difference between the docking results of the 14-O-substituted and 14-NH-substituted naltrexone derivatives for the KOR and DOR was observed. In these two receptors, the conserved Asp anchor residue not only interacts with the 17-position nitrogen, it also hydrogen bonds to the amide hydrogen at the 14-position. This extra hydrogen bonding interaction only present in the 14-NH-substituted naltrexone derivatives may be responsible for increasing their affinity for the KOR and DOR. In this computational study, one extra hydrogen in otherwise identical series of compounds seems to be the reason for the differing selectivity profiles.

The isosteric replacement of the O atom by NH led to the 14-N-substituted naltrexone derivatives having a different selectivity profile than the 14-O-substituted naltrexone derivatives. Based on the computational studies this was not a bioisosteric replacement, since the extra hydrogen in the amide linkage was able to participate in a hydrogen bonding interaction, thus increasing its affinity for the KOR and DOR compared to the ester-linked compounds.

In summary, the compounds **9** and **28** can be seen as lead compounds for the development of mu-kappa selective dual-antagonists. It is well established that mu opioid receptor antagonists by themselves can be effective at treating various forms of addiction. Furthermore, there is growing evidence that suggests kappa opioid receptor antagonists may be beneficial in lowering drug cravings and preventing relapse in addicts. MOR-KOR dual-antagonists may find clinical utility as a therapeutic agent in the treatment of opioid dependence and other addictions. The KOR antagonist component of the drug will block the dysphoric and anxiolytic effects associated with

chronic drug withdrawal thus decreasing the chance of relapse. While the MOR antagonist component will inhibit the euphoric and rewarding effects of exogenously administered addictive drugs. Further development of these two MOR-KOR selective dual-antagonists may lead to the discovery of innovative new treatment options for opioid dependence.

Future directions regarding this project may involve either of two paths. Using structure activity relationship studies the MOR-KOR dual-selective lead compounds could be optimized by increasing their selectivity over the DOR and by decreasing agonist activity at both MOR and KOR. For these compounds the amide linker seems to be essential for high affinity at both MOR and KOR. Introducing rotational flexibility to the side chain of compound **9** by selectively reducing the carbonyl group at 14-position into a methylene might decrease KOR agonism. The linker length of compound **28** seems to be ideal for antagonism at both KOR and MOR, but the affinity for DOR should be reduced. Based on the molecular modeling study as the linker length increased, the pyridine ring of compound **28** seemed to be interacting with a Leu residue in the DOR binding site. Therefore polar functional groups can be introduced into the pyridine ring to clash with the nonpolar Leu residue in the DOR, thus decreasing the binding affinity at this receptor.

The alternative path may involve development of MOR selective antagonists. In this case, the ester carbonyl of compound **1** should be reduced to give an ether group at the 14-position, which is much more stable than the ester and these compounds will retain their high selectivity for the MOR due to the lack of a hydrogen bond donor at this position. Similar approach would involve the replacement of the amide linker in

compound **9** by a methylene group. This approach may be synthetically more challenging compared to the reduction of the ester carbonyl.

Since the 14-position heteroaromatic side chains of these naltrexone derivatives were not interacting with the putative address site of the MOR, new address site needs to be defined and targeted. Clocinnamox, selective irreversible MOR antagonist, is also a 14-position substituted naltrexone derivative and it only irreversibly inhibits the MOR. If the specific amino acid residue that interacts with clocinnamox is identified, it could be used as the address for the MOR receptor. Clocinnamox could be docked into the MOR crystal structure, to identify the amino acid residue that alkylates it. This residue should not be conserved in the other two opioid receptors, since clocinnamox only selectively inhibits the MOR. Identifying and targeting the amino acid residue that covalently binds to clocinnamox, might lead to the development of selective MOR antagonist.

V. Experimental Procedure

1. Synthesis of 14-NH-Heterocyclic Substituted Natrexone Derivatives

All reagents were purchased from Sigma-Aldrich or as otherwise stated. Melting points were obtained with a Fisher scientific micro melting point apparatus without correction. All IR spectra were recorded on a Nicolet iS10 FT-IR instruments from Thermo Fisher Scientific. Proton (400 MHz) and Carbon-13 (100 MHz) nuclear magnetic resonance (NMR) spectra were recorded at ambient temperature with tetramethylsilane as the internal standard on a Varian Mercury 400 MHz NMR spectrometer. GC/MS analysis was performed on a Hewlett Packard 6890 (Palo Alto, CA). TLC analyses were carried out on the Analtech Uniplate F254 plates. Chromatographic purification was carried out on silica gel columns (230~400 mesh, Merck). Yields were not maximized.

1.1 Synthetic Route Towards 14-Amino Naltrexone

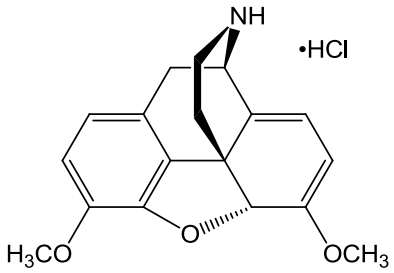

Northebaine hydrochloride (19). To a refluxing solution of thebaine (2.0 g, 6.42 mmol) in benzene was added diethylazodicarboxylate (1.56 g, 4.1 mL, 9.0 mmol) slowly. The solution was allowed to reflux overnight. After cooling to room temperature, the solvent was evaporated under reduced pressure. Pyridine hydrochloride (1.18 g,

10.27 mmol), water (5.0 mL), and EtOH (10 mL) were added to the dry residue of crude intermediate. The solution was refluxed for 2 hours and stirred overnight at room temperature. The title compound was crystallized as the hydrochloride salt (1.77 g, 83%). ^{1}H NMR (400 MHz, DMSO): δ 9.57 (b, 1 H, exchangeable), 9.24 (b, 1 H, exchangeable), 6.80 (d, J = 8.2 Hz, 1 H), 6.69 (d, J = 8.2 Hz, 1 H), 5.85 (d, J = 6.6 Hz, 1 H), 5.45 (s, 1 H), 5.20 (d, J = 6.6 Hz, 1 H), 4.55 (m, 1 H), 3.75 (s, 3 H), 3.58 (s, 3 H), 3.34 (m, 1 H), 3.22 (m, 1 H), 3.08 (m, 2 H), 2.20 (m, 1 H), 1.86 (m, 1 H).

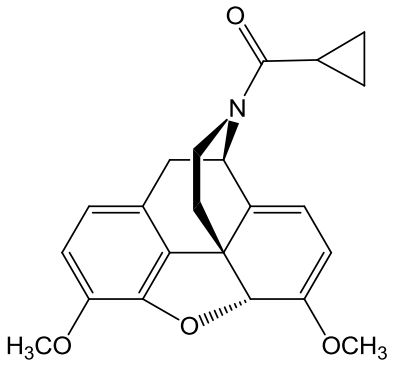

17-Cyclopropylcarbonylnorthebaine (20). To a solution of northebaine hydrochloride (2.37 g, 7.10 mmol) in anhydrous CH_2Cl_2 was added Et_3N (2.57 mL, 18.46 mmol) and the reaction mixture was put on ice-water bath. To the cooled solution was added cyclopropyl carbonyl chloride (0.89 g, 0.77 mL, 8.52 mmol) slowly, dropwise. The mixture was allowed to warm up to room temperature and stirred overnight. The mixture was then washed with 1 N HCl, water, and dried over Na_2SO_4. The solvent was evaporated under vacuum to give the product (2.61 g, 100%). ^{1}H NMR (400 MHz, $CDCl_3$): δ 6.69 (d, J = 8.2 Hz, 1 H), 6.61 (d, J = 8.2 Hz, 1 H), 5.63 (d, J = 6.36 Hz, 1 H), 5.31 (s, 1 H), 5.04 (d, J = 6.48 Hz, 1 H), 4.12 (m, 1 H), 3.86 (s, 3 H), 3.60 (s, 3 H), 3.30-

3.00 (2 m, 1 H each), 2.95 (m, 1 H), 2.15 (m, 1 H), 1.93-1.68 (2 m, 1 H each), 1.23 (m, 1 H), 1.00 (m, 2 H), 0.75 (m, 2 H).

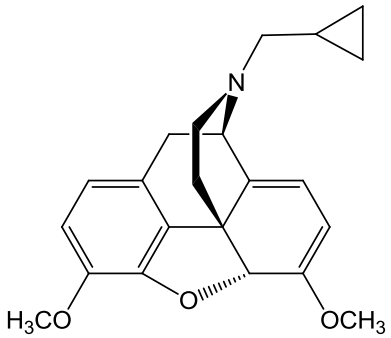

17-Cyclopropylmethylnorthebaine (21). To a stirred slurry of $LiAlH_4$ (0.20 g, 5.4 mmol) in anhydrous THF was slowly added a solution of 17-cyclopropylcarbonylnorthebaine (1.24 g, 3.4 mmol) in dry THF. The reaction mixture was refluxed for 1.5 h and allowed to cool down to room temperature and placed on an ice-water bath. Wet diethyl ether was added to the mixture dropwise, until there was no bubbling. The mixture was filtered and the precipitate was washed several times with THF. The filtrate was evaporated in vacuo and the residue was dissolved in EtOAc. The solution was washed with water twice and dried over Na_2SO_4. The solvent was evaporated and the crude mixture was purified using flash chromatography (2:1 Hex:EtOAc) to give the title compound (0.93 g, 77%). ^{1}H NMR (400 MHz, DMSO): δ 6.69 (d, J = 8.2 Hz, 1 H), 6.57 (d, J = 8.2 Hz, 1 H), 5.51 (d, J = 6.08 Hz, 1 H), 5.23 (s, 1 H), 5.11 (d, J = 6.5 Hz, 1 H), 3.84 (m, 1 H), 3.73 (s, 3 H), 3.54 (s, 3 H), 3.14 (m, 1 H), 2.78 (m, 1 H), 2.66 (m, 2 H), 2.41 (m, 2 H), 2.10 (m, 1 H), 1.51 (m, 1 H), 0.83 (m, 1 H), 0.47 (m, 2 H), 0.12 (m, 2 H).

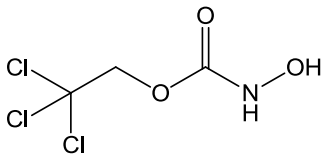

2,2,2-Trichloroethyl N-hydroxycarbamate (22). To a vigorously stirred solution of hydroxylamine hydrochloride (6.95 g, 100 mmol) and NaOH (4.8 g, 120 mmol) on ice-water bath was added dropwise 2,2,2-trichloroethylchloroformate (4.24 g, 20 mmol). The reaction mixture was vigorously stirred at room temperature for 1 h, then acidified with HCl to pH=5, and extracted with EtOAc (5 x 50 mL). The combined extract was washed with brine, dried over Na_2SO_4, and the solvent was removed under vacuum. The product was recrystallized from toluene (2.3 g, 55%). IR (KBr, cm^{-1}) V_{max}: 3371, 3264, 1710. ^1H NMR (400 MHz, $CDCl_3$): δ 7.56 (b, 1 H, exchangeable), 6.67 (b, 1 H, exchangeable), 4.79 (s, 2 H).

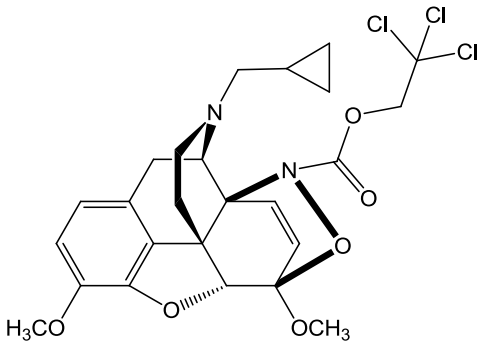

19-(2,2,2-Trichloroethoxycarbonyl)-6,14-dihydro-6β,14β-epoxyimino-17-cyclopropyl-methylnorthebaine (24). To a vigorously stirred and ice-cold mixture of 17-cyclopropylmethyl-northebaine (1.4 g, 4.0 mmol) in EtOAc and $NaIO_4$ (1.28 g, 5.98 mmol) in aqueous 0.5 M NaOAc previously adjusted to pH=6 by HCl was added 2,2,2-trichloroethyl N-hydroxycarbamate (1.25 g, 5.98 mmol) in small portions. The mixture was stirred at 0 ºC for 1 h then made alkaline by addition of saturated aqueous

$NaHCO_3$. The EtOAc layer was separated, washed with aqueous sodium thiosulfate ($Na_2S_2O_3$) and then brine, dried over Na_2SO_4, and evaporated to afford the crude mixture. The product was recrystallized from MeOH as white solid (1.63 g, 73%). ^{1}H NMR (400 MHz, DMSO): δ 6.72 (d, J = 8.2 Hz, 1 H), 6.57 (d, J = 8.2 Hz, 1 H), 6.31 (d, J = 8.9 Hz, 1 H), 6.24 (d, J = 8.9 Hz, 1 H), 4.95 (d, J = 12.3 Hz, 1 H), 4.80 (m, 2 H), 4.44 (s, 1 H), 3.69 (s, 3 H), 3.54 (s, 3 H), 3.18 (d, J = 18.8 Hz, 1 H), 2.73 (m, 1 H), 2.65 (m, 1 H), 2.40-2.07 (3 m, 1 H each), 1.84 (d, J = 12.1 Hz, 1 H), 0.84 (m, 1 H), 0.47 (m, 2 H), 0.10 (m, 2 H).

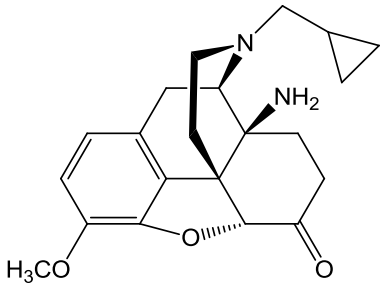

14β-Amino-7,8-dihydro-17-cyclopropylmethylnorcodeinone (25). The compound 19-(2,2,2-Trichloroethoxycarbonyl)-6,14-dihydro-6β,14β-epoxyimino-17-cyclopropyl-methylnorthebaine (0.7 g, 1.26 mmol) in MeOH and 2 N AcOH/1.5 N NaOAc was hydrogenated at 60 PSI in the presence of 70 mg of 10% Pd/C catalyst. After 5 h, the catalyst was filtered off and washed with 2 N AcOH. The filtrate was stirred on ice-water bath and neutralized with concentrated NH_4OH solution and extracted with $CHCl_3$ (4 x 50 mL). The combined extract was dried over Na_2SO_4 and the solvent removed *in vacuo*, the residue was chromatographed on silica gel using 1:1 Hex:EtOAc as an eluent to afford the product (0.18 g, 40%). ^{1}H NMR (400 MHz, DMSO): δ 6.77 (d, J = 8.2 Hz, 1 H), 6.68 (d, J = 8.2 Hz, 1 H), 5.03 (s, 1 H), 3.78 (s, 3 H), 3.72 (m, 1 H), 3.24

(m, 1 H), 3.02 (d, J = 18.8 Hz, 1 H), 2.95 (m, 1 H), 2.70 (m, 1 H), 2.55 (m, 1 H), 2.42-2.23 (3 m, 1 H each), 2.17 (m, 1 H), 1.98 (m, 2 H), 1.52 (m, 1 H), 1.36 (m, 1 H), 1.23 (m, 1 H), 0.91 (m, 1 H), 0.49 (m, 2 H), 0.15 (m, 2 H). ^{13}C NMR (100 MHz, DMSO) δ: 207.72, 144.38, 142.09, 128.46, 125.43, 119.44, 114.92, 88.99, 59.46, 58.37, 56.32, 54.87, 48.79, 48.55, 43.38, 35.84, 28.86, 21.30, 8.88, 3.82, 3.51. IR *v* (diamond, cm^{-1}): 2919, 1717, 1495, 1437, 1277, 1053.

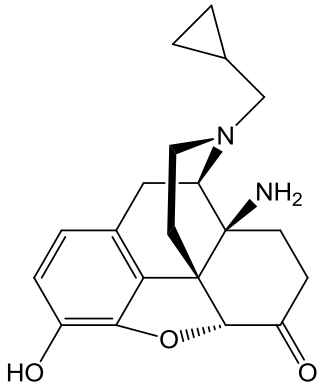

14β-Amino-7,8-dihydro-17-cyclopropylmethylnormorphinone (26). To a solution of 14β-Amino-7,8-dihydro-17-cyclopropylmethylnorcodeinone (0.71 g, 2.0 mmol) in dry CH_2Cl_2 on ice-water bath and N_2 protection was added 1 M solution of BBr_3 (1.5 g, 6.0 mmol) in CH_2Cl_2. The mixture was allowed to warm up to room temperature and stirred for 1.5 h. Water was added to the reaction mixture and the solution was refluxed for 5 h. The reaction mixture was cooled, placed on an ice-water bath and basified (NH_4OH, pH = 10). The organic layer was extracted with CH_2Cl_2 (4 x 50 mL). The extract was washed with brine and dried over Na_2SO_4. The crude product was purified with flash chromatography (40:1 CH_2Cl_2:CH_3OH) to afford the title compound (0.3 g, 44%). ^{1}H NMR (400 MHz, DMSO): δ 9.10 (b, 1 H, exchangeable), 6.52 (d, J = 8.1 Hz, 1 H), 6.48 (d, J = 8.1 Hz, 1 H), 4.60 (s, 1 H), 2.94 (m, 1 H), 2.89 (m, 2 H), 2.63 (m, 1 H), 2.42 (m, 2

H), 2.40-2.18 (m, 4 H), 2.04 (m, 1 H), 1.93 (m, 1 H), 1.62 (m, 1 H), 1.45 (m, 1 H), 1.23 (m, 1 H), 0.83 (m, 1 H), 0.46 (m, 2 H), 0.11 (m, 2 H). ^{13}C NMR (100 MHz, DMSO) δ: 209.40, 143.38, 138.92, 129.93, 124.08, 118.86, 116.64, 89.13, 62.57, 58.77, 51.83, 49.61, 43.60, 36.19, 31.05, 29.59, 21.62, 9.34, 3.63, 3.42.

1.2 Synthesis of Final Compounds

General Procedure 1. To a solution of 14β-Amino-7,8-dihydro-17-cyclopropylmethyl-normorphinone (**26**, 1 equiv) in CH_2Cl_2 was added acyl chloride (2 equiv) and Et_3N (4 equiv) on ice-water bath under N_2 protection. The mixture was allowed to stir overnight at room temperature. After concentrating to remove the solvent, the resulting residue was dissolved in CH_3OH and potassium carbonate (2 equiv) added. The reaction mixture was stirred overnight at room temperature. After concentration, the residue was partitioned between water and CH_2Cl_2. The aqueous layer was extracted with CH_2Cl_2. The combined extract was washed with brine and dried over Na_2SO_4. After concentration, the residue was purified by silica gel column with a CH_2Cl_2/CH_3OH (50:1) (1% NH_3H_2O) solvent system as eluent to give the aim product.

General Procedure 2. To a solution of carboxylic acid (3 equiv) in DMF was added N-(3-dimethylaminopropyl)-N'-ethylcarbodiimide hydrochloride (EDCI, 3 equiv), hydroxybenzotriazole (HOBt, 3 equiv), molecular sieves, and Et_3N (5 equiv) on an ice-water bath under N_2 protection. After 15 min, a solution of 14β-Amino-7,8-dihydro-17-cyclopropylmethyl-normorphinone (**26**, 1 equiv) in DMF was added. The reaction mixture was stirred overnight at room temperature. The mixture was filtered through

celite and the filtrate concentrated in vacuum to remove DMF. The residue was dissolved in CH_3OH and added with potassium carbonate (2 equiv). The resulting mixture was stirred overnight at room temperature. After concentration, the residue was partitioned between water and CH_2Cl_2. The water layer was extracted with CH_2Cl_2, the combined extract was washed with brine, and dried over Na_2SO_4. After concentration, the residue was purified by silica gel column with a CH_2Cl_2/CH_3OH (50:1) (1% NH_3H_2O) solvent system as eluent to give the aim product.

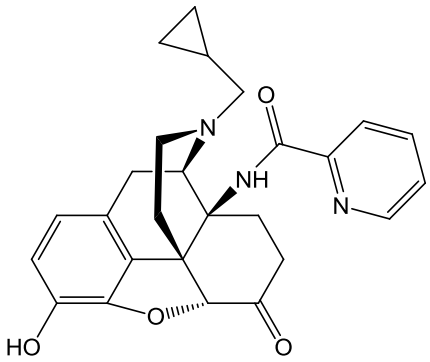

17-cyclopropylmethyl-4,5α-epoxy-3-hydroxy-14β-N-[(2'pyridyl)acetamido]morphinan-6-one (9). This compound was prepared by following the general procedure 2 in 45% yield. ^{1}H NMR (400 MHz, DMSO): δ 9.21 (s, 1 H, exchangeable), 9.19 (s, 1 H, exchangeable), 8.69 (m, 1 H), 8.13-8.01 (2 m, 1 H each), 7.65 (m, 1 H), 6.61(2 d, J = 8.1 Hz, 1 H each), 4.91 (s, 1 H), 3.67 (d, J = 5.4 Hz, 1 H), 3.04 (d, J = 18.4 Hz, 1 H), 2.76 (m, 1 H), 2.55 (m, 2 H), 2.33 (m, 2 H), 2.15 (m, 1 H), 2.10-1.88 (m, 3 H), 1.71 (m, 1 H), 1.35 (m, 1 H), 0.83 (m, 1 H), 0.44 (m, 2 H), 0.16 (m, 2 H). ^{13}C NMR (100 MHz, DMSO) δ: 207.26, 163.73, 149.58, 148.36, 143.36, 138.96, 138.01, 128.31, 126.70, 124.06, 121.56, 119.01, 117.29, 88.59, 58.97, 58.27,

55.85, 47.96, 43.31, 36.34, 30.01, 29.28, 21.03, 9.25, 3.75, 3.46. MS (ESI) *m/z*: 446.3 $(M+H)^+$. IR *v* (diamond, cm^{-1}): 2949, 1722, 1682, 1505, 1302, 1112. m.p. 195 ^{0}C.

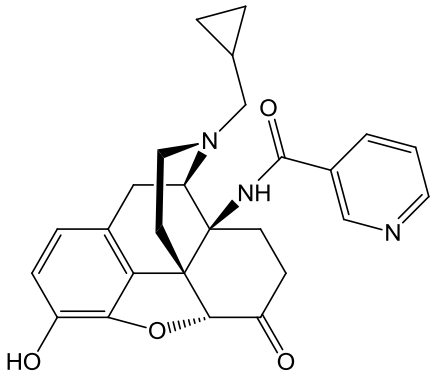

17-cyclopropylmethyl-4,5α-epoxy-3-hydroxy-14β-N-[(3'-pyridyl)acetamido]morphinan-6-one (10). This compound was prepared by following the general procedure 1 in 62% yield. ^{1}H NMR (400 MHz, DMSO): δ 9.19 (s, 1 H, exchangeable), 9.03 (s, 1 H), 8.74 (m, 1 H), 8.26 (s, 1 H, exchangeable), 8.17 (m, 1 H), 7.55 (m, 1 H), 6.57 (2 d, J = 8.1 Hz, 1 H each), 5.00 (s, 1 H), 4.06 (d, J = 5.4 Hz, 1 H), 2.97 (d, J = 18.4 Hz, 1 H), 2.71 (m, 2 H), 2.44-2.23 (m, 5 H), 2.11 and 2.04 (2 m, 1 H each), 1.56 (m, 1 H), 1.32 (m, 1 H), 0.78 (m, 1 H), 0.39 (m, 2 H), 0.06 (m, 2 H). ^{13}C NMR (100 MHz, DMSO) δ: 208.30, 165.59, 151.61, 148.36, 143.38, 139.02, 135.26, 131.55, 128.37, 124.28, 123.44, 118.94, 117.11, 88.52, 58.86, 57.66, 57.23, 48.57, 43.14, 36.38, 29.36, 28.12, 21.42, 9.60, 3.85, 3.20. MS (ESI) *m/z*: 446.5 $(M+H)^+$. IR *v* (diamond, cm^{-1}): 2924, 1712, 1677, 1523, 1241. m.p. 192-195 ^{0}C.

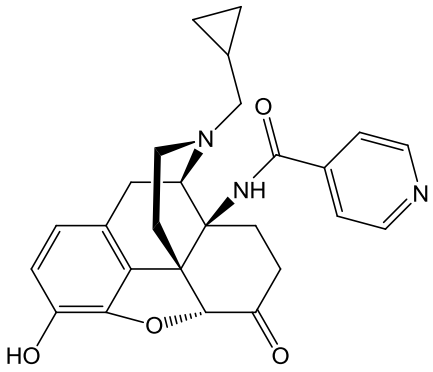

17-cyclopropylmethyl-4,5α-epoxy-3-hydroxy-14β-N-[(4'-pyridyl)acetamido]morphinan-6-one (11). This compound was prepared by following the general procedure 1 in 77% yield. ^{1}H NMR (400 MHz, DMSO): δ 9.19 (s, 1 H, exchangeable), 8.76 (d, J = 6.0 Hz, 2 H), 8.28 (s, 1 H, exchangeable), 7.75 (d, J = 6.0 Hz, 2 H), 6.57 (2 d, J = 8.1 Hz, 1 H each), 5.00 (s, 1 H), 4.07 (d, J = 5.2 Hz, 1 H), 2.97 (d, J = 18.4 Hz, 1 H), 2.69 (m, 2 H), 2.44-2.23 (m, 5 H), 2.11 and 2.04 (2 m, 1 H each), 1.55 (m, 1 H), 1.31 (m, 1 H), 0.78 (m, 1 H), 0.40 (m, 2 H), 0.06 (m, 2 H). ^{13}C NMR (100 MHz, DMSO) δ: 208.37, 165.68, 150.09, 143.40, 142.98, 139.06, 128.35, 124.32, 121.59, 119.04, 117.18, 88.54, 58.88, 57.79, 57.15, 48.61, 43.21, 36.39, 29.38, 28.03, 21.40, 9.62, 3.85, 3.37. MS (ESI) *m/z*: 446.5 $(M+H)^{+}$. IR *v* (diamond, cm^{-1}): 3270, 1710, 1686, 1604, 1510, 1221. m.p. 195 ^{0}C.

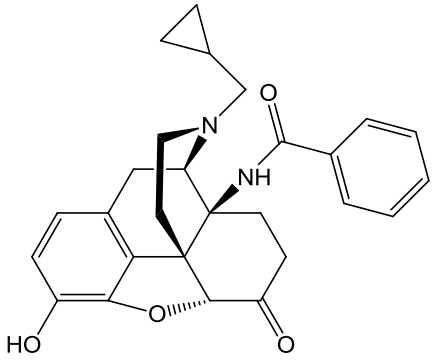

17-cyclopropylmethyl-4,5α-epoxy-3-hydroxy-14β-N-(benz-amido)morphinan-6-one (12). This compound was prepared by following the general procedure 2 in 60% yield. ^{1}H NMR (400 MHz, DMSO): δ 9.18 (s, 1 H, exchangeable), 8.06 (s, 1 H, exchangeable), 7.86 (m, 2 H), 7.53 (m, 3 H), 6.59 (2 d, J = 8.1 Hz, 1 H each), 5.00 (s, 1 H), 3.95 (d, J = 5.2 Hz, 1 H), 2.98 (d, J = 18.5 Hz, 1 H), 2.70 (m, 2 H), 2.32 (m, 3 H), 2.23 (m, 1 H), 2.07 (m, 2 H), 1.59 (m, 1 H), 1.32 (m, 1 H), 1.23 (m, 1 H), 0.81 (m, 1 H), 0.42 (m, 2 H), 0.09 (m, 2 H). ^{13}C NMR (100 MHz, DMSO) δ: 208.10, 167.23, 143.40, 138.97, 135.79, 131.09, 128.47, 128.28, 127.29, 124.31, 118.92, 117.14, 88.59, 58.82, 57.84, 57.04, 48.40, 43.15, 36.38, 29.53, 28.44, 21.32, 9.58, 3.83, 3.30. MS (ESI) *m/z*: 445.3 $(M+H)^{+}$. IR *v* (diamond, cm^{-1}): 2958, 1721, 1659, 1508, 1302, 1112. m.p. 180-185 ^{0}C.

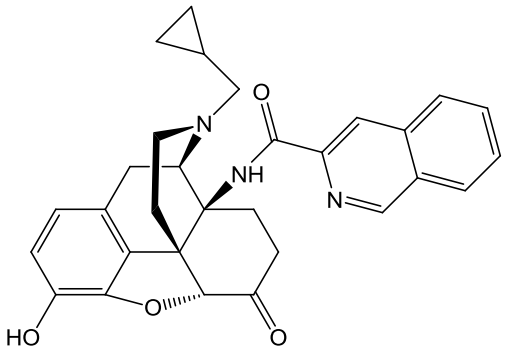

17-cyclopropylmethyl-4,5α-epoxy-3-hydroxy-14β-N-[(3'-isoquinolyl)acetamido]-morphinan-6-one (13). This compound was prepared by following the general procedure 2 in 44% yield. ^{1}H NMR (400 MHz, DMSO): δ 9.43 (s, 1 H), 9.42 (s, 1 H, exchangeable), 9.20 (s, 1 H, exchangeable), 8.63 (s, 1 H), 8.27 (d, J = 8.1Hz, 1 H), 8.19 (d, J = 8.1Hz, 1 H), 7.89 (m, 1 H), 7.82 (m, 1 H), 6.61 (2 d, J = 8.1 Hz, 1 H each), 4.93 (s, 1 H), 3.68 (d, J = 5.4 Hz, 1 H), 3.06 (d, J = 18.4 Hz, 1 H,), 2.84 (m, 1 H), 2.60 (m, 2 H), 2.39 (m, 2 H), 2.19 (m, 1 H), 2.05 (m, 3 H), 1.78 (m, 1 H), 1.36 (d, J = 11.7 Hz, 1 H), 0.89 (m, 1 H), 0.50 (m, 2 H), 0.23 (m, 2 H). ^{13}C NMR (100 MHz, DMSO) δ: 207.39,

164.26, 151.54, 143.41, 138.94, 135.39, 131.53, 129.23, 128.42, 127.94, 127,86, 127.24, 124.23, 119.62, 119.12, 117.36, 88.70, 59.19, 58.33, 55.89, 54.69, 48.01, 43.38, 36.39, 30.13, 29.46, 21.06, 9.32, 3.85, 3.53. MS (ESI) *m/z*: 497.7 $(M+H)^+$. IR *v* (diamond, cm^{-1}): 2953, 1721, 1676, 1508, 1305, 1111. m.p. 251-253 ^{0}C.

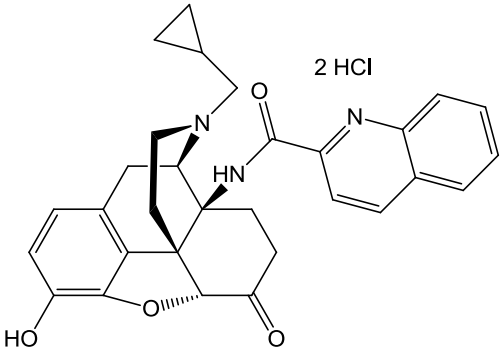

17-cyclopropylmethyl-4,5α-epoxy-3-hydroxy-14β-N-[(2'-quinolyl)acetamido]-morphinan-6-one (14). The title compound was prepared by following the general procedure 2 in 40% yield. ^{1}H NMR (400 MHz, DMSO) (hydrochloride salt): δ 9.23 (s, 1 H, exchangeable), 9.12 (b, 1 H, exchangeable), 8.65 (d, J = 8.6 Hz, 1 H), 8.34 (d, J = 8.4 Hz, 1 H), 8.21 (d, J = 8.5 Hz, 1 H), 8.14 (d, J = 8.1 Hz, 1 H), 7.94 (m, 1 H), 7.78 (m, 1 H), 6.79 (d, J = 8.1 Hz, 1 H), 6.71 (d, J = 8.1 Hz, 1 H), 5.57 (s, 1 H), 5.49 (d, J = 5.8 Hz, 1 H), 3.46 (m, 2 H), 3.17 (m, 2 H), 2.93 (m, 1 H), 2.68 (m, 4 H), 2.23 (m, 1 H), 1.73 and 1.61 (2 m, 1 H each), 1.07 (m, 1 H), 0.69 (m, 2 H), 0.50 (m, 2 H). ^{13}C NMR (100 MHz, DMSO) δ: 204.73, 163.58, 147.50, 143.19, 141.16, 137.77, 135.94, 128.41, 126.94, 126.66, 126.18, 125.74, 124.35, 118.50, 117.89, 116.33, 115.92, 85.60, 55.57, 54.92, 45.49, 43.65, 33.12, 24.56, 19.73, 3.22, 3.09. MS (ESI) *m/z*: 496.7 $(M+H)^+$. IR *v* (diamond, cm^{-1}): 2946, 1722, 1680, 1499, 1320, 1112. m.p. 200-202 ^{0}C.

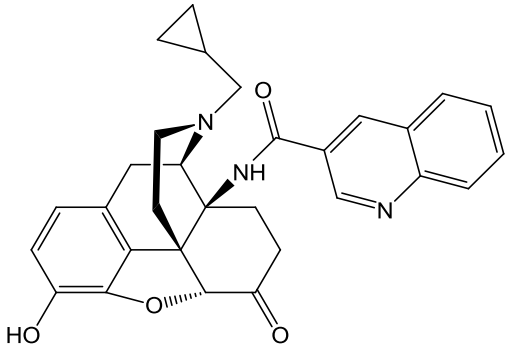

17-cyclopropylmethyl-4,5α-epoxy-3-hydroxy-14β-N-[(3'-quinolyl)acetamido]morphinan-6-one (15). This compound was prepared by following the general procedure 2 in 48% yield. ^{1}H NMR (400 MHz, DMSO): δ 9.29 (m, 1 H), 9.20 (s, 1 H, exchangeable), 8.82 (m, 1 H), 8.42 (m, 1 H, exchangeable), 8.13 (m, 2 H), 7.88 (m, 1 H), 7.72 (m, 1 H), 6.59 (2 d, J = 8.1 Hz, 1 H each), 5.04 (s, 1 H), 4.10 (d, J = 5.3 Hz, 1 H), 2.99 (d, J = 18.4 Hz, 1 H), 2.77 (m, 2 H), 2.55 (m, 1 H), 2.37 (m, 4 H), 2.15 and 2.08 (2 m, 1 H each), 1.61 (m, 1 H), 1.35 (m, 1 H), 0.84 (m, 1 H), 0.41 (m, 2 H), 0.09 (m, 2 H). ^{13}C NMR (100 MHz, DMSO) δ: 208.28, 165.62, 148.96, 148.29, 143.41, 139.04, 135.57, 131.09, 128.93, 128.66, 128.61, 128.41, 127.41, 126.46, 124.31, 118.97, 117.15, 88.57, 58.86, 57.76, 57.42, 48.61, 43.19, 36.42, 29.46, 28.22, 21.48, 9.62, 3.88, 3.25. MS (ESI) *m/z*: 496.3 $(M+H)^{+}$. IR *v* (diamond, cm^{-1}): 2929, 1715, 1659, 1499, 1305, 1102. m.p. 185 ^{0}C.

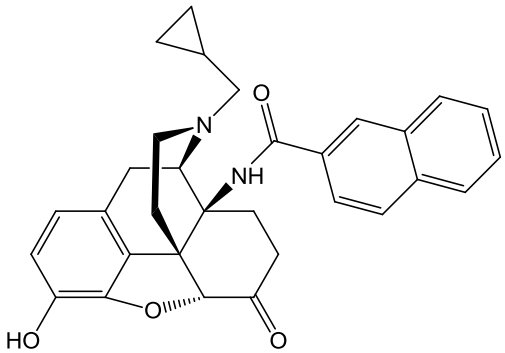

17-cyclopropylmethyl-4,5α-epoxy-3-hydroxy-14β-N-[(2'-naphthalyl)acetamido]-morphinan-6-one (16). The title compound was prepared by following the general procedure 2 in 45% yield. ^{1}H NMR (400 MHz, DMSO): δ 9.19 (s, 1 H, exchangeable), 8.46 (s, 1 H), 8.24 (s, 1 H, exchangeable), 8.03 (m, 3 H), 7.94 (m, 1 H), 7.62 (m, 2 H), 6.59 (2 d, J = 8.1 Hz, 1 H each), 5.03 (s, 1 H, C_5–H), 4.00 (d, J = 5.3 Hz, 1 H), 3.01 (d, J = 18.4 Hz, 1 H), 2.73 (m, 2 H), 2.56 (m, 1 H), 2.34 (m, 4 H), 2.09 (m, 2 H), 1.63 (m, 1 H), 1.35 (m, 1 H), 0.83 (m, 1 H), 0.43 (m, 2 H), 0.12 (m, 2 H). ^{13}C NMR (100 MHz, DMSO) δ: 208.05, 167.19, 143.42, 138.98, 134.02, 133.05, 132.02, 128.64, 128.48, 127.88, 127.59, 127.52, 127.40, 126.76, 124.30, 118.92, 117.14, 88.62, 58.81, 58.00, 57.15, 48.42, 43.17, 36.41, 29.61, 28.53, 21.36, 9.61, 3.90, 3.31. MS (ESI) *m/z*: 495.7 $(M+H)^+$. IR *v* (diamond, cm^{-1}): 3029, 1717, 1668, 1506, 1302, 1021. m.p. 192-195 ^{0}C.

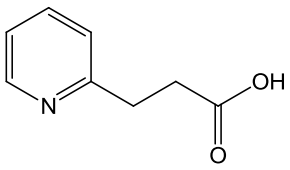

3-(pyridin-2-yl)propanoic acid (30). To a stirred solution of 2-Pyridine propanol (1.0 g, 7.3 mmol), concentrated H_2SO_4 (0.3 mL), and 13 mL of water was added over 30 min period $KMnO_4$ (1.8 g, 1.6 mmol), while the reaction temperature was maintained at 50 ^{0}C. After the addition was complete, the reaction mix was held at 50 ^{0}C until the color of the reaction mix turned brown, then the reaction mix was heated to 80 ^{0}C for 1 hour and filtered through celite. The filtrate was evaporated to dryness. The crude residue was dissolved in EtOH, added with 100 mg of activated carbon and refluxed for 10 min. The solution was filtered through celite once again and product was recrystallized from hot EtOH as white crystalline solid (0.48 g, 43%). ^{1}H NMR (400 MHz, DMSO): δ 12.09

(s, 1 H), 8.47 (d, J = 4.0 Hz, 1 H), 7.68 (m, 1 H), 7.27 (d, J = 7.8 Hz, 1 H), 7.19 (m, 1 H), 2.97 (t, 2 H), 2.66 (t, 2 H).

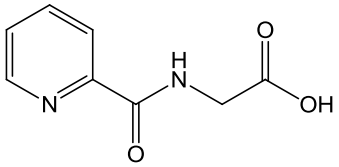

2-(picolinamido)acetic acid (31). To a mixture of 2-picolinic acid (465 mg, 3.76 mmol), HOBt (726 mg, 5.37 mmol), and molecular sieves was added dry DCM. Then 2 mL of TEA was added and the reaction was put on ice-water bath. To the reaction mixture under N_2 protection was added EDCI (1.03 g, 5.37 mmol). After stirring for 10 minutes, glycine ethyl ester hydrochloride (0.50 g, 3.58 mmol) dissolved in DMF was added dropwise. The reaction was stirred at ambient temperature overnight. The reaction mixture was filtered through celite, washed couple of times with MeOH and evaporated in vacuo to remove DMF. The dried residue was dissolved in 5 mL of THF and placed on ice-water bath. The mixture was added with 10 mL of 1:1 solution of MeOH and 1 N NaOH and stirred at ambient temperature for 2 hours. After evaporating off MeOH and THF, the pH of the aqueous layer was adjusted to 5. The aqueous layer was extracted with EA, dried over Na_2SO_4, and concentrated to afford the product as white solid (0.27 g, 40%). ^{1}H NMR (400 MHz, DMSO): δ 12.66 (s, 1 H), 8.96 (t, 1 H), 8.67 (d, J = 4.4 Hz, 1 H), 8.04 (m, 2 H), 7.63 (m, 1 H), 3.99 (d, J = 6.1 Hz, 2 H). ^{13}C NMR (100 MHz, DMSO) δ: 171.00, 164.03, 149.46, 148.50, 137.82, 126.69, 121.86, 40.97.

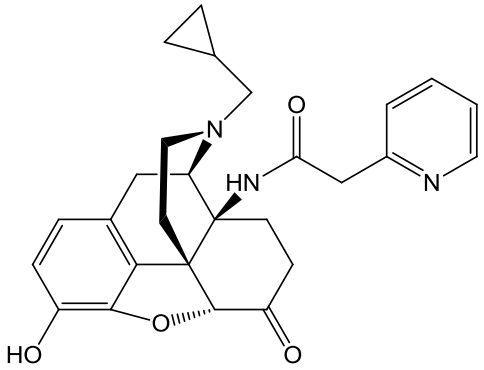

17-cyclopropylmethyl-4,5α-epoxy-3-hydroxy-14β-N-[2'-(pyridine-2"-yl)acetamido]morphinan-6-one (27). The title compound was prepared by following the general procedure 2 in 43% yield. ^{1}H NMR (400 MHz, DMSO): δ 9.17 (s, 1 H, exchangeable), 8.51 (d, J = 4.2 Hz, 1 H), 8.10 (b, 1 H, exchangeable), 7.74 (m, 1 H), 7.51 (d, J = 7.8 Hz, 1 H), 7.25 (m, 1 H), 6.57 (d, J = 8.0 Hz, 1 H), 6.52 (d, J = 8.0 Hz, 1 H), 4.82 (s, 1 H), 3.92 (s, 1 H), 3.78 (m, 1 H), 2.91 (d, J = 18.1 Hz, 1 H), 2.71 (m, 1 H), 2.59 (m, 1 H), 2.41 (m, 1 H), 2.25 (m, 4 H), 2.02 (m, 2 H), 1.47 (m, 1 H), 1.24 (m, 2 H), 0.70 (m, 1 H), 0.41 (m, 2 H), 0.07 (m, 2 H). ^{13}C NMR (100 MHz, DMSO) δ: 208.02, 169.21, 156.41, 148.85, 143.35, 139.06, 136.60, 128.53, 123.67, 121.80, 119.04, 117.14, 88.45, 58.90, 56.83, 56.76, 54.82, 48.36, 45.79, 43.45, 36.21, 29.04, 27.86, 21.24, 9.12, 3.62, 3.47. MS (ESI) *m/z*: 460.2 $(M+H)^{+}$. IR *v* (diamond, cm^{-1}): 3011, 1720, 1689, 1537, 1304, 1015. m.p. 195-198 ^{0}C.

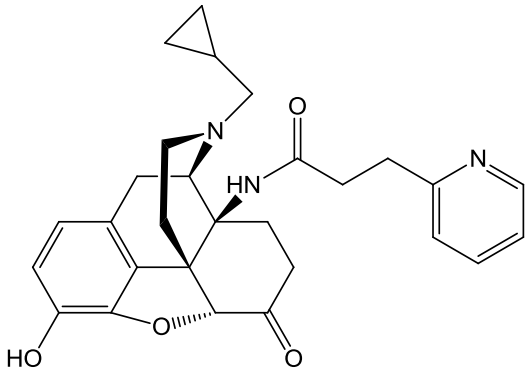

17-cyclopropylmethyl-4,5α-epoxy-3-hydroxy-14β-N-[3'-(pyridine-2"-yl)propan-amido]morphinan-6-one (28). The title compound was prepared by following the general procedure 2 in 38% yield. ^{1}H NMR (400 MHz, DMSO): δ 9.15 (s, 1 H, exchangeable), 8.46 (m, 1 H), 7.68 (m, 1 H), 7.67 (s, 1 H, exchangeable), 7.30 (d, J = 7.8 Hz, 1 H), 7.19 (m, 1 H), 6.56 (d, J = 8.1 Hz, 1 H), 6.51 (d, J = 8.1 Hz, 1 H), 4.80 (s, 1 H), 3.96 (d, J = 5.1 Hz, 1 H), 3.03 (m, 2 H), 2.89 (d, J = 18.4 Hz, 1 H), 2.68 (m, 2 H), 2.55 (m, 2 H), 2.38 (m, 1 H), 2.20 (m, 4 H), 1.96 (m, 2 H), 1.41 (m, 1 H), 1.18 (m, 1 H), 0.76 (m, 1 H), 0.42 (m, 2 H), 0.09 (m, 2 H). ^{13}C NMR (100 MHz, DMSO) δ: 208.44, 171.68, 160.43, 148.76, 143.34, 138.97, 136.44, 128.63, 124.46, 122.82, 121.35, 118.99, 117.03, 88.49, 58.81, 56.64, 56.58, 48.40, 43.39, 36.17, 35.32, 33.18, 28.96, 27.83, 21.25, 9.35, 3.61, 3.52. MS (ESI) *m/z*: 474.3 $(M+H)^{+}$. IR *v* (diamond, cm^{-1}): 3020, 1721, 1674, 1505, 1304, 1031. m.p. 210-212 ^{0}C.

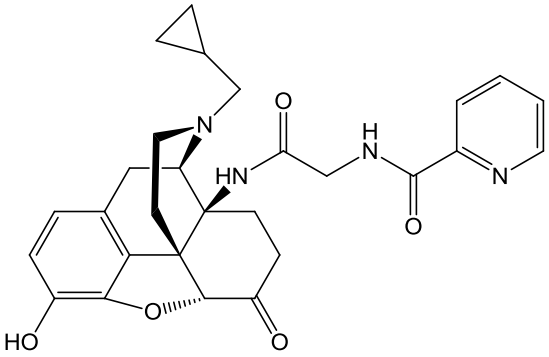

17-cyclopropylmethyl-4,5α-epoxy-3-hydroxy-14β-N-{2'-[(pyridine-2"-yl)carbox-amido]acetamido}morphinan-6-one (29). The title compound was prepared by following the general procedure 2 in 37% yield. ^{1}H NMR (400 MHz, DMSO): δ 9.15 (s, 1 H, exchangeable), 9.08 (t, 1 H, exchangeable), 8.66 (m, 1 H), 8.07 (m, 1 H), 8.00 (m, 1 H), 7.84 (s, 1 H, exchangeable), 7.62 (m, 1 H), 6.57 (d, J = 8.0 Hz, 1 H), 6.51 (d, J = 8.1

Hz, 1 H), 4.73 (s, 1 H), 4.06 (d, J = 5.8 Hz, 2 H), 3.69 (d, J = 5.3 Hz, 1 H), 2.89 (d, J = 18.4 Hz, 1 H), 2.71 (m, 1 H), 2.52 (m, 1 H), 2.46 (m, 1 H), 2.16 (m, 4 H), 1.97 (m, 2 H), 1.55 (m, 1 H), 1.23 (m, 1 H), 0.53 (m, 1 H), 0.27 (m, 2 H), 0.02 (m, 2 H). ^{13}C NMR (100 MHz, DMSO) δ: 207.64, 168.78, 164.19, 149.30, 148.52, 143.30, 138.97, 137.81, 128.54, 126.74, 124.20, 121.86, 119.04, 117.24, 88.43, 58.59, 57.58, 56.13, 48.20, 43.47, 42.95, 36.25, 29.31, 28.37, 21.06, 9.06, 3.48, 3.25. MS (ESI) *m/z*: 503.2 $(M+H)^+$. IR *v* (diamond, cm^{-1}): 3014, 1718, 1691, 1652, 1532, 1319, 1029. m.p. 205-208 ^{0}C.

1.3 HPLC Methods and Results for the Final Compounds

HPLC System: Varian Prostar 210;

Column: Microsorb-MV 100–5 C18 (250 × 4.6 mm);

Injection Volume: 5–15 µL;

Sample Concentrations: 0.3 – 0.5 mg/0.5 mL in mobile phase;

Method A: acetonitile (0.1% TFA)/water (35/65) at 1 mL/min over 30 min at 254 nm;

Method B: acetonitile (0.1% TFA)/water (40/60) at 1 mL/min over 15 min at 210 nm.

Method C: acetonitile (0.1% TFA)/water (65/35) at 1 mL/min over 16 min at 254 nm;

Table 12. HPLC analysis of final compounds.

Compd	Compound code in spectrum	Retention Time (min)	Purity (%)	Method
9	VZMN052	4.609	96.61	B
10	VZMN047	6.766	95.74	A
11	VZMN046	5.863	97.25	A
12	VZMN053	5.439	97.38	B
13	VZMN051	9.992	96.30	A
14	VZMN058	7.438	95.01	B
15	VZMN050	6.952	97.51	A
16	VZMN057	3.845	95.53	C
27	VZMN074	3.903	97.34	B
28	VZMN075	3.807	99.73	B
29	VZMN076	4.408	99.18	B

2 In Vitro Pharmacological Assays

In order to determine the affinity, selectivity, and the agonist activity of the newly synthesized naltrexone derivatives, a number of pharmacological assays were performed. For these assays, CHO (Chinese hamster ovary) cells that over expressed each of the opioid receptors were used. MOR-CHO cells and KOR-CHO cells were received from Dr. Dana Selley's laboratory at VCU. DOR-CHO cells were provided by Dr. Liu-Chen at Temple University. The CHO cells were grown in DMEM/F12 (Invtrogen) cell media consisting of 5-10% FBS (Invitrogen), 1% penicillin/streptomycin (Invitrogen), and 0.25 mg/mL G418 (Genetecin, Invitrogen). The naltrexone derivatives that are being tested were dissolved in deionized water and 5 mM stock solution of each compound was made. The compounds were aliquoted into 20 µL portions and stored at -20 ºC until used for the assay.

2.1 Cell Culture Protocol

The general procedure for growing the cells to make membrane preparations and cell freezebacks is outlined below.

The tube containing the cells are removed from the -80 ºC freezer and put in a 37 ºC water bath for 1 minute. After thawing, the cells are gently pipetted into culture dish (100 mm x 20 mm) containing 12 mL of warm cell media and placed in the incubator set at 30 ºC with 5% CO_2 and 95% humidity. The next morning, the old media is removed and fresh media is added. The cells are grown until they are 85-95% confluent and

then split into 4 culture dishes by vacuuming off the old media and adding 4 mL of Trypsin with 0.05% EDTA (Invitrogen). The cells are put back in the incubator for 3-4 minutes until all the cells are detached. Then 1 mL of cells is added into 3 new culture dishes and added with 12 mL of warm complete cell media. The cells are put back in the incubator and grown, while changing the media if necessary. It usually takes 1-2 days before the cells are grown to confluency and needs to be split again. The cells are passed one more time until there are 8 culture dishes with confluent cells. These cells can either be made into freezebacks or split into 16 large culture dishes (150 mm x 20 mm) and turned into membrane preparations for the pharmacological assays.

A. Freezeback Preparation

The freezebacks are prepared by vacuuming off the old media and adding 3 mL of trypsin to each plate. The plates are incubated for 3-4 mins and when all the cells detach from the culture dish, they are put in a falcon tube and spun down at 5000 rpms for 5 minutes. The supernatant is poured off and the appropriate amount of freezeback solution, which consists of cell media, 10% FBS, and 10% sterile DMSO, is added. The cells are aliquoted into 1 mL portions in cryovials and stored in the -80 ºC freezer.

B. Membrane Preparation

After the cells in 16 large culture dishes are confluent, they are harvested and made into membrane preparations. The old media is poured off and 7 mL of warm membrane prep media is added. The membrane prep media consists of DMEM/F12 with 5% FBS. The cells are manually detached from the culture dish by using a cell scraper and the cells are added into a large 40 mL spin tube on ice. The culture dish is

rinsed with 2 mL of membrane buffer that contains 50 mM Tris, 3 mM $MgCl_2$, and 1 mM EGTA. After all 16 plates are scraped and the cells transferred into 4 spin tubes, they are centrifuged at 1000 x g for 10 minutes. The supernatant is poured off, 8 mL of membrane buffer is added into each tube and the cells are homogenized. The contents within the spin tubes are combined into one tube and centrifuged once more at 50000 x g for 10 minutes. The supernatant is discarded and the cells are added with 12-17 mL (depends on pellet size) of membrane buffer and homogenized. Finally, a Bradford protein assay is used to quantitate the amount of protein. The cells are then divided into 3 mg portions in 2 mL cryovials and kept at -80 ºC.

2.2 Radioligand Binding Assays

A. Competition Binding Assay

The affinity and the selectivity of the newly synthesized naltrexone derivatives were determined using competitive radioligand binding assay. In this assay, the binding of the radioligand at a constant concentration that is usually around the K_d value, is measured while competing with varying concentrations of unlabeled drug of interest. The IC_{50} values of the drugs under investigation were obtained from Hill plots, analyzed by linear regression using Microsoft Excel. The K_i values, affinity of the naltrexone derivatives for the receptor, were calculated from the IC_{50} using the Cheng-Prusoff equation. The K_i value of each compound was determined for the mu, kappa, and delta opioid receptors.

The assay was performed in triplicates. The protein concentration used for the assay was usually 30 µg. The total volume of the assay was generally 500 µL and TME buffer (with no NaCl) which consists of 50 mM Tris, 3 mM $MgCl_2$, 0.2 mM EGTA, with pH adjusted to 7.7 is used. Each assay rack included three types of tubes: total binding, non-specific binding, and drug competition binding. The total binding tubes contained the buffer, radioligand, and the protein. The non-specific binding tubes included all of the components in total binding as well as excess unlabeled drug. For each rack, 2 new drugs can be tested at 7 different concentrations. These tubes contained the buffer, drugs of interest, radioligand and the protein. Using serial dilution, the drug curve with 7 different concentrations is made 10 times more concentrated than the desired concentration needed to be tested. After the initial assay, the concentration range can be optimized in order to get more usable data.

The general step-by-step protocol for the competition binding assay:

1. Pour out the appropriate amount of buffer (TME with no NaCl) into a beaker and place in ice bucket. (Everything needs to be on ice!)
2. Remove membrane preparation from the -80 ºC freezer and thaw. Add cells into a spin tube containing ~5 mL of buffer.
3. Homogenize cells and centrifuge at 50000 ^{x} g for 10 mins
4. Pour out supernatant, add 7 mL of buffer into the pellet, and homogenize. Rinse the homogenizer with 1 mL of buffer
5. Perform the Bradford Assay, use varying concentrations of BSA in order to construct the standard curve. Determine the protein concentration and dilute accordingly to get the desired concentration of protein for the assay.

6. Make the stock solution of the radioligand 10 times more concentrated than the desired concentration using the buffer and put on ice.
7. Prepare standards by adding 50 µL of radioligand into a 7 mL scintillation vials in triplicate. Add 4 mL of scintillation fluid in each vial, cap, and vortex. Determine the radioactivity in each vial using the scintillation counter and make sure the radioligand is at a proper concentration.
8. Make the appropriate concentration of the cold drug using the buffer and place on ice.
9. Add test tubes to the experimental rack and label according to the setup sheet. Add test tubes to the drug curve rack and label by concentration. Place both racks on ice.
10. Make dilutions of the drugs of interest using the buffer by following the excel setup sheet. The drugs are made 10 times more concentrated than the desired concentration because there is a 10 fold dilution when the drugs are added into the experiment tubes.
11. By this point, the proper concentrations of the protein, radioligand, excess unlabeled drug, and the 7 different concentrations of the two new drugs that are being tested should be made and kept on ice.
12. Add the appropriate amounts of buffer into the all experimental tubes. Add 50 µL of excess cold drug into non-specific tubes. Add 50 µL of drugs into the drug tubes. Add 50 µL of radioligand into all tubes. Add 100 µL of protein into all tubes.

13. Vortex each tube and rearrange tubes into a new rack. Place the test tubes in the shaking water bath at 30 ºC for 90 minutes.
14. Fill blue racks with scintillation vials leaving the first and last slots open. Three blue racks are needed for each rack of test tubes.
15. Right before the incubation is complete, place GF/B glass fiber filters in the Brandel harvester and rinse through with small amount of cold Tris buffer.
16. Filter to separate the bound radioligand from the free. Rinse through three times with cold Tris buffer.
17. Place filter papers on the blue rack with scintillation tubes. Transfer filter paper into the vials using the Brandel puncher/filler. Fill tubes with 4 mL of scintillation fluid and cap.
18. Label tubes and place in the scintillation counter to determine bound radioactivity.

B. The [^{35}S]GTPγS Binding Functional Assay

The [^{35}S]GTPγS functional assay is used to measure the level of G-protein activation following the binding of an agonist to a GPCR. This assay was used to determine the functional activity of the naltrexone derivatives for the mu and kappa opioid receptors. In the assay, DAMGO (3 µM) and U-50488 (5 µM) were included as a maximally effective concentrations of full agonists at the mu and kappa opioid receptors respectively, for determination of relative efficacy values. The E_{max}, the maximum effect of the drug or the efficacy and the EC_{50}, the concentration that produces half-maximal effect or potency can be determined from this assay.

In the functional assay, [^{35}S]GTPγS replaces the endogenous GTP and binds to the Gα when the receptor is activated. Since the γ-thiophosphate bond is resistant to hydrolysis by the GTPase, the G-protein is not able to reform the heterotrimer. Therefore, [^{35}S]GTPγS labeled Gα subunits accumulate and can be measured by counting the amount of [^{35}S] label incorporated.[72] The amount of stimulation produced by each novel ligand is normalized to that obtained with the full agonist DAMGO or U50-488. The resulting data were fit by nonlinear regression to a one-site binding model, using GraphPad Prism software, to determine EC_{50} and E_{max} values for the naltrexone derivatives.

The assay was performed in triplicates. The protein concentration used for the assay was usually 10 µg. The total volume of the assay was 500 µL and TME buffer (with NaCl) which consists of 50 mM Tris, 3 mM $MgCl_2$, 0.2 mM EGTA, 100 mM NaCl with pH adjusted to 7.7 is used. The concentration of the radioligand [^{35}S]GTPγS needs to be around 0.1 nM which corresponds to 125000 DPMs. For this assay, there are four different experimental tubes: basal, non-specific binding, positive standard binding and drug binding. The basal test tubes will include buffer, GDP, [^{35}S]GTPγS, and protein. For the non-specific binding, the tubes will include all the components in basal plus excess cold GTPγS. The positive standard tubes are added with buffer, GDP, DAMGO or U-50488, [^{35}S]GTPγS, and the protein. For each rack, 2 different drugs can be tested, one with 6 different concentrations and the other with 7 different concentrations. These tubes will include buffer, GDP, drugs of interest, [^{35}S]GTPγS, and the protein. Using serial dilution, the drug curve with 6 and 7 different concentrations is made 10

times more concentrated than the desired concentration needed to be tested. After the initial assay, the concentration range can be optimized in order to get more usable data.

The general step-by-step protocol for the functional [^{35}S]GTPγS binding assay:

1. Pour out the appropriate amount of buffer (TME with NaCl) into a beaker and place in ice bucket. (Everything needs to be on ice!)
2. Remove membrane preparation from the -80 ºC freezer and thaw. Add cells into a spin tube containing ~5 mL of buffer.
3. Homogenize cells and centrifuge at 50000 x g for 10 mins
4. Pour out supernatant, add 7 mL of buffer into the pellet, and homogenize. Rinse the homogenizer with 1 mL of buffer.
5. Perform the Bradford Assay, use varying concentrations of BSA in order to construct the standard curve. Determine the protein concentration and dilute accordingly to get the desired concentration of protein for the assay.
6. Make the stock solution of the [^{35}S]GTPγS by adding ~5 mL of buffer into pre-aliquoted [^{35}S]GTPγS in 15 mL vial
7. Prepare standards by adding 50 µL of [^{35}S]GTPγS into a 7 mL scintillation vials in triplicate. Add 4 mL of scintillation fluid in each vial, cap, and vortex. Determine the radioactivity in each vial using the scintillation counter and make sure the DPM is between 115000 – 135000.
8. Make the appropriate concentration of the cold GTPγS which is used to determine the non-specific and place on ice.
9. Make appropriate concentration of the full agonist used as the positive standard and place on ice.

10. Following the setup sheet, dilute the pre-aliquoted GDP with buffer to get the proper concentration and put on ice.
11. Add test tubes to the experimental rack and label according to the setup sheet. Add test tubes to the drug curve rack and label by concentration. Place both racks on ice.
12. Make dilutions of the drugs of interest using the buffer by following the setup sheet. The drugs are made 10 times more concentrated than the desired concentration because there is a 10 fold dilution when the drugs are added into the experiment tubes.
13. By this point, the proper concentrations of the protein, radioligand [^{35}S]GTPγS, excess unlabeled GTPγS, GDP, full agonist standard, and the different concentrations of the two new drugs that are being tested should be made and kept on ice.
14. Add the appropriate amounts of buffer into the all experimental tubes. Add 50 µL of cold GTPγS into non-specific tubes. Add 50 µL of full agonist standard into the designated tubes. Add 50 µL of drugs into the drug tubes. Add 50 µL of GDP into all tubes. Add 50 µL of [^{35}S]GTPγS into all tubes. Add 100 µL of protein into all tubes.
15. Vortex each tube and rearrange tubes into a new rack. Place the test tubes in the shaking water bath at 30 ºC for 90 minutes.
16. Fill blue racks with scintillation vials leaving the first and last slots open. Three blue racks are needed for each rack of test tubes.

17. Right before the incubation is complete, place GF/B glass fiber filters in the Brandel harvester and rinse through with small amount of cold Tris buffer.
18. Filter to separate the bound radioligand from the free. Rinse through three times with cold Tris buffer.
19. Place filter papers on the blue rack with scintillation tubes. Transfer filter paper into the vials using the Brandel puncher/filler. Fill tubes with 4 mL of scintillation fluid and cap.
20. Label tubes and place in the scintillation counter to determine bound radioactivity.

3. In Vivo Pharmacological Assays

Compounds **9**, **10**, and **13** were chosen based on their in vitro assay results for in vivo studies. Initially, these compounds were tested for acute agonistic and antagonistic effects in mice. The 14-NH-substituted naltrexone derivatives were assessed for their ability to produce antinociception and to antagonize the antinociceptive effects of morphine in the mouse tail immersion assay. Additionally, these compounds were characterized in the comparative opioid withdrawal precipitation study using mice chronically exposed to morphine. The procedures for these assays were previously reported[29,73] and the basic protocol is summarized below.

3.1 Handling of Mice

Male Swiss Webster mice weighing 25-30 g were housed six to a cage in animal care quarters and maintained at 22 ºC on a 12 hour light-dark cycle. Food and water

were available ad libitum. The mice were brought to a test room, marked for identification and allowed 18 hours to recover from transport and handling. Protocols and procedures were approved by the IACUC at VCU Medical Center and comply with the recommendations of the IASP.

3.2 Tail Immersion Test

The warm-water tail immersion test was performed using a water bath with the temperature maintained at 56 ºC. To test for agonist properties, mice with predetermined tail immersion baseline, were injected s.c. with morphine (10 mg/kg; a dose that produces maximal antinociception) or test compound at increasing doses and were reassessed for their tail immersion reaction time 20 minutes later. To test for antagonistic properties, mice with predetermined tail immersion baseline, were injected s.c. with either naloxone (1 mg/kg; a dose that totally block the antinociception indced by 10 mg/kg morphine) or the test compound at various doses and 5 minutes later they were administered morphine (10 mg/kg; s.c.). Mice were reassessed for their tail immersion reaction time 20 minutes later. ED_{50} values were calculated using least-squares linear regression analysis followed by calculation of 95% confidence limits by the method of Bliss.

3.3 Opioid Withdrawal Assay

Male Swiss Webster mice were anesthetized with 2.5% isoflurane and a 75 mg morphine pellet was surgically implanted at the base of the neck following the proper procedure. Withdrawal was precipitated in mice at 72 hours from pellet implantation with naloxone (1.0 mg/kg, s.c.), naltrexone (1.0 mg/kg, s.c.), and the test compounds at

increasing doses. Mice were allowed for 30 minutes to habituate to an open-topped, square, clear Plexiglas observation chamber (26 x 26 x 26 cm^3) with lines partitioning the bottom into quadrants then given antagonist. Withdrawal commenced within 1 minute after antagonist administration. Escape jumps and wet dog shakes were quantified by counting their occurrences over 20 minutes.

Data are expressed as mean values ± SEM. Analysis of variance (ANOVA) followed by the post hoc Dunnett test performed to assess significance using the Instat 3.0 software (GraphPad Software). The withdrawal signs of jumping and wet dog shakes were counted and subjected to two-factor ANOVA.

4. Molecular Modeling Study

All ligands used in the molecular modeling study were built with standard bond lengths and angles using the molecular modeling package SYBYL 8.1. The small molecules were assigned Gasteiger-Huckel charges and energy minimized with the Tripos Force Field (TFF).

4.1 Dynamics Simulation

The compound **1** of the 14-O-substituted series and compound **9** of the 14-NH-substituted series of naltrexone derivatives were subjected to a short dynamics simulation inside a water box in order to compare their lowest energy conformations. The water box was constructed automatically with Tripos Force Field and the ligands

placed inside. The dynamics was run for 1000 fs with steps of 1 fs. In order to get the final model after dynamics run, the final 20 conformations were averaged.

4.2 Docking Study

The naltrexone derivatives were docked into the crystal structures of mu, kappa, and delta opioid receptors. Each receptor crystal structure was downloaded from the protein data bank as a pdb file. The crystal structures were prepared for docking by adding hydrogens and deleting extra proteins, fatty acids, cholesterols, water molecules, and the bound ligands inside each binding pocket.

The binding site for the docking study was set to be all atoms within 15 Å of an oxygen atom on an Asp residue that is conserved in all three opioid receptors that is known to interact with the basic amine functionality of most opioid compounds. For the mu opioid receptor crystal structure, oxygen atom OD2 of Asp147 was set to be the center of the binding pocket. For the kappa opioid receptor, oxygen atom OD1 of Asp138 was used to define the binding site. For the delta opioid crystal structure, oxygen atom OD2 of Asp128 was used to define the binding site. All 19 naltrexone derivatives were docked 40 times each into the opioid receptor crystal structures using GOLD 5.1. The docking was done with mostly default parameters, the option to flip amide bonds and ring corners were turned on. Also the option to generate diverse solutions was on. The CHEMPLP score was used as the default scoring function and all solutions were rescored using the GOLD score. The best ranked docking solutions for all compounds are tabulated in the appendix section.

List of References

List of References

1. Yaksh, T. L.; Wallace, M. S. Opioids, Analgesia, and Pain Management. In *Goodman & Gilman's The Pharmacological Basis of Therapeutics*; Brunton, L. L., Ed.; McGraw-Hill, 2011.
2. Woods, T. M.; Hilaire, M. L. Opioid abuse and dependence: treatment review and future options. *Formulary*. **2010**, *45* (9), 284-291.
3. Pert, C. B.; Snyder, S. H. Opiate receptor: demonstration in nervous tissue. *Science*. **1973**, *179* (4077), 1011-1014
4. Simon, E. J.; Hiller, J. M.; Edelman, I. Stereospecific binding of the potent narcotic analgesic tritium-labeled etorphine to rat-brain homogenate. *Proc. Natl. Acad. Sci. U.S.A*. **1973**, *70* (7), 1947-1949.
5. Terenius, L. Stereospecific interaction between narcotic analgesics and a synaptic plasma membrane fraction of rat cerebral cortex. *Acta Pharmacol. Toxicol*. **1973**, *32*, 317-320.
6. Berezniuk, I.; Fricker, L. D. Endogenous opioids. In *The Opiate Receptors*; Pasternak, G. W., Ed.; Humana Press: New York, NY., 2011.
7. Corbett, A. D.; Henderson, G.; McKnight, A. T.; Paterson, S. J. 75 years of opioid research: the exciting but vain quest for the Holy Grail. *Br. J. Pharmacol*. **2006**, *147*, 153-162.
8. Law, P.; Wong, Y. H.; Loh, H. H. Molecular mechanisms and regulation of opioid receptor signaling. *Annu. Rev. Pharmacol. Toxicol*. **2000**, *40*, 389-430.

9. Trigo, J. M.; Martin-Garcia, E.; Berrendero, F.; Robledo, P.; Maldonado, R. The endogenous opioid system: A common substrate in drug addiction. *Drug Alcohol Depend*. **2010**, *108* (3), 183-194
10. Matthes, H. W.; Maldonado, R.; Simonin, F.; Valverde, O.; Slowe, S.; et. al. Loss of morphine-induced analgesia, reward effect and withdrawal symptoms in mice lacking the mu-opioid-receptor gene. *Nature*. **1996**, *383*, 819-823.
11. Loh, H. H.; Liu, H.; Cavalli, A.; Yang, W.; Chen, Y.; Wei, L. *μ* Opioid receptor knockout in mice: effects on ligand-induced analgesia and morphine lethality. *Mol. Brain Res*. **1998**, *54* (2), 321-326.
12. Zimmerman, D. M.; Leander, J. D. Selective opioid receptor agonists and antagonists: research tools and potential therapeutic agents. *J. Med. Chem*. **1990**, *33* (3), 895-902.
13. Hart, E. R.; McCawley, E. L. The pharmacology of N-allylnormorphine as compared with morphine. *J. Pharmacol. Exp. Ther*. **1944**, *82*, 339-348.
14. Lasagna, L.; Beecher, H. K. The analgesic effectiveness of nalorphine and nalorphine-morphine combinations in man. *J. Pharmacol. Exp. Ther*. **1954**, *112*, 356-363.
15. Foldes, F. F.; Lunn, J. N.; Moore, J.; Ian, B. N-allylnoroxymorphone: a new potent narcotic antagonist. *Am. J. Med. Sci*. **1963**, *245*, 57-64.
16. Glass, P. S. A.; Jhaveri, R. M.; Smith, L. R. Comparison of potency and duration of action of nalmefene and naloxone. *Anesth. Analg*. **1994**, *78*, 536-541.
17. Julius, D. A. Research and development of naltrexone: a new narcotic antagonist. *Am. J. Psych*. **1979**, *136*, 782-786.

18. Eguchi, M. Recent advances in selective opioid receptor agonists and antagonists. *Med. Res. Rev*. **2004**, *24*, 182-212
19. Tucker, T. K.; Ritter, A. J. Naltrexone in the treatment of heroin dependence: a literature review. *Drug Alc. Rev*. **2000**, *19*, 73-82.
20. Goodman, A. J.; Le Bourdonnec, B.; Dolle, R. E. Mu opioid receptor antagonists: recent developments. *ChemMedChem*. **2007**, *2*, 1552-1570.
21. Tetrault, J. M.; Fiellin, D. A. Current and potential pharmacological treatment options for maintenance therapy in opioid-dependent individuals. *Drugs*. **2012**, *72*, 217-228.
22. White, K. L.; Roth, B. L. Psychotomimetic effects of kappa opioid receptor agonists. *Biol. Psychiatry*. **2012**, *72*, 797-798
23. Hollister, L. E.; Johnson, K.; Boukhabza, D.; Gillespie, H. K. Aversive effects of naltrexone in subjects not dependent on opiates. *Drug Alcohol Depend*. **1981**, *8*, 37-41
24. Crowley, T. J.; Wagner, J. E.; Zerbe, G.; Macdoald, M. Naltrexone-induced dysphoria in former opioid addicts. *Am. J. Psych*. **1985**, *142*, 1081-1084.
25. Portoghese, P. S.; Larson, D. L.; Sayre, L. M.; Fries, D. S.; Takemori, A. E. A novel opioid receptor site directed alkylating agent with irreversible narcotic antagonistic and reversible agonistic activities. *J. Med. Chem*. **1980**, *23* (3), 233-234.
26. Chen, C.; Yin, J.; de Riel, K. J.; DesJarlais, R. L.; Raveglia, L. F.; Zhu, J.; Liu-Chen, L. Determination of the amino acid residue involved in [^{3}H]β-

Funaltrexamine covalent binding in the cloned rat μ opioid receptor. *J. Biol. Chem*. **1996**, *271*, 21422-21429.

27. Zernig, G.; Burke, T.; Lewis, J. W.; Woods, J. H. Mechanism of clocinnamox blockade of opioid receptors: evidence from in vitro and ex vivo binding and behavioral assays. *J. Pharmacol. Exp. Ther*. **1996**, *279*, 23-31.
28. Wentland, M. P.; Lou, R.; Lu, Q.; Bu, Y.; Denhardt, C. et. al. Synthesis of novel high affinity ligands for opioid receptors. *Bioorg. Med. Chem. Lett*. **2009**, *19*, 2289-2294.
29. Li, G.; Aschenbach, L. C.; Chen, J.; Cassidy, M. P.; Stevens, D. L.; Gabra, B. H.; Selley, D. E.; Dewey, W. L.; Westkaember, R. B.; Zhang, Y. Design, synthesis, and biological evaluation of 6α- and 6β-N-heterocyclic substituted naltrexamine derivatives as mu opioid receptor selective antagonists. *J. Med. Chem*. **2009**, *52*, 1416-1427.
30. Kramer, T. H.; Shook, J. E.; Kazmierski, W.; Ayres, E. A.; Wire, W. S.; Hruby, V. J.; Burks, T. F. Novel peptidic mu opioid antagonists: pharmacologic characterization in vitro and in vivo. *J. Pharmacol. Exp. Ther*. **1989**, *249*, 544-551.
31. Pelton, J. T.; Kazmierski, W.; Gulya, K.; Yamamura, H. I.; Hruby, V. J. Design and synthesis of conformationally constrained somatostatin analogs with high potency and specificity for μ opioid receptors. *J. Med. Chem*. **1986**, *29*, 2370-2375
32. Schmidhammer, H.; Burkard, W. P.; Eggstein-Aeppli, L.; Smith, C. F. C. Synthesis and biological evaluation of 14-alkoxymorphinans. 2. (-)-N-

(Cyclopropylmethyl)-4,14-dimethoxymorphinan-6-one, a selective μ opioid receptor antagonist. *J. Med. Chem*. **1989**, *32*, 418-421.

33. Spetea, M.; Schuellner, F.; Moisa, R. C.; Berzetei-Gurske, I. P.; Schraml, B.; Doerfler, C.; Aceto, M. D.; Harris, L. S.; Coop, A.; Schmidhammer, H. Synthesis and biological evaluation of 14-Alkoxymorphinans. 21. Novel 4-alkoxy and 14-phenylpropoxy derivatives of the μ opioid receptor antagonist cyprodime. *J. Med. Chem*. **2004**, *47*, 3242-3247.
34. Schmidhammer, H.; Smith, C. F. C.; Erlach, D.; Koch, M.; Krassnig, R.; Schwetz, W.; Wechner, C. Synthesis and biological evaluation of 14-alkoxymorphinans. 3. Extensive study on cyprodime-related compounds. *J. Med. Chem*. **1990**, *33*, 1200-1206.
35. Portoghese, P. S.; Sultana, M.; Takemori, A. E. Design of peptidomimetic δ opioid receptor antagonists using the message-address concept. *J. Med. Chem*. **1990**, *33*, 1714-1720.
36. Jones, R. M.; Portoghese, P. S. 5'-Guanidinonaltrindole, a highly selective and potent κ-opioid receptor antagonist. *Eur. J. Pharmcol*. **2000**. *396*, 49-52.
37. Schwyzer, R. ACTH: a short introductory review. *Ann. N.Y. Acad. Sci*. **1977**, *297*, 3-26.
38. Portoghese, P. S.; Sultana, M.; Nagase, H.; Takemori, A. E. Application of the message-address concept in the design of highly potent and selective non-peptide δ opioid receptor antagonists. *J. Med. Chem*. **1988**, *31*, 281-282.
39. Portoghese, P. S. The role of concepts in structure-activity relationship studies of opioid ligands. *J. Med. Chem*. **1992**, *35*, 1927-1937.

40. Stevens, W. C.; Jones, R. M.; Subramanian, G.; Metzger, T. G.; Ferguson, D. M.; Portoghese, P. S. Potent and selective indomorphinan antagonists of the kappa-opioid receptor. *J. Med. Chem*. **2000**, *43*, 2759-2769.
41. Jones, R. M.; Hjorth, S. A.; Schwartz, T. W.; Portoghese, P. S. Mutational evidence for a common κ antagonist binding in the wild-type κ and mutant μ[K303E] opioid receptors. *J. Med. Chem*. **1998**, *41*, 4911-4914.
42. National Institute on Drug Abuse. Topics in brief: prescription drug abuse. http://www.drugabuse.gov/publications/topics-in-brief/prescription-drug-abuse/ (accessed November 22, 2012).
43. Okie, S. A flood of opioids, a rising tide of deaths. *N. Engl. J. Med*. **2010**, *363*, 1981-1985.
44. Xue, J.; Chen, C.; Zhu, J.; Kunapuli, S. P.; de Riel, J. K.; Yu, L.; Liu-Chen, L. The third extracellular loop of the μ opioid receptor is important for agonist selectivity. *J. Biol. Chem*. **1995**, *270*, 12977-12979.
45. Bonner, G.; Meng, F.; Akil, H. Selectivity of μ-opioid receptor determined by interfacial residues near third extracellular loop. *Eur. J. Pharmacol*. **2000**, *403*, 37-44.
46. Li, G.; Aschenbach, L. C. K.; He, H.; Selley, D. E.; Zhang, Y. 14-O-Heterocyclic-substituted naltrexone derivatives as non-peptide mu opioid receptor selective antagonists: design, synthesis, and biological studies. *Bioorg. Med. Chem. Lett*. **2009**. *19*, 1825-1829.
47. Manglik, A.; Kruse, A. C.; Kobilka, T. S.; Thian, F. S.; Mathiesen, J. M.; Sunahara, R. K.; Pardo, L.; Weis, W. I.; Kobilka, B. K.; Granier, S. Crystal

structure of the μ-opioid receptor bound to a morphinan antagonist. *Nature*. **2012**, *485*, 321-326.

48. Wu, H.; Wacker, D.; Mileni, M.; Katritch, V.; Han, G. W.; Vardy, E.; Liu, W.; Thompson, A. A; Huang, X.; Carroll, F. I.; Mascarella, S. W.; Westkaemper, R. B.; Mosier, P. D.; Roth, B. L.; Cherezov, V.; Stevens, R. C. Structure of the human κ-opioid receptor in complex with JDTic. *Nature*. **2012**, *485*, 327-332.
49. Granier, S.; Manglik, A.; Kruse, A. C.; Kobilka, T. S.; Thian, F. S.; Weis, W. I.; Kobilka, B. K. Structure of the δ-opioid receptor bound to naltrindole. *Nature*. **2012**, *485*, 400-405.
50. Jones, G.; Willett, P.; Glen, R. C.; Leach, A. R.; Taylor, R. Development and validation of a genetic algorithm for flexible docking. *J. Mol. Biol*. **1997**, *267*, 727-748.
51. Pohland, A.; Sullivan, H. R. Normorphines. U.S. Patent 3,342,824, December 7, 1964. (accessed 2009); SciFinder.
52. Bentley, K. W.; Bower, J. D.; Lewis, J. W. Novel analgesics and molecular rearrangements in the morphine-thebaine group. XVI. Some derivatives of 6,14-endo-etheno-7,8-dihydromorphine. *J. Chem. Soc*. **1969**, *18*, 2569-2572.
53. Kirby, G. W.; McGuigan, H.; Mackinnon, J. W. M.; McLean D.; Sharma, R. P. Formation and reactions of C-nitrosoformate esters, a new class of transient dienophiles. *J. Chem. Soc*. **1985**, *7*, 1437-1442.
54. Kirby, G. W.; Mclean, D. An efficient synthesis of 14β-aminocodeinone from thebaine. *J. Chem. Soc*. **1985**, *7*, 1443-1445.

55. Sebastian, A.; Bidlack J. M.; Jiang, Q.; Deecher, D.; Teitler, M.; Glick, S. D.; Archer, S. 14-beta-[(p-Nitrocinnamoyl)amino]morphinones, 14-beta-[(p-nitrocinnamoyl)amino]-7,8-dihydromorphinones, and their codeinone analogs: synthesis and receptor activity. *J. Med. Chem*. **1993**, *36*, 3154-3160.
56. Archer, S.; Seyed-Mozaffari, A.; Jiang, Q.; Bidlack, J. M. 14-alpha, 14'-beta-[Dithiobis[(2-oxo-2,1-ethanediyl)imino]]bis(7,8-dihydromorphinone) and 14-alpha, 14'-beta-[Dithiobis[(2-oxo-2,1-ethanediyl)imino]]bis-7,8-dihydro-N-(cyclopropyl-methyl)normorphinone: chemistry and opioid binding properties. *J. Med. Chem*. **1994**, *37*, 1578-1585.
57. Braun, V. J. Resolution of cyclic bases by means of bromcyanogen. *Chem. Ber*. **1909**, *42*, 2035-2057.
58. Abdel-Monem, M. M.; Portoghese, P. S. N-demethylation of morphine and structurally related compounds with chloroformate esters. *J. Med. Chem*. **1972**, *15*, 208-210.
59. Montzka, T. A.; Matiskella, J. D.; Partyka, R. A. 2,2,2-Trichloroethyl chloroformate. General reagent for demethylation of tertiary methylamines. *Tetrahedron Lett*. **1974**, *14*, 1325-1327.
60. Zuo, L.; Yao, S.; Wang, W.; Duan, W. An efficient method for demethylation of aryl methyl ethers. *Tetrahedron Lett*. **2008**, *49*, 4054-4056.
61. Chae, J. Practical demethylation of aryl methyl ethers using an odorless thiol reagent. *Arch. Pharmacal Res*. **2008**, *31*, 305-309.

62. Vass, A.; Dudas, J.; Borbely, L.; Haasz, F.; Jekkel, P. A new process for the preparation of phenolic hydroxyl-substituted compounds. U.S. Patent 7,973,185, July 5, 2011. (accessed 2011); SciFinder.
63. Reddy, G.; Sagar, V.; Venkat, R. G.; Subramanyam, R. V. K.; Ivengar, D. S. A new novel and practical one pot methodology for conversion of alcohols to amines. *Synth. Commun*. **2000**, *30*, 2233-2237.
64. Wright, S. W.; Ammirati, M. J.; Andrews, K. M.; Brodeur, A. M.; Danley, D. E.; Doran, S. D.; Lillquist, J. S.; McClure, L. D.; McPherson, R. K.; Orena, S. J. cis-2,5-Dicyanopyrrolidine inhibitors of dipeptidyl peptidase IV: Synthesis and in vitro, in vivo, and x-ray crystallographic characterization. *J. Med. Chem*. **2006**, *49*, 3068-3076.
65. Koziara, A.; Zwierzak, A. Iminophosphorane-mediated transformation of tertiary alcohols into tert-alkylamines and their N-phosphorylated derivatives. *Tetrahedron Lett*. **1987**, *28*, 6513-6516.
66. Hartsel, J. A.; Craft, D. T.; Chen, Q.; Ma, M.; Carlier, P. R. Acess to “Friedel-Crafts-Restricted” tert-alkyl aromatics by activation/methylation of tertiary benzylic alcohols. *J. Org. Chem*. **2012**, *77*, 3127-3133.
67. Lyssikatos, J. P.; La Greca, S. D.; Yang, B. V. Preparation of quinolin-2-ones as anticancer agents. U.S. Patent 6,495,564, December 17, 2002. (accessed 2011); SciFinder.
68. Gololobov, Y. G.; Zhmurova, I. N.; Kasukhin, L. F. Sixty years of Staudinger reaction. *Tetrahedron*. **1981**, *37*, 437-472.

69. Montalbetti, C. A. G. N.; Virginie, F. Amide bond formation and peptide coupling. *Tetrahedron*. **2005**, *61*, 10827-10852.

70. Cheng, Y.; Prusoff, W. H. Relation between the inhibition constant (K1) and the concentration of inhibitor which causes fifty per cent inhibition (I50) of an enzymatic reaction. *Biochem. Pharmacol*. **1973**, *22*, 3099-3108.

71. Bradford, M. M. A rapid and sensitive method for the quantification of microgram quantities of protein utilizing the principle of protein-dye binding. *Anal. Biochem*. **1976**, *72*, 248-254.

72. Harrison, C.; Traynor, J. R. The [^{35}S]GTPγS binding assay: approaches and application in pharmacology. *Life Sci*. **2003**, *74*, 489-508.

73. Yuan, Y.; Li, G.; He, H.; Stevens, D. L.; Kozak, P.; Scoggins, K. L.; Mitra, P.; Gerk, P. M.; Selley, D. E.; Dewey, W. L.; Zhang, Y. Characterization of 6α- and 6β-N-Heterocyclic substituted naltrexamine derivatives as novel leads to development of mu opioid receptor selective antagonists. *ACS Chem. Neurosci*. **2011**, *2*, 346-351.

74. Yuan, Y.; Elbegdorj, O.; Chen, J.; Akubathini, S. K.; Zhang, F.; Stevens, D. L.; Beletskaya, I. O.; Scoggins, K. L.; Zhang, Z.; Gerk, P. M.; Selley, D. E.; Akbarali, H. I.; Dewey, W. L.; Zhang, Y. Design, synthesis, and biological evaluation of 17-cyclopropylmethyl-3,14*β*-dihydroxy-4,5*α*-epoxy-6*β*-[(4'-pyridyl)carboxamido]morphinan derivatives as peripheral selective *μ* opioid receptor agents. *J. Med. Chem*. **2012**, *55*, 10118-10129.

75. Mitra, P.; Venitz, J.; Yuan, Y.; Zhang, Y.; Gerk, P. M. Preclinical disposition (in vitro) of novel *μ*-opioid receptor selective antagonists. *Drug Metab. Dispos*. **2011**, *39*, 1589-1596.

76. Walker, E. A.; Sterious, S. N. Opioid antagonists differ according to negative intrinsic efficacy in a mouse model of acute dependence. *Br. J. Pharmacol*. **2005**, *145*, 975-983.

77. Garbutt, J. C. Efficacy and tolerability of naltrexone in the management of alcohol dependence. *Curr. Pharm. Des*. **2010**, *16*, 2091-2097.

78. Hutchison, K. E.; Monti, P. M.; Rohsenow, D. J.; Swift, R. M.; Colby, S. M.; Gnys, M.; Niaura, R. S.; Sirota, A. D. Effects of naltrexone with replacement on smoking cue reactivity: preliminary results. *Psychopharmacology*. **1999**, *142*, 139-143.

79. Gerra, G.; Fantoma, A.; Zaimovic, A. Naltrexone and buprenorphine combination in the treatment of opioid dependence. *J. Psychopharm*. **2006**, *20*, 806-814.

80. Bruchas, M. R.; Land, B. B.; Chavkin, C. The dynorphin/kappa opioid system as a modulator of stress-induced and pro-addictive behaviors. *Brain Res*. **2010**, *1314*, 44-55.

81. Wee, S.; Koob, G. F. The role of the dynorphin-κ opioid system in the reinforcing effects of drugs of abuse. *Psychopharmacology*. **2010**, *210*, 121-135.

82. Butelman, E. R.; Yuferov, V.; Kreek, M. J. κ-opioid receptor/dynorphin system: genetic and pharmacotherapeutic implications for addiction. *Trends Neurosci*. **2012**, *35*, 587-596.

83. McLaughlin, J. P.; Marton-Popovici, M.; Chavkin, C. κ opioid receptor antagonism and prodynorphin gene disruption block stress-induced behavioral responses. *J. Neurosci.* **2003**, *23*, 5674-5683.
84. Redila, V. A.; Chavkin, C. Stress-induced reinstatement of cocaine seeking is mediated by the kappa opioid system. *Psychopharmacology*. **2008**, *200*, 59-70.
85. Smith, J. S.; Schindler, A. G.; Martinelli, E.; Gustin, R. M.; Bruchas, M. R.; Chavkin, C. Stress-induced activation of the dynorphin/κ-opioid receptor system in the amygdala potentiates nicotine conditioned place preference. *J. Neurosci*. **2012**, *32*, 1488-1495.
86. Nestler, E. J. Historical review: molecular and cellular mechanisms of opiate and cocaine addiction. *Trends Pharmacol. Sci*. **2004**, *25*, 210-218.
87. Koob, G. F. The neurobiology of addiction: a neuroadaptational view relevant for diagnosis. *Addiction*. **2006**, *101*, 23-30.
88. Zhang, H.; Shi, Y.; Woods, J. H.; Watson, S. J.; Ko, M. Central κ-opioid receptor-mediated antidepressant-like effects of nor-Binaltorphimine: behavioral and BDNF mRNA expression studies. *Eur. J. Pharmacol*. **2007**, *570*, 89-96.
89. Chartoff, E.; Sawyer, A.; Rachlin, A.; Potter, D.; Pliakas, A.; Carlezon, W. A. Blockade of kappa opioid receptors attenuates the development of depressive-like behaviors induced by cocaine withdrawal in rats. *Neuropharmacology*. **2012**, *62*, 167-176.

Appendix

HPLC spectrum for the final compounds and the GOLD docking scores for the best-scoring poses are enclosed in the appendix.

Compound **9**

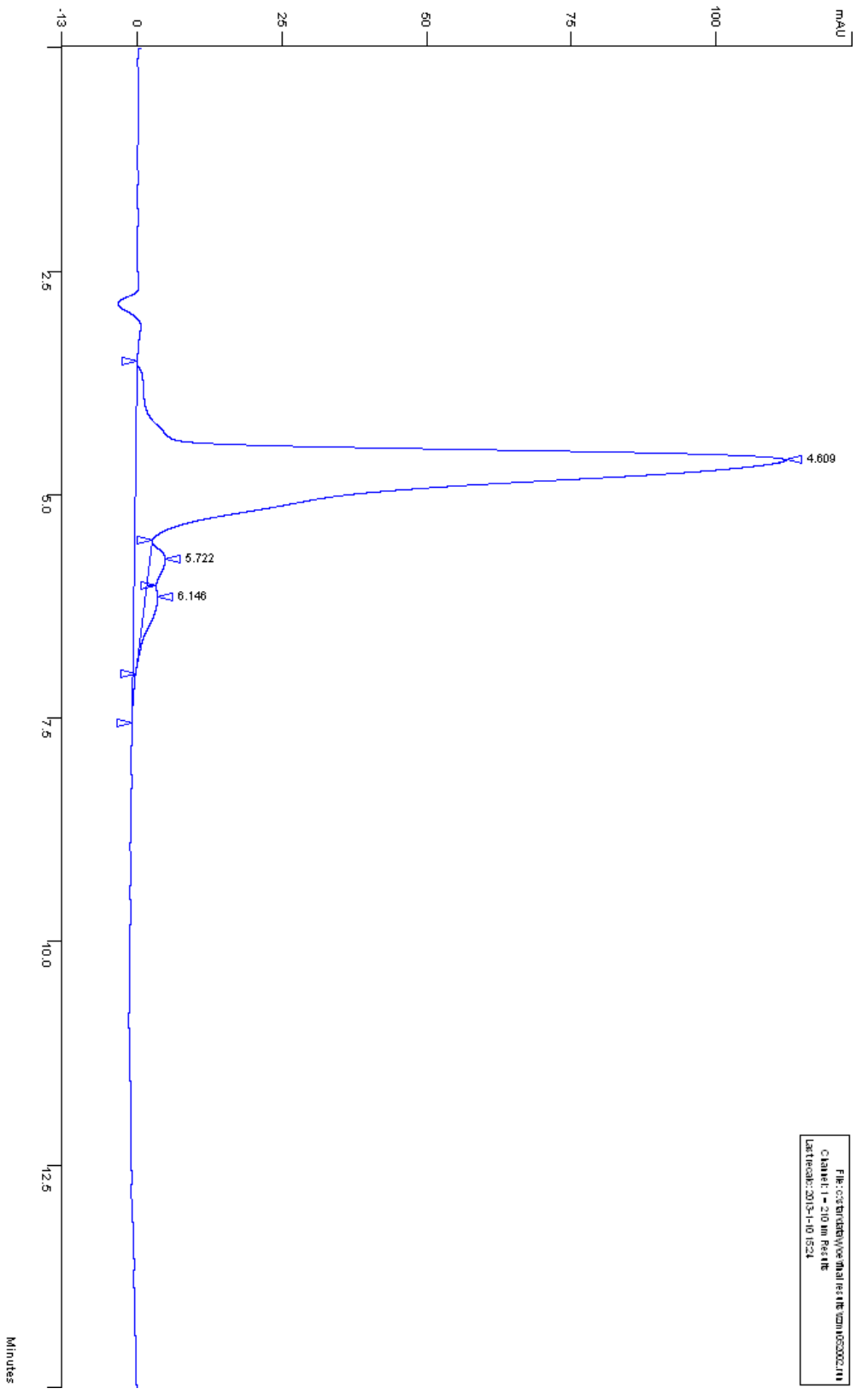

Compound **10**

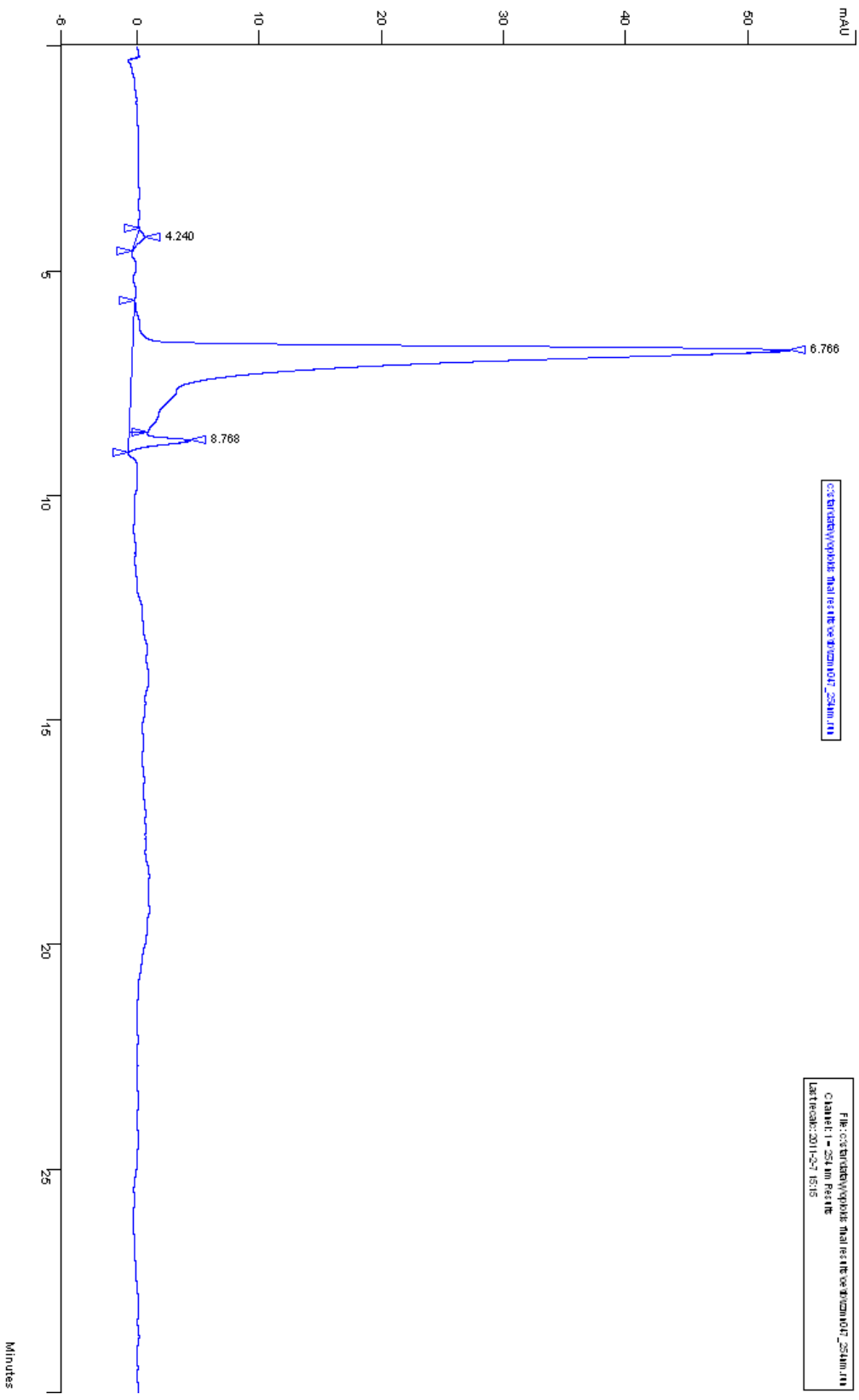

Compound **11**

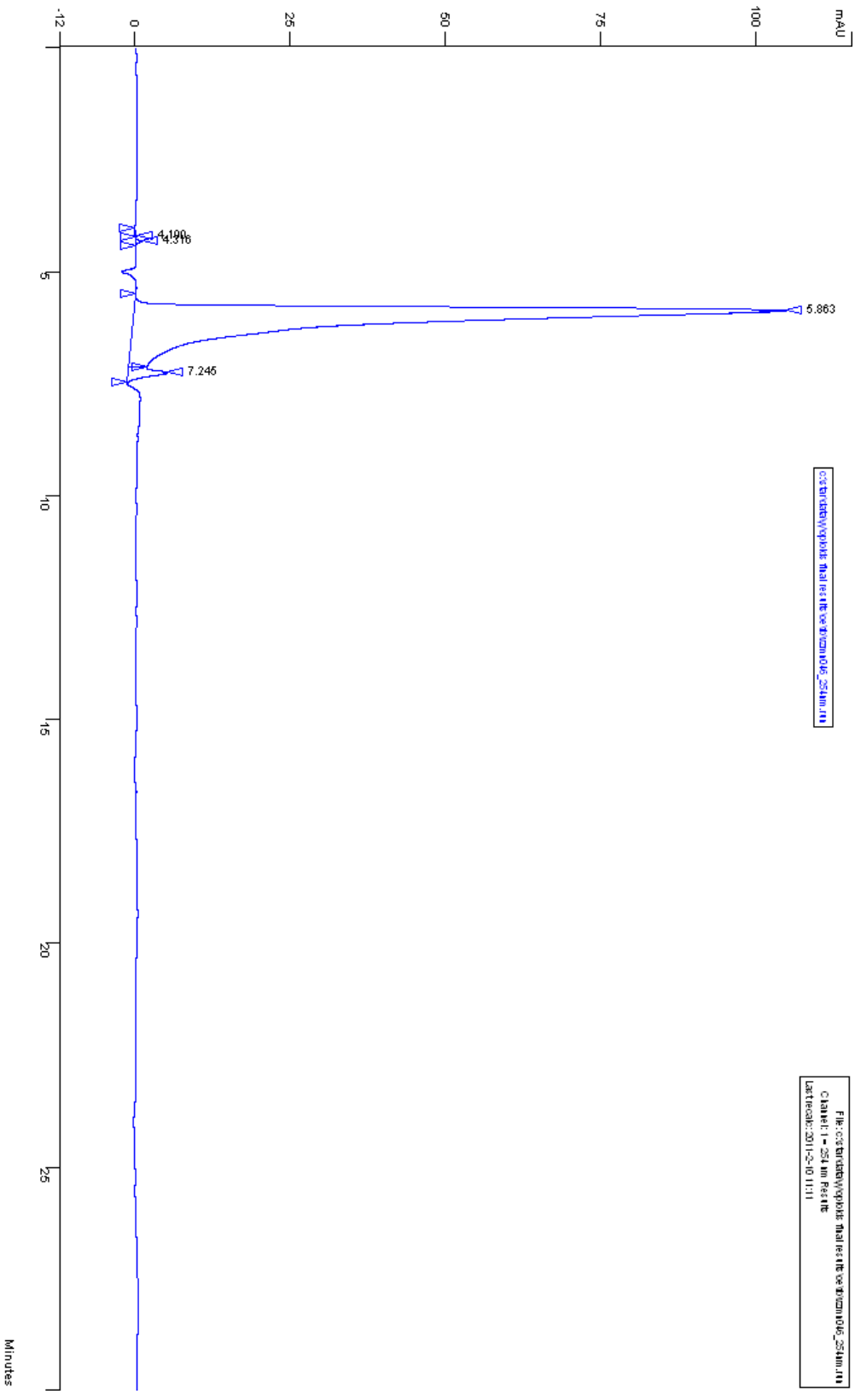

Compound **12**

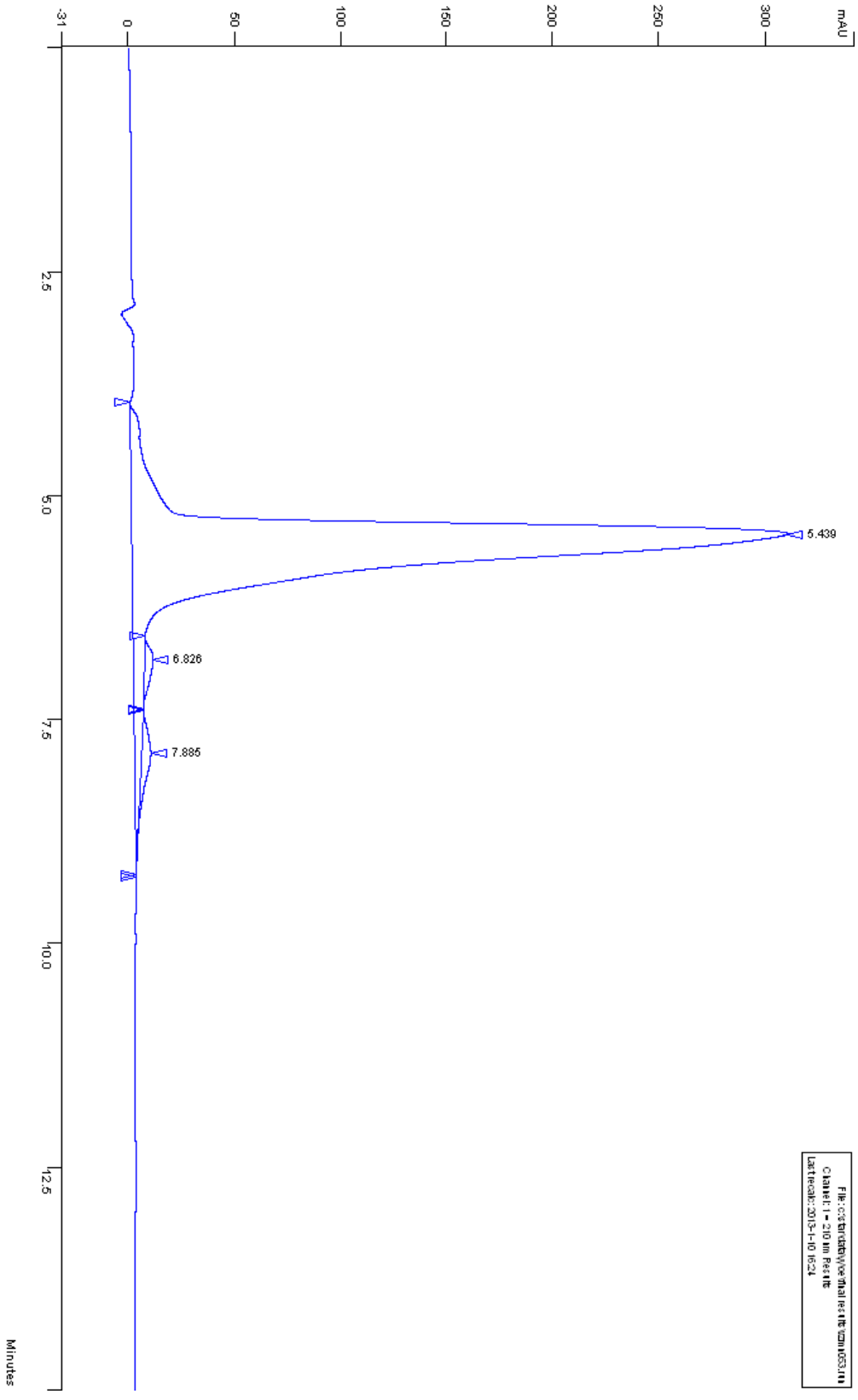
mAU
-31
0
50
100
150
200
250
300
2.5
5.0
7.5
10.0
12.5
Minutes
5.439
6.826
7.885

Compound **13**

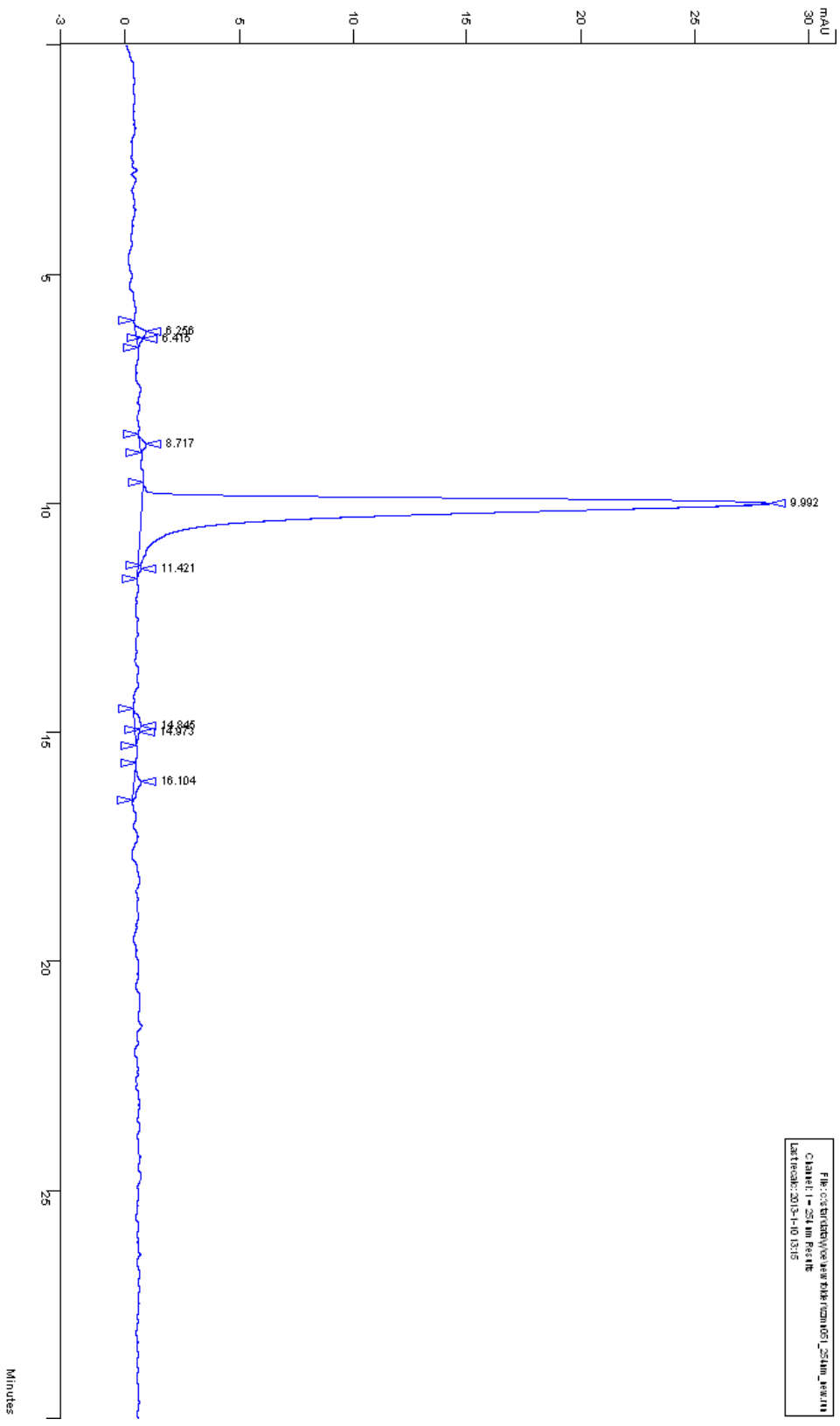
mAU
30
25
20
15
10
5
0
-3
Minutes
5
10
15
20
25
6.256
6.415
8.717
9.992
11.421
14.845
14.973
16.104

Compound **14**

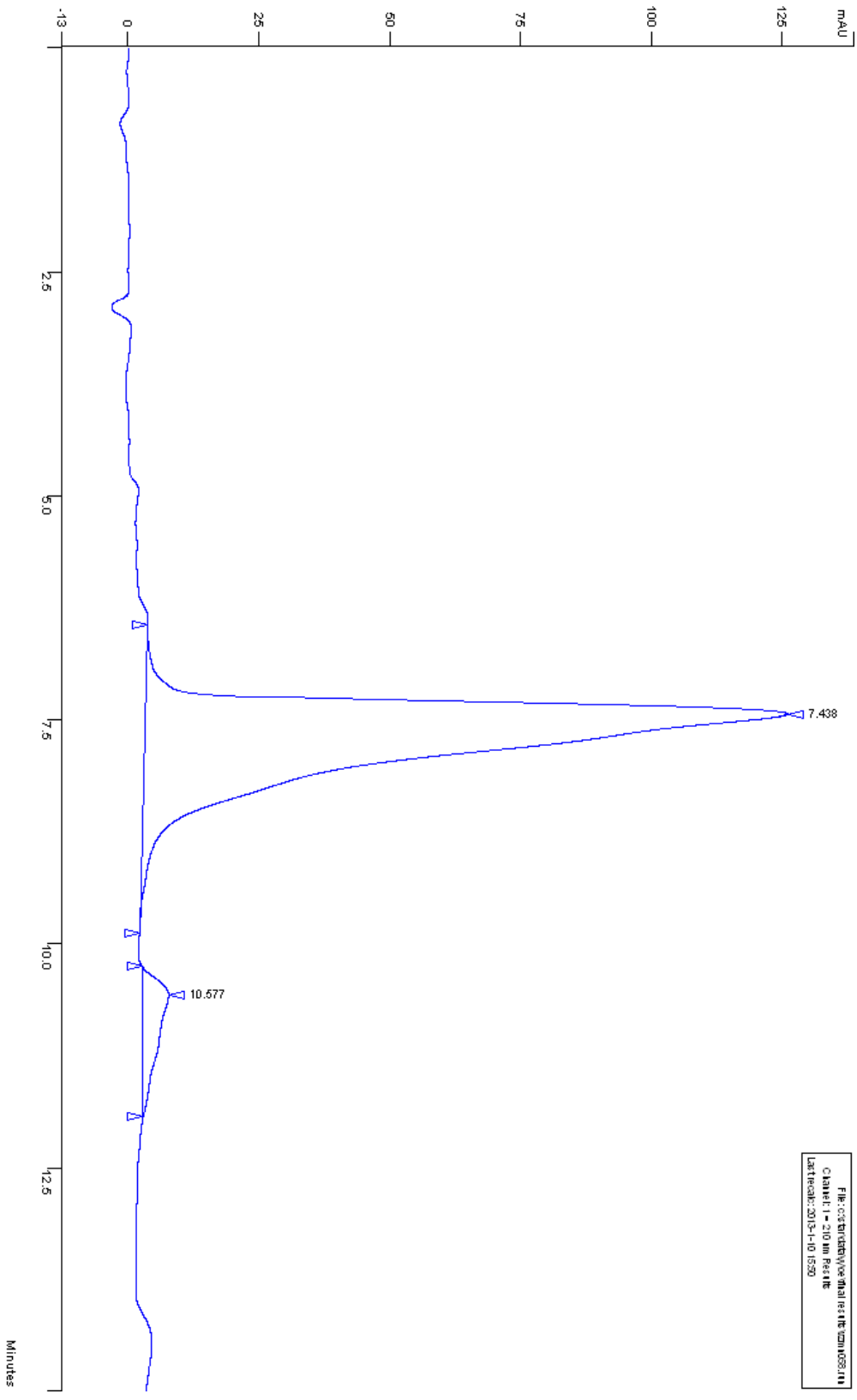

Compound **15**

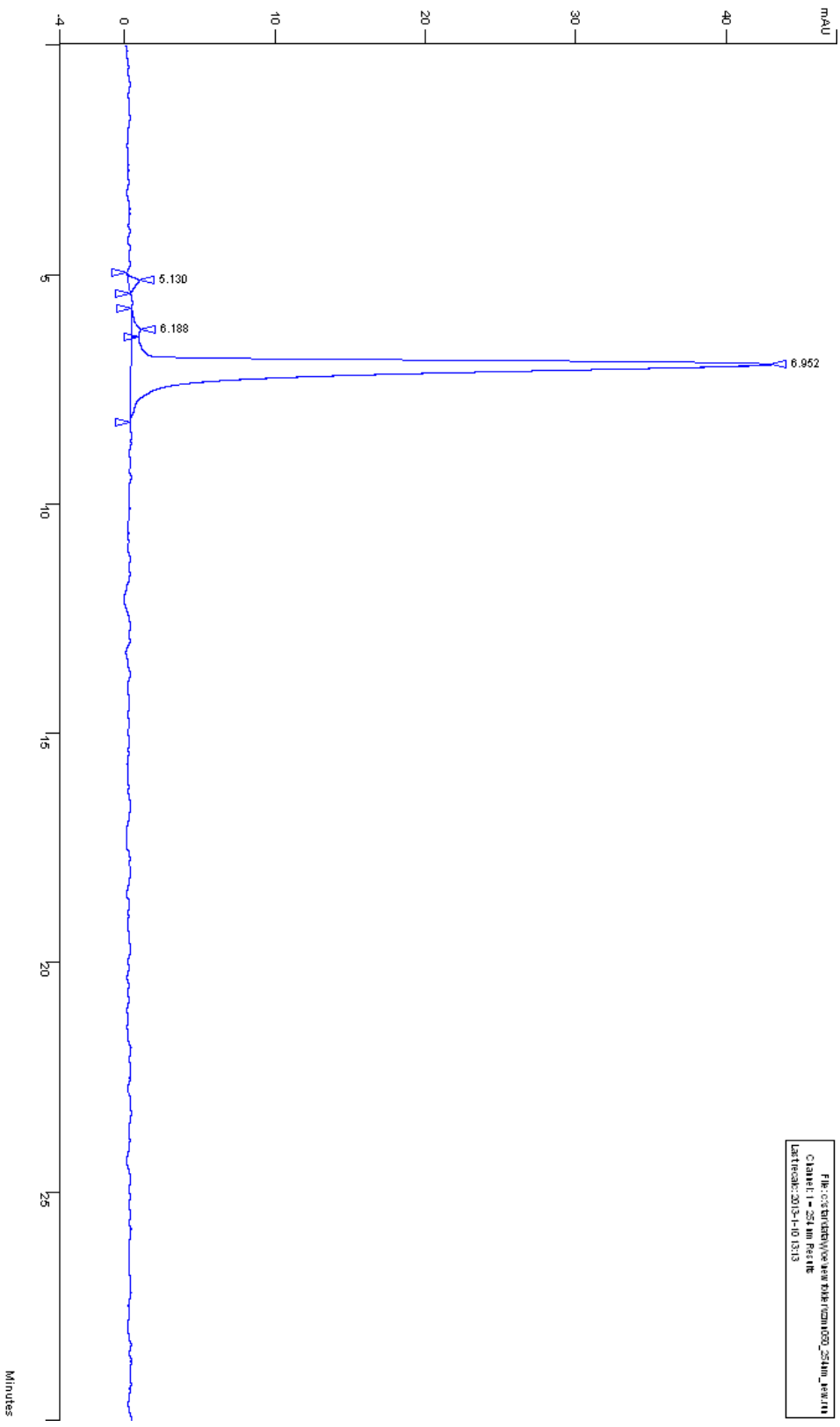

Compound **16**

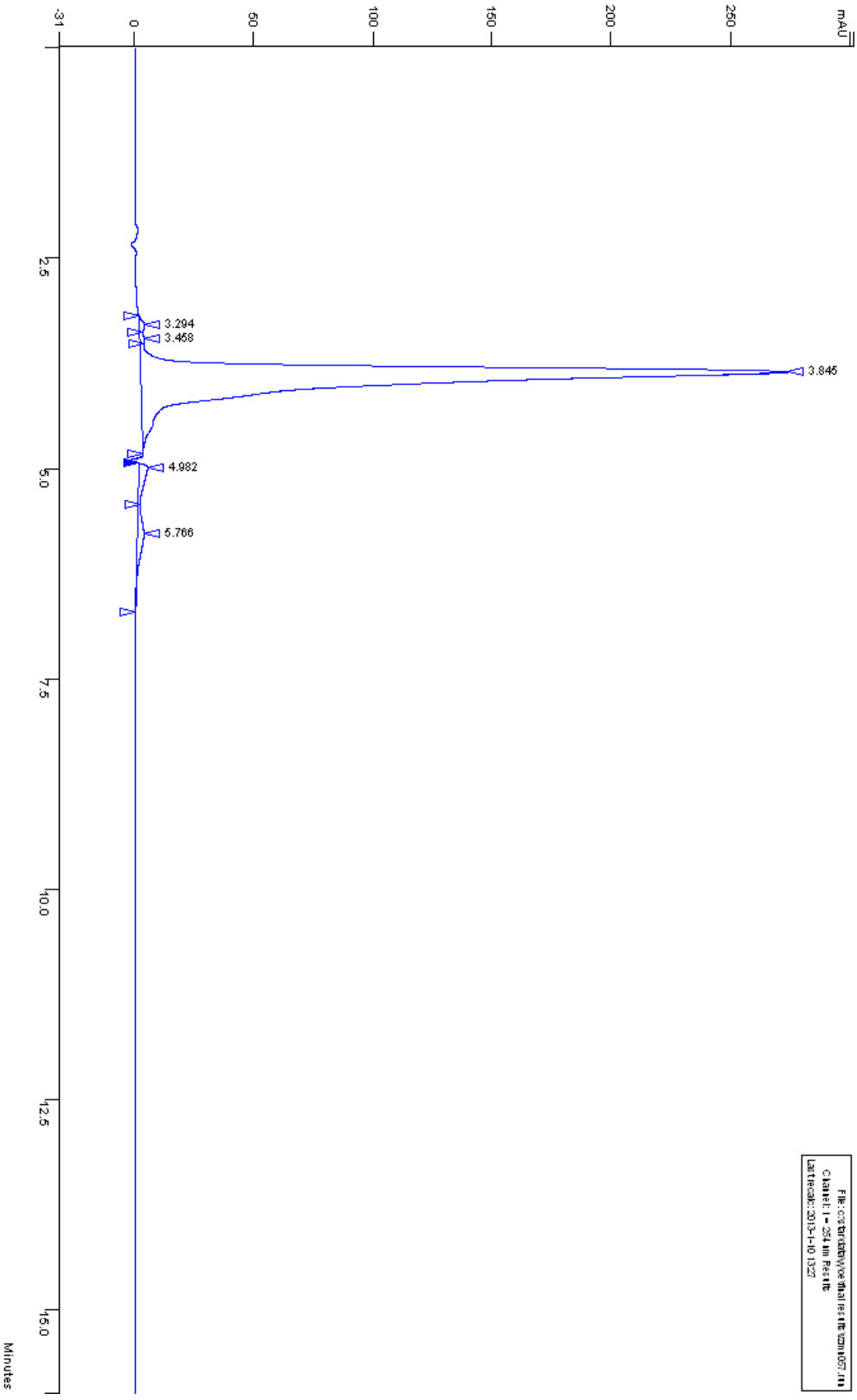
mAU
-31
0
50
100
150
200
250
2.5
5.0
7.5
10.0
12.5
15.0
Minutes
3.294
3.458
3.845
4.982
5.766

Compound **27**

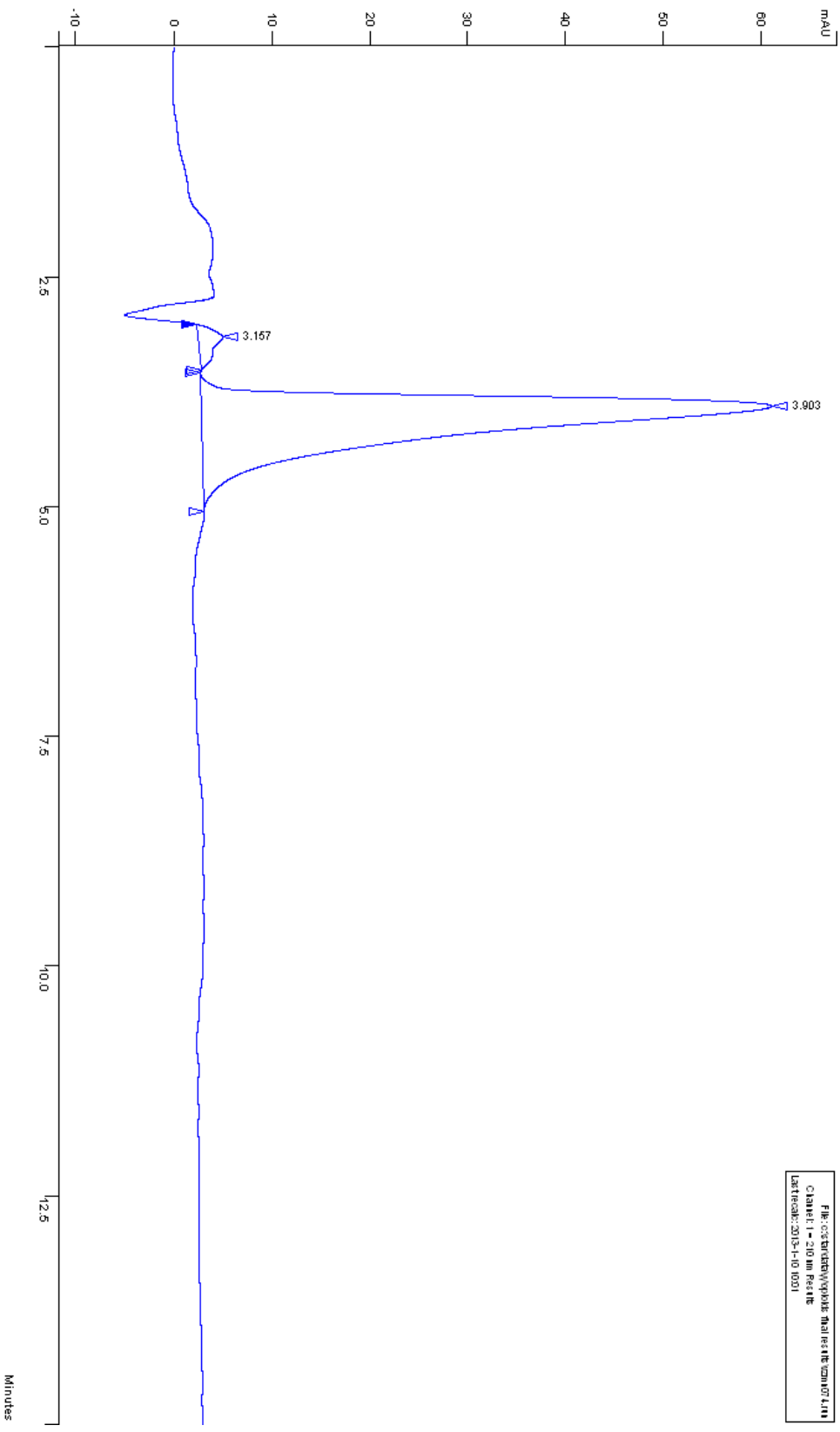

Compound **28**

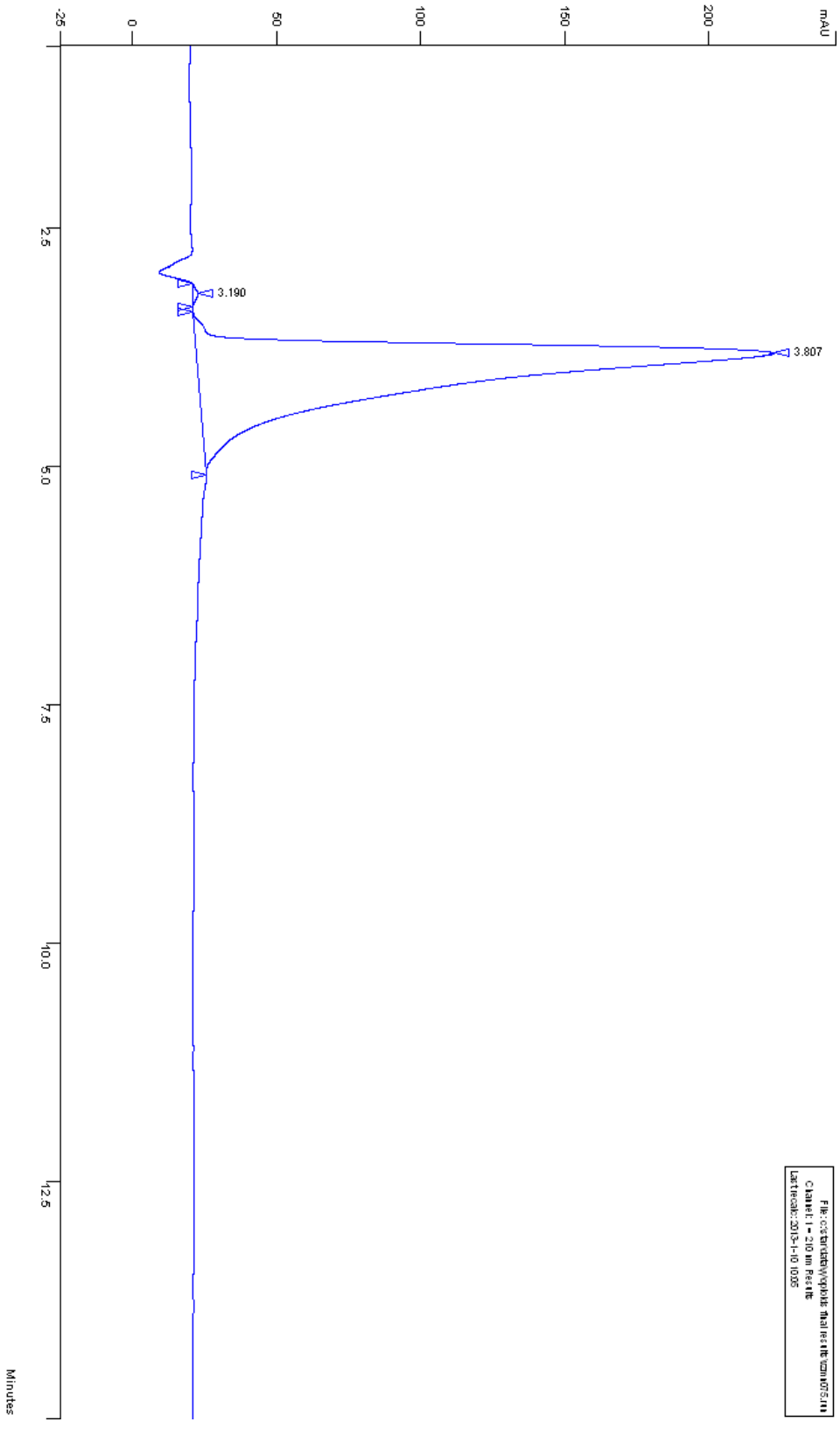

Compound **29**

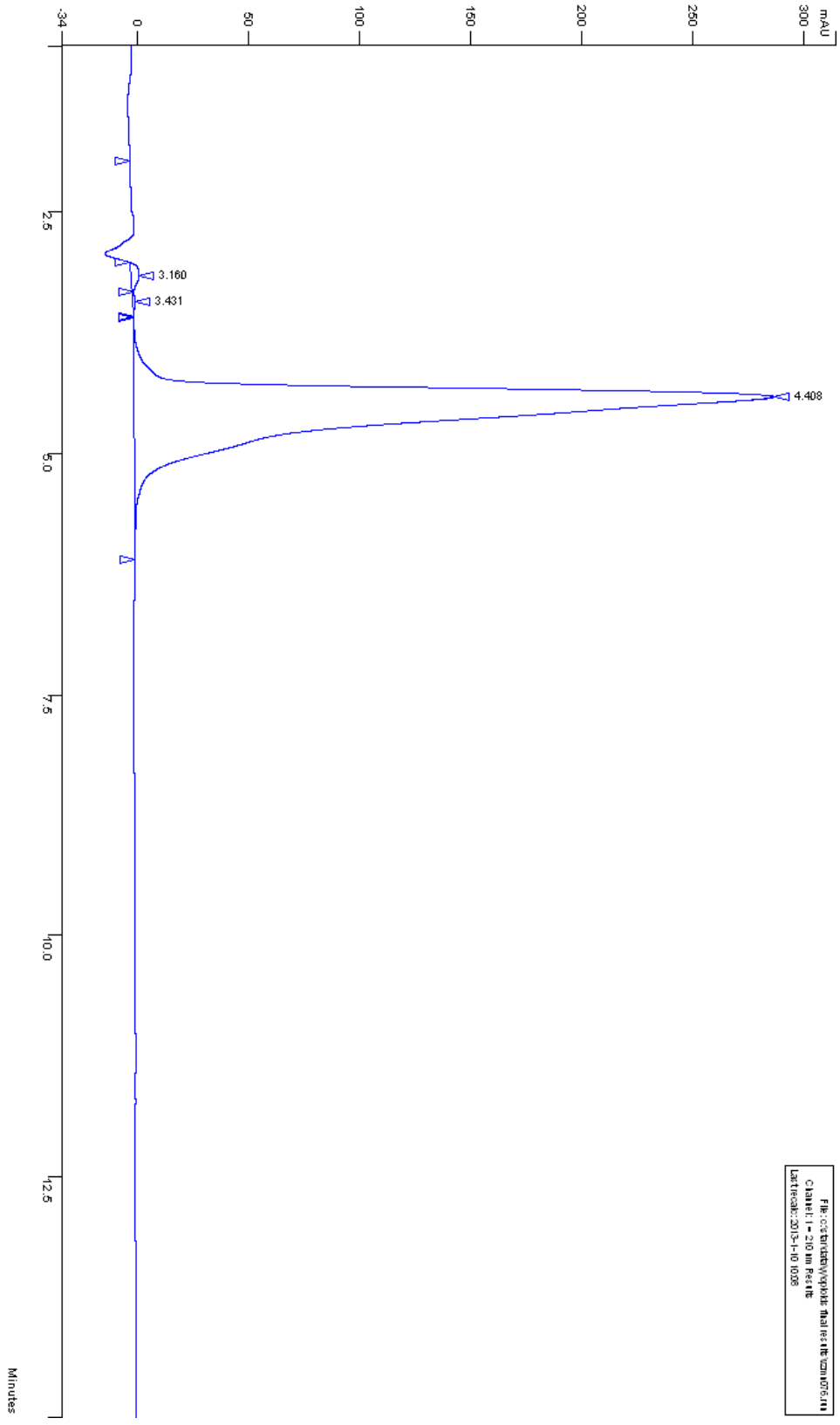
mAU
300
250
200
150
100
50
0
-34
2.5
5.0
7.5
10.0
12.5
Minutes
3.160
3.431
4.408

Table 1. Best Ranked CHEMPLP Docking Scores for MOR

Compd	CHEMPLP Score	S(PLP)	S(hbond)	S(cho)	DE(tors)
1	80.61	-72.37	2.00	1.00	1.53
2	74.42	-68.20	2.29	0.00	1.43
3	76.22	-67.02	2.67	0.69	1.57
4	76.11	-70.75	1.92	0.00	1.35
5	84.08	-78.15	2.56	0.00	1.99
6	85.92	-80.80	1.98	0.00	1.52
7	84.66	-79.04	2.36	0.00	1.84
8	86.97	-81.90	1.98	0.00	1.55
9	80.46	-75.40	2.00	0.00	1.79
10	78.02	-72.08	2.00	0.00	1.39
11	80.16	-74.44	2.00	0.00	1.51
12	79.60	-72.17	2.50	0.00	1.40
13	89.37	-81.16	3.00	0.00	1.72
14	88.79	-83.09	2.00	0.00	1.49
15	86.47	-76.10	3.00	0.71	1.71
16	89.44	-83.75	2.00	0.00	1.50
27	89.42	-80.89	2.00	1.00	1.65
28	86.73	-79.52	2.00	0.97	2.22
29	89.42	-83.82	2.00	0.00	1.54

Table 2. Best Ranked CHEMPLP Docking Scores for the Kappa Opioid Receptor

Compd	CHEMPLP Score	S(PLP)	S(hbond)	S(cho)	DE(tors)
1	74.36	-67.84	3.11	0.00	2.51
2	72.46	-66.61	2.96	0.00	2.68
3	75.72	-67.31	2.95	1.00	2.86
4	75.15	-68.75	3.09	0.00	2.56
5	85.23	-77.71	3.36	0.00	2.45
6	85.65	-78.88	3.24	0.00	2.60
7	79.58	-75.72	2.86	0.00	3.48
8	86.66	-80.05	3.14	0.00	2.53
9	71.56	-62.54	4.33	0.00	3.36
10	74.48	-63.21	3.42	0.66	1.85
11	75.06	-60.01	4.50	1.00	2.09
12	75.46	-63.81	4.11	0.00	1.70
13	81.92	-71.86	4.54	0.00	3.10
14	83.41	-72.66	4.43	0.00	2.66
15	83.22	-70.60	4.33	0.52	2.30
16	83.82	-72.83	4.33	0.00	2.40
27	88.58	-74.77	4.40	1.00	2.59
28	83.06	-71.63	4.17	0.00	1.90
29	88.19	-77.74	4.54	0.00	3.02

Table 3. Best Ranked CHEMPLP Scores for the Delta Opioid Receptor

Compd	CHEMPLP Score	S(PLP)	S(hbond)	S(cho)	DE(tors)
1	74.07	-67.98	1.45	1.00	1.74
2	75.48	-67.90	2.88	0.00	1.68
3	84.18	-73.61	2.85	1.00	1.61
4	73.70	-69.24	1.89	0.00	1.74
5	73.44	-70.99	2.35	0.00	3.42
6	66.55	-64.51	1.80	0.00	2.85
7	75.16	-68.71	1.60	0.99	1.77
8	72.77	-69.80	2.44	0.00	3.28
9	71.12	-63.36	3.62	0.14	3.07
10	74.20	-65.13	3.05	1.00	2.90
11	73.89	-64.75	2.42	1.00	2.00
12	67.13	-62.26	2.66	0.00	2.93
13	80.08	-73.82	3.31	0.00	3.19
14	79.32	-74.69	2.79	0.00	3.22
15	65.46	-70.55	2.66	0.00	3.29
16	63.66	-67.25	2.96	0.00	2.83
27	85.05	-77.34	2.10	1.00	2.21
28	89.46	-81.81	3.03	0.00	2.12
29	93.68	-81.99	4.15	0.00	1.91

Table 4. Best Ranked GOLD Fitness Scores for the Ligands Docked into the Mu Opioid Receptor

Compd	GOLD Score	S(hb_ext)	S(vdw_ext)	S(int)
1	70.62	3.47	49.76	-1.27
2	70.55	3.68	48.72	-0.11
3	68.95	3.61	48.04	-0.72
4	70.72	3.66	49.12	-0.47
5	76.70	3.27	54.48	-1.48
6	75.62	3.36	53.22	-0.91
7	77.18	3.27	54.29	-0.74
8	78.15	3.63	54.87	-0.93
9	70.70	5.03	48.10	-0.47
10	70.18	4.23	48.45	-0.67
11	70.02	4.13	48.43	-0.70
12	71.06	4.32	49.27	-1.01
13	76.85	2.31	55.18	-1.34
14	76.29	2.70	55.31	-2.47
15	78.98	4.59	54.98	-1.21
16	78.02	2.63	55.27	-0.60
27	70.62	4.25	49.19	-1.26
28	79.58	4.20	56.25	-1.97
29	75.86	4.10	53.37	-1.62

Table 5. Best Ranked GOLD Fitness Scores for the Ligands Docked into the Kappa Opioid Receptor

Compd	GOLD Score	S(hb_ext)	S(vdw_ext)	S(int)
1	59.38	2.74	42.78	-2.18
2	61.35	2.42	43.77	-1.24
3	58.85	2.91	41.91	-1.68
4	58.72	2.70	42.15	-1.93
5	68.33	2.96	49.27	-2.37
6	68.26	2.45	50.13	-3.11
7	67.30	3.01	47.88	-1.55
8	67.85	3.16	48.29	-1.71
9	60.95	3.86	43.00	-2.03
10	63.91	2.40	44.98	-0.34
11	62.54	2.45	44.65	-1.31
12	63.99	2.68	45.55	-1.32
13	65.54	1.76	47.53	-1.58
14	67.27	3.27	48.86	-3.19
15	66.14	3.94	46.11	-1.19
16	67.42	4.20	47.16	-1.63
27	63.25	1.86	45.29	-0.88
28	68.44	2.89	49.04	-1.88
29	69.37	1.51	52.09	-3.77

Table 6. Best Ranked GOLD Fitness Scores for the Ligands Docked into the Delta Opioid Receptor

Compd	GOLD Score	S(hb_ext)	S(vdw_ext)	S(int)
1	73.33	6.52	52.30	-5.11
2	70.51	6.82	50.13	-5.24
3	68.90	2.95	48.87	-1.24
4	70.57	6.22	50.62	-5.25
5	76.13	5.26	54.54	-4.12
6	71.97	3.48	53.59	-5.19
7	72.14	3.21	54.33	-5.77
8	73.91	6.33	52.38	-4.44
9	75.49	6.58	51.60	-2.05
10	75.39	5.97	53.10	-3.60
11	76.42	5.69	51.98	-0.75
12	76.16	3.85	53.02	-0.59
13	83.81	4.67	60.24	-3.69
14	81.32	7.34	55.73	-2.66
15	82.80	4.88	58.15	-2.03
16	81.97	5.13	57.15	-1.74
27	77.52	7.34	51.58	-0.74
28	79.14	3.82	56.72	-2.67
29	80.45	7.02	54.57	-1.61

Vita

Orgil Elbegdorj was born on May 12, 1986, in Ulaanbaatar, Mongolia, and is a Mongolian citizen. He graduated from Patrick Henry High School, Roanoke, Virginia in 2004. He received his Bachelor of Science in Biochemistry from Virginia Tech in 2008. He joined the Medicinal Chemistry department in the School of Pharmacy at Virginia Commonwealth University in August 2008.